Distribution and Dynamics of Endoplasmic Reticulum-Plasma Membrane Junctions in Pancreatic Acinar and Pancreatic Cancer Cells

Thesis submitted in accordance with the requirements of the University of Liverpool for the degree of Doctor of Philosophy by

Hayley Dingsdale

December 2012

Dedicated to John D. Dingsdale

Table of Contents

TABLE OF CONTENTS **3**

ABSTRACT **5**

ACKNOWLEDGEMENTS **6**

ABBREVIATIONS **7**

CHAPTER 1: INTRODUCTION **10**

1.1 ENDOPLASMIC RETICULUM-PLASMA MEMBRANE JUNCTIONS 10

1.1.1 Overview *10*

1.1.2 The ER *11*

1.1.3 The ER and Ca^{2+} signalling *12*

1.1.4 Store-operated Ca^{2+} entry *14*

1.1.5 ER-PM junctions *18*

1.1.6 SOCE junctions *19*

1.2 CELL MIGRATION 23

1.2.1 Overview *23*

1.2.2 Cell polarity *23*

1.2.3 Actin polymerisation *24*

1.2.4 Focal adhesions *25*

1.2.5 Ras GTPases *26*

1.2.6 Calcium in cell migration *27*

1.2.7 Caveolae in SOCE and cell migration *31*

1.3 CA^{2+} SIGNALLING IN PANCREATIC ACINAR CELLS 33

1.3.1 Overview *33*

1.3.2 Ca^{2+} signalling *33*

1.4 AIMS 34

CHAPTER 2: MATERIALS AND METHODS **36**

2.1 MATERIALS 36

2.1.1 General reagents and equipment for pancreatic cancer cell culture and transfection *36*

2.1.2 Constructs *36*

2.1.3 Reagents for isolation and overnight maintenance of pancreatic acinar cells *39*

2.1.4 Immunocytochemistry *39*

2.1.5 Chemicals *40*

2.2 METHODS 40

2.2.1 Pancreatic cancer cell culture and transfection *40*

2.2.2 Isolation of pancreatic acinar cells *41*

2.2.3 Viral transfection of pancreatic acinar cells *42*

2.2.4 Immunocytochemistry *42*

2.2.5 Confocal microscopy *43*

2.2.6 Migration assays *45*

2.2.7 Rapamycin-inducible linkers *45*

2.2.8 Image and statistical analysis *45*

CHAPTER 3: DYNAMICS OF ER-PM JUNCTIONS **49**

3.1 OVERVIEW 49

3.1.1 The role of phospholipids in the placement of ER-PM junctions *50*

3.1.2 The role of microtubules in the placement of ER-PM junctions *51*

3.2 PROTOCOL OPTIMISATION 52

3.3 MODIFYING SOCE CAN INHIBIT MIGRATION OF PANC-1 CELLS 58

3.4 ER-PM JUNCTIONS CONCENTRATE AT THE LEADING EDGE OF MIGRATING CELLS 64

3.5 Distribution of constitutively active STIM1 mutant in non-store depleted PANC-1 cells 72
3.6 Effect of deletion of the C-terminal polybasic region of STIM1 on the distribution of STIM1 puncta 75
3.7 Distribution of STIM1(NN) in store-depleted PANC-1 cells 77
3.8 STIM1 puncta formation at the leading edge of cells is saltatory, and does not involve sliding from the cell interior 83
3.9 Puncta can travel long distances during retraction of the cell tail 94
3.10 STIM1 puncta at the leading edge co-localise with Orai1 102
3.11 Summary 104
3.11.1 Overview 104
3.11.2 Effects of SOCE regulation on cell migration 104
3.11.3 Concentration of STIM1 puncta at the periphery of cells 105
3.11.4 Mechanism of STIM1 puncta concentration at the periphery of cells 106
3.11.5 Saltatory formation of puncta 109
3.11.6 Long distance translocation of STIM1 puncta during tail withdrawal 110
3.11.7 Conclusion 111

CHAPTER 4: DISTRIBUTION OF ER-PM JUNCTIONS IN RELATION TO MIGRATORY PROTEINS 114
4.1 Overview 114
4.1.1 Actin 115
4.1.2 Focal adhesions 115
4.1.3 Calnexin 116
4.1.4 Caveolin 116
4.2 Use of linker constructs as a mechanism for highlighting junctions 117
4.3 Distribution of ER-PM junctions in relation to actin 126
4.4 Distribution of ER-PM junctions in relation to vinculin 141
4.5 The concentration of STIM1 puncta at the leading edge of cells is not due to an increased density of ER 147
4.6 Localisation of caveolin in relation to STIM1 puncta 152
4.7 Summary 159
4.7.1 Overview 159
4.7.2 Verification of ER-PM junction distribution in polarised PANC-1 cells 159
4.7.3 Relationship between ER-PM junctions and actin 160
4.7.4 Relationship between ER-PM junctions and focal adhesions 161
4.7.5 Relative distribution of calnexin 161
4.7.6 Caveolin and ER-PM junctions in migrating cells 162
4.7.7 Conclusion 163

CHAPTER 5: LOCALISATION OF ORAI1 IN PANCREATIC ACINAR CELLS 165
5.1 Overview 165
5.2 Apical IP_3R2 and Orai1 in pancreatic acinar cells 166
5.3 Testing the localisation of Orai1 in pancreatic acinar cells 169
5.4 Summary 178

CHAPTER 6: GENERAL DISCUSSION & CONCLUDING REMARKS 183
6.1 Overview 183
6.2 ER-PM junctions and migration 183
6.3 SOCE complexes in pancreatic acinar cells 186
6.4 Concluding remarks 187

REFERENCES 188

APPENDIX 1: VIDEO LEGENDS 210

Abstract

Endoplasmic reticulum (ER)-plasma membrane (PM) junctions are found in many different cell types. They function as important calcium (Ca^{2+}) signalling structures, as sites of store-operated calcium entry (SOCE) and play many other crucial roles. Their distribution in polarised migrating pancreatic cancer cells, and in the polarised pancreatic acinar cells, was the subject of this investigation. In migrating cells, the specific spatial pattern of Ca^{2+} signalling has been shown to be of paramount importance, but is produced by an unknown mechanism that I aimed to investigate. In acinar cells, Ca^{2+} influx (via the SOCE complex) occurs basolaterally, whilst Ca^{2+} signals are generated apically, physically separating the two processes. The presence of the Ca^{2+} influx channel normally present in SOCE complexes (Orai1) in the apical region therefore, is a conundrum this investigation set out to untangle.

I found that ER-PM junctions and SOCE complexes localise to the leading edge of migrating cells and are ideally positioned for Ca^{2+}-dependent regulation of actin dynamics and focal adhesion turnover – processes crucial to migration. The appearance of junctions at the leading edge was saltatory, suggesting that it develops as a result of the formation of new junctions, not from a relocation of junctions from a more interior position. I also saw long distance translocation and dissolution of junctions in the retracting tails of migrating cells, in a manner similar to the dynamics of focal adhesions. In pancreatic acinar cells, PM-localised Orai1 was found on basal and lateral membranes, whilst apical Orai1 was found to be absent from the PM and instead in a structure just beneath it, co-localising with ER-located Ca^{2+}-release channels.

Acknowledgements

I would like to thank my supervisor Alexei Tepikin for his kind words of encouragement, his contagious sense of optimism and his unending support. His supervision and advice have been consistently amazing.
Thank you also to my co-supervisor David Criddle for his advice and for always being happy to provide a friendly ear.

Thanks to Robert Sutton for his valuable advice during my project and for donating the use of the 710 microscope, which was central to this investigation.

Special thanks to Gyorgy Lur for training me during my first year, and for passing on his extensive laboratory expertise. Special thanks also to Lee Haynes for the production of many of the constructs used, and for his help with all the molecular biology carried out during my Ph.D.

Thank you to Svetlana Voronina, Misha Chvanov and David Booth for their help with laboratory work, and Muhammad Awais for training me on the 710. Thanks also to Emmanuel Okeke for proofreading my thesis and to Mark Houghton for patiently helping me make diagrams and for all his administrative support.

Thanks to all the external collaborators – Stefan Feske, David Yule, Richard Lewis, Tamas Balla and Tobias Meyer – for generously supplying us with their essential constructs and antibodies.

Thank you to the whole of Blue Block for helping me keep my spirits high and for being a friendly and entertaining bunch, I hope to see you all again soon. Thanks also to all my friends who have supported me throughout this thesis, especially to Matthew Cane.

Thank you to my family for their love and support throughout this process, their motivational speeches, care packages, and house-moving skills – I promise to never move house so many times in four years again. Finally, thank you to George Dingsdale, for the inspiration.

This project was funded by the Wellcome Trust.

Abbreviations

ACCM	Acinar cell culture media
AOBS	Acousto-optical beam splitter
ARPC2	Actin related protein 2/3 complex, subunit 2, 34kDa
ATCC	American Type Culture Collection
ATP	Adenosine triphosphate
AU	Arbitrary unit
BSA	Bovine serum albumin
Ca^{2+}	Calcium
$[Ca^{2+}]_c$	Cytosolic Ca^{2+} concentration
$[Ca^{2+}]_{ER}$	Endoplasmic reticulum Ca^{2+} concentration
CDI	Ca^{2+}-dependent inhibition
CFP	Cyan fluorescent protein
CICR	Ca^{2+} induced Ca^{2+} release
CMV	Cytomegalovirus
CPA	Cyclopiazonic acid
DMEM	Dulbecco's modified eagle medium
DNA	Deoxyribonucleic acid
DPBS	Dulbecco's phosphate buffered saline
EB1	End-binding protein 1
EDTA	Ethylenediaminetetraacetic acid
EGFP	Enhanced green fluorescent protein
EM	Electron microscopy
ER	Endoplasmic reticulum
EtOH	Ethanol
FBS	Heat-inactivated foetal bovine serum
FKBP	FK506-binding protein
FRB	Fragment of mTOR that binds FKBP12
GDP	Guanosine diphosphate
GFP	Green fluorescent protein
HEPES	4-(2-hydroxyethyl)-1-piperazineethanesulphonic acid
IP_3	Inositol 1,4,5-trisphosphate
IP_3R	IP_3 receptor
LSM	Laser scanning microscope

MEFs	Murine embryonic fibroblasts
MEM	Minimum essential media
MeOH	Methanol
NA	Numerical aperture
PBS	Phosphate buffered saline
PFA	Paraformaldehyde
PH	Pleckstrin homology
PI	Phosphoinositide
PM	Plasma membrane
PSG	PenStrep Glutamine
RFP	Red fluorescent protein
RPM	Revolutions per minute
RT	Room temperature
SERCA	Sarco(endo)plasmic reticulum Ca^{2+}-ATPase
SOCE	Store-operated Ca^{2+} entry
SP	Signal peptide
SR	Sarcoplasmic reticulum
STIM	Stromal interaction molecule
TACs	Tip attachment complexes
TG	Thapsigargin
TIRF	Total internal reflection fluorescence
TK	Thymidine kinase
TRP	Transient receptor potential
WGA	Wheat germ agglutinin
WT	Wild type
YFP	Yellow fluorescent protein

Chapter 1: Introduction

Chapter 1: Introduction

1.1 Endoplasmic reticulum-plasma membrane junctions

1.1.1 Overview

The endoplasmic reticulum (ER) is an intracellular organelle present in and vital for the function of all eukaryotic cells. Its diverse array of functions include the synthesis, modification and transport of proteins and lipids; it functions also as a calcium (Ca^{2+}) signalling hub for the cell (Berridge *et al.*, 2000). The cellular ER network is wide reaching, extending throughout the cell and to the cell periphery; this allows it to efficiently communicate with other intracellular organelles (Levine & Loewen, 2006; English *et al.*, 2009). Direct or indirect communication between the ER and other cellular organelles provides the means for lipid transfer between the production site (the ER) and the destination organelles (Holthuis & Levine, 2005), and allows the ER to strictly regulate the Ca^{2+} content of individual cellular compartments, in particular that of the mitochondria (Rizzuto *et al.*, 1998). It also means that intracellular Ca^{2+} signalling events originating from the ER can be tightly restricted spatially (Rizzuto & Pozzan, 2006).

Communication between the ER and other intracellular organelles mainly occurs via two main mechanisms: vesicular transport, such as that occurring between the ER and the Golgi (Lee *et al.*, 2004) and via tight physical junctions, such as those present between the ER and both the mitochondria (Copeland & Dalton, 1959; Giorgi *et al.*, 2009) and the plasma membrane (PM) (Fawcett & Revel, 1961; Reger, 1961; Brandt *et al.*, 1965; Franzini-

Armstron, 1974; Gardiner & Grey, 1983). The junctions found between the ER and the PM are the main focus of this investigation.

1.1.2 The ER

With a diverse array of functions comes a diverse range of structural requirements. The ER negotiates these requirements with three distinct structural entities – rough ER, smooth ER, and the nuclear envelope. Transitional ER is a fourth type of ER that communicates with the Golgi and which is occasionally mentioned as another specialised form of the organelle (Jamieson & Palade, 1967; Voeltz *et al.*, 2002). The nuclear envelope is a double bilayer structure containing nuclear pores – sites of import and export of materials in and out of the nucleus. The outer layer is continuous with the rough ER, whilst the inner membranous region is separate, linked to the nuclear outer membrane at the sites of nuclear pore complexes (Hetzer *et al.*, 2005). This region of ER encircles the nucleus and therefore does not interact with the cell periphery or PM.

The rough ER is heavily involved in protein production. It is so called because its surface is covered with ribosomes, relatively large (26 nm) nucleoprotein structures that carry out protein synthesis and which create the 'rough' appearance when imaged using electron microscopy (EM) (Lur *et al.*, 2009). Smooth ER lacks ribosomes and is preferentially involved in the production of lipids and sterols. A specialised form of smooth ER called the sarcoplasmic reticulum (SR) plays a role in Ca^{2+} signalling in muscle cells (Rossi & Dirksen, 2006). The specific composition of the ER in individual cells (i.e. the balance of smooth to rough ER) is largely dependent on cell function, for example rough ER will be predominant in cells with a high protein export requirement (Voeltz *et al.*, 2002).

1.1.3 The ER and Ca^{2+} signalling

The ER Ca^{2+} concentration ($[Ca^{2+}]_{ER}$) is ~ 100 – 800 μM at rest (Burdakov *et al.*, 2005), a thousand fold higher than the cytosolic Ca^{2+} concentration ($[Ca^{2+}]_c$) of ~ 100 nM. Ca^{2+} release from the ER is the main mechanism by which non-excitable cells (cells without voltage-gated ion channels) create intracellular Ca^{2+} signals. Release occurs as a consequence of stimulation of receptor-operated Ca^{2+}-release channels located in the ER. Agonists for these receptors include the second messengers inositol 1,4,5-trisphosphate (IP_3) which activates IP_3 receptors (IP_3Rs) (Berridge, 1993), and cyclic adenosine diphosphate ribose and nicotinic acid adenine dinucleotide phosphate which can both activate ryanodine receptors (Galione *et al.*, 1993). Ca^{2+} influx through PM channels (e.g. voltage-gated channels activated by depolarisation of the cell) can also stimulate Ca^{2+} release from the ER, as Ca^{2+} itself can act as a co-agonist for IP_3 receptors, and as an agonist for ryanodine receptors; this is called Ca^{2+} induced Ca^{2+} release (CICR) (Berridge *et al.*, 2003).

Downstream effects of ER Ca^{2+} release are many and varied, and range from fast responses such as stimulating cell contraction (Bers, 2002) or secretion (Petersen & Tepikin, 2008), to slower responses such as up-regulation of gene expression (Parekh & Muallem, 2011) or promotion of cell differentiation (Berridge *et al.*, 2000) or death (Berridge *et al.*, 2000; Orrenius *et al.*, 2003).

Many of the downstream effects are reliant on the cells' ability to increase Ca^{2+} in a specific and precise spatiotemporal pattern. A myriad of inappropriate downstream responses would be activated if $[Ca^{2+}]_c$ was allowed to remain elevated for erroneously long time periods and / or was spatially unregulated. Certainly, it is well known that excessively prolonged

Ca^{2+} elevations are toxic to cells and can lead to apoptosis or necrosis (Orrenius *et al.*, 2003). Two features of the ER and the whole cell help minimise the possibility of this occurrence.

First is the extensive distribution of the ER and the presence of Ca^{2+} release channels throughout the organelle. By limiting Ca^{2+} release through ER channels to specific regions of the cell, small Ca^{2+} microdomains can be created, able to activate local signalling cascades without affecting the rest of the cell. A high concentration of intracellular Ca^{2+} buffers also helps to prevent the spread of Ca^{2+} throughout the cell, increasing the spatial specificity of Ca^{2+} signals (Neher & Augustine, 1992; Mogami *et al.*, 1999; Schwaller, 2010).

Secondly, Ca^{2+} pumps present on the ER and the PM help rapidly remove Ca^{2+} from the cytosol after signalling events (Blaustein & Lederer, 1999; Di Leva *et al.*, 2008), transforming Ca^{2+} signals into short transients instead of sustained elevations. Increases in $[Ca^{2+}]_c$ stimulate increases in the rate of activity of these pumps (Camello *et al.*, 1996; Petersen, 2003). The pumps located on the ER are called sarco(endo)plasmic Ca^{2+}-ATPases (SERCA; ATP: adenosine triphosphate) pumps, and in quiescent cells they work to balance the Ca^{2+} leak from the ER that occurs via a poorly defined leak channel (Wuytack *et al.*, 2002). By returning Ca^{2+} back into the ER, these pumps also help prevent excessive depletion of ER Ca^{2+} stores, itself a dangerous prospect for cells. Without sufficient $[Ca^{2+}]_{ER}$, Ca^{2+}-dependent chaperones in the ER would not be able to fold newly synthesised proteins, leading to a backlog of incorrectly folded proteins and, further downstream, apoptosis (Michalak *et al.*, 2002; Kaufman, 2004; Groenendyk & Michalak, 2005; Tabas & Ron, 2011). By continuously returning $[Ca^{2+}]_c$ to baseline conditions and refilling the ER Ca^{2+} stores, these pumps allow cells to create Ca^{2+} oscillations,

transient Ca^{2+} elevations that can be repeated over multiple cycles without causing damage to the cell (Parekh, 2011). The Ca^{2+} pumps present on the PM are called the plasma membrane Ca^{2+}-ATPases (PMCAs), pumps with a high affinity for Ca^{2+} when stimulated, but a relatively low pumping activity (Di Leva *et al.*, 2008).

As $[Ca^{2+}]_c$ is returned to basal levels after signalling by both returning Ca^{2+} to the ER and by extrusion across the PM, the ER Ca^{2+} store would gradually be diminished if the loss to the external environment was not compensated (Putney & Bird, 2008). Compensation occurs through store-operated Ca^{2+} entry (SOCE), a process that occurs at specialised junctions between the ER and PM (Putney, 2007).

1.1.4 Store-operated Ca^{2+} entry

SOCE is a process stimulated by depletion of $[Ca^{2+}]_{ER}$ by which cells refill their internal Ca^{2+} stores. Though the existence of this process was first postulated in 1986 (Putney, 1986), the integral proteins involved were only determined 20 years later: the stromal interaction molecule (STIM) family (STIM1 and STIM2)(Liou *et al.*, 2005; Roos *et al.*, 2005) and the Orai family (Orai1, Orai2 and Orai3)(Feske *et al.*, 2006; Gwack *et al.*, 2007). Controversy over the exact components involved in SOCE still rages today, for example the role of transient receptor potential (TRP) channels is much debated, with strong evidence for and against their involvement (for: e.g. (Zeng *et al.*, 2008; Pani *et al.*, 2009), against: e.g. (Dietrich *et al.*, 2007; DeHaven *et al.*, 2009)).

STIM is a protein found in the ER membrane that can sense the status of the Ca^{2+} store. When the store is full, STIM binds Ca^{2+} at its EF hand domains. As the stores are depleted, this Ca^{2+} is lost, allowing STIM to oligomerise and

translocate towards the PM. Oligomerisation of the STIM proteins is thought to allow sufficient aggregation of positively charged regions found in the cytosolic regions of STIM to attract them towards the negatively charged PM (Ercan *et al.*, 2009; Park *et al.*, 2009). Here they bind directly to and activate pore-forming Orai proteins allowing formation of Ca^{2+} conducting, store-operated channels at ER-PM junctions (Mercer *et al.*, 2006; Xu *et al.*, 2006; Luik *et al.*, 2008; Park *et al.*, 2009). A visual representation of this is shown in Figure 1.1.

Though the primary function of SOCE is the refilling of ER Ca^{2+} stores, it also acts to initiate several downstream signalling events. The Ca^{2+} microdomains produced by SOCE can locally activate specific Ca^{2+}-dependent adenylyl cyclases (Willoughby *et al.*, 2010), or promote gene transcription via nuclear factor of activated T cells (Kar *et al.*, 2011). The ER-PM junctions that act as sites for SOCE are therefore critical for both refilling of the ER Ca^{2+} store and as platforms for downstream signalling cascades (Luik *et al.*, 2006; Lewis, 2007; Lee *et al.*, 2010; Carrasco & Meyer, 2011).

Figure 1.1 STIM translocation upon ER Ca^{2+} store depletion. STIM in resting conditions has Ca^{2+} bound at its EF hand (1). When stores are depleted, this Ca^{2+} is lost and STIM oligomers form (2). These oligomers translocate to ER-PM junctions where they activate Ca^{2+} channels consisting of Orai proteins (3). The aggregation of positive charges in the cytosolic region of STIM are thought to attract STIM oligomers to the negatively charged PM phospholipids. ER: endoplasmic reticulum; PM: plasma membrane; STIM: stromal interaction molecule.

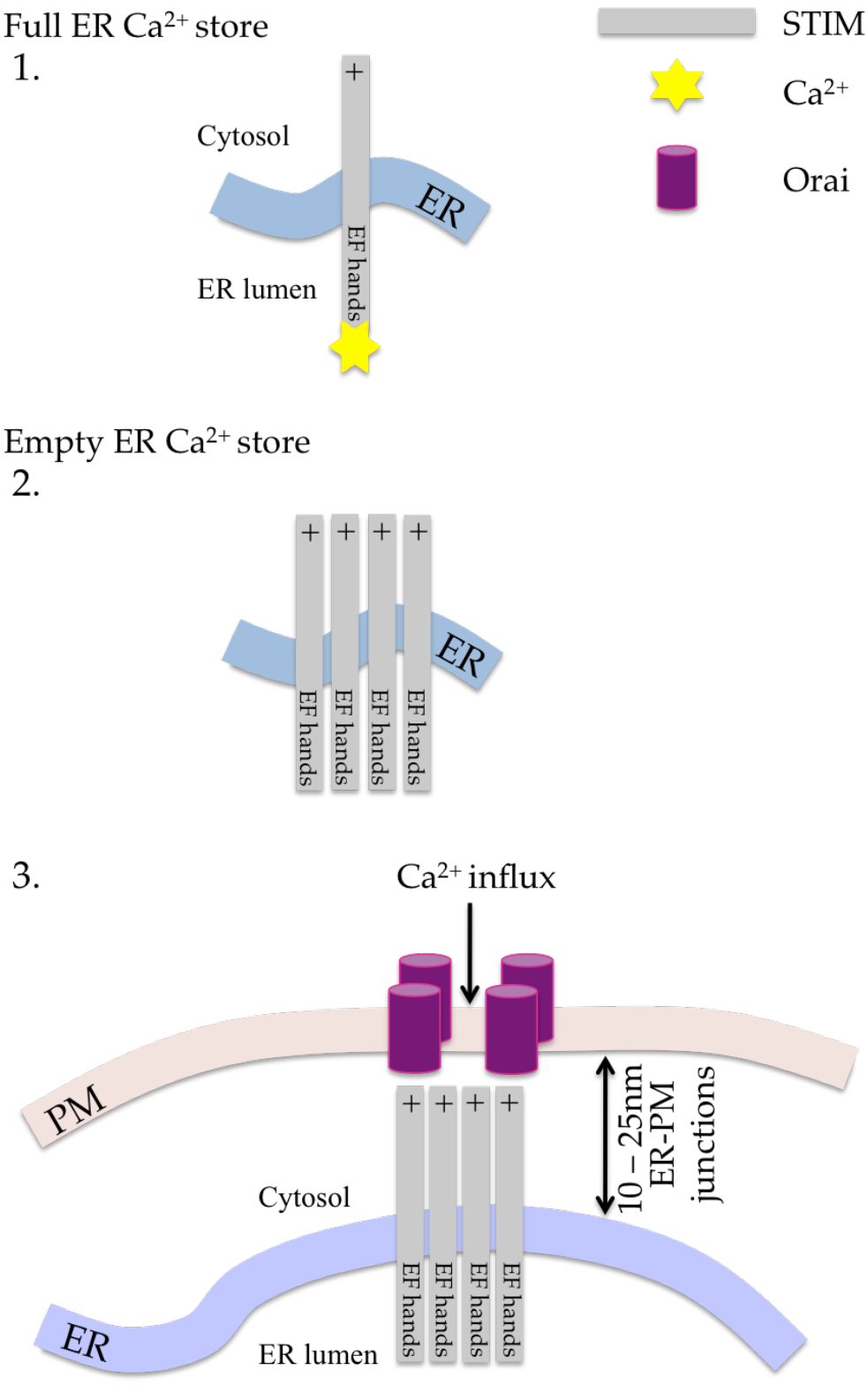

Figure 1.1 STIM translocation upon ER Ca^{2+} store depletion.

1.1.5 ER-PM junctions

ER-PM junctions act as the sites for SOCE and other forms of Ca^{2+} influx. One of the earliest EM images of ER-PM junctions was produced in 1957 using striated muscle cells (Porter & Palade, 1957). Discovery of the ER-PM junctions in these cells was quickly followed by identification of junctions in several other cell types (Engstrom, 1958; Fawcett & Revel, 1961; Reger, 1961; Rosenbluth, 1962; Brandt *et al.*, 1965; Franzini-Armstron, 1974). Several key characteristics of the ER-PM junctions defined at this early stage included a gap between the two membranes of ~ 4 – 10 nm, a lack of ribosomes in the space between the two membranes and a higher density of mitochondria near the junctional site (Rosenbluth, 1962). In the cell types used during this investigation – pancreatic acinar cells and PANC-1 cells, relatively little is still known. Several studies have demonstrated both the basic morphology of the pancreatic acinar cell (Bolender, 1974), and the distribution of key organelles (Tinel *et al.*, 1999; Gerasimenko *et al.*, 2002), but not until the recent paper by Lur and colleagues (Lur *et al.*, 2009) had direct investigation of the ER-PM junctions been carried out. To the best of my knowledge, no literature on ER-PM junctions in PANC-1 cells existed (prior to the publication arising from this thesis).

Though research into SOCE-related ER-PM junctions has been an area of heightened activity recently, the best-characterised ER-PM junctions are those found in striated muscle. The junctions here form between the SR and specialised, invaginated regions of the PM (T tubules). The physical link between the two membranes allows changes in membrane potential to activate signalling cascades that lead to activation of Ca^{2+}-release channels in the SR, producing excitation-contraction coupling (Eisenberg & Eisenberg,

1982; Fill & Copello, 2002; Rossi & Dirksen, 2006). Specialised forms of ER-PM junctions are also found in neuronal cells where they function to coordinate the interaction of IP_3Rs with receptors at the PM (Tu *et al.*, 1998).

1.1.6 SOCE junctions

Although the basic components of SOCE complexes are relatively simple, the actual creation and composition of these junctions is complex. SOCE-competent ER-PM junctions consist primarily of Ca^{2+}-free STIM oligomers (sitting in the ER membrane) bound to Orai tetramers (located in the PM), with a ratio of approximately 8 STIM proteins per tetramer (Hoover & Lewis, 2011). The junctions themselves however have several strict structural prerequisites. Similar to as described in 1962, the gap between the two membranes is estimated to be between 10 – 25 nm wide (Wu *et al.*, 2006; Várnai *et al.*, 2007; Lur *et al.*, 2009). The absence of ribosomes between the two membranes has also been reiterated in recent studies, even in those cells that manipulate rough ER to form the ER-PM junctions, such as pancreatic acinar cells (Lur *et al.*, 2009). These cells secrete large amounts of digestive enzymes and therefore require a large amount of rough ER to cope with the demand for protein production. In this highly polarised cell type SOCE occurs at the basolateral region, a region in which rough ER is predominant (Lur *et al.*, 2009). To form ER-PM junctions with a sufficiently small gap between the two membranes as to enable STIM-Orai binding, the ribosomes are stripped from the ER membrane facing the PM, whilst those on the opposing side of the organelle (i.e. facing the cytoplasm) remain (Lur *et al.*, 2009). The removal of ribosomes from the membrane is not the only structural reorganisation that the ER must perform – proteins containing the KDEL signal sequence

(such as BiP) are also excluded from the ER at sites of ER-PM junctions, by an as yet unknown mechanism (Orci *et al.*, 2009).

An additional structural requirement for ER-PM junctions is an increased density of mitochondria in regions surrounding the junctions, via a mechanism potentially dependent on mitochondrial-ER tethers (Csordas *et al.*, 2010). Mitochondria have been suggested to play several roles in the regulation of SOCE (Hoth *et al.*, 1997; Parekh, 2003; Barrow *et al.*, 2008; Parekh, 2008; Walsh *et al.*, 2009; Singaravelu *et al.*, 2011). Even before activation of Orai channels, mitochondria (especially subplasmalemmal mitochondria) are thought to regulate the translocation of STIM to ER-PM junctions (via mitofusin2) (Singaravelu *et al.*, 2011). ATP or reactive oxygen species produced by the mitochondria have also been suggested to regulate SOCE (Bogeski *et al.*, 2010).

The ER-PM junctions themselves consist of other proteins aside from their basic components, and the number of reported participants is growing rapidly. One of the best-defined additional members are the SERCA pumps, mentioned previously as a mechanism for refilling ER Ca^{2+} stores. These pumps create a pathway by which external Ca^{2+} entering through Orai channels can reach the ER lumen (to refill the store) and are thought to concentrate near ER-PM junctions and SOCE complexes (Jousset *et al.*, 2007). This localisation should help buffer the local Ca^{2+} influx, helping to shape local Ca^{2+} microdomains and prevent premature Ca^{2+}-dependent inhibition (CDI) of SOCE, a mechanism whereby Ca^{2+} itself inactivates Orai channels (Mullins *et al.*, 2009). The exact positioning of the pumps is not fully determined, but evidence suggests that they encircle the STIM-Orai complexes and do not directly interact (Manjarres *et al.*, 2010), based on both

the close proximity of the pumps with STIM and Orai, and the inability of FRET protocols to pick up an interaction between SERCA and either STIM or Orai.

Other proteins thought to be present at SOCE complexes and to regulate SOCE include junctate (Treves *et al.*, 2004; Srikanth *et al.*, 2012), partner of STIM (POST) (Krapivinsky *et al.*, 2011), Golli (Walsh *et al.*, 2010b), CRACR2A (Srikanth *et al.*, 2010) and effectors of the downstream cAMP signalling cascade (Lefkimmiatis *et al.*, 2009), all of which must be correctly positioned and co-ordinated by the cell to appropriately regulate or be regulated by SOCE at ER-PM junctions.

The complexity of ER-PM junctions and the large array of proteins and structures involved suggest that creating an ER-PM junction is not a simple, easily reversible process for cells. There are still debates ongoing as to how and when ER-PM junctions form, especially as to whether they form upon depletion of the ER Ca^{2+} store, or are consistently present but only activated after store-depletion. EM studies of pancreatic acinar cells showed that store-depletion does not increase the number of junctions present in these cells (Lur *et al.*, 2009), whilst studies looking at the locations of junctions during repeated, cyclical store-depletion (i.e. involving shuttling of STIM in and out of junctions) indicated that STIM was translocating back and forth to the same junctions (Smyth *et al.*, 2008). Evidence for the creation of junctions upon store-depletion includes a study using Jurkat cells that showed translocation of STIM to ER-PM junctions that formed upon store-depletion as well as to pre-existing junctions (Wu *et al.*, 2006). The existence or non-existence of pre-formed junctions may well be a cell-type dependent phenomenon.

No research to date has suggested how pre-formed or newly formed junctions may behave in migrating cells. As ER-PM junctions are structures present at the interface between two organelles, the dynamics of both structures affects the dynamics of the junctions. The ER network is a very motile and dynamic structure, undergoing constant movement, expansion and shrinking. Its dynamics are mostly mediated via the microtubular network, and it can travel and expand by either sliding along non-motile microtubules with the aid of motor proteins, or attaching to polymerising microtubules and using the growth of the microtubules as a means of expansion (Baba *et al.*, 2006; Borgese *et al.*, 2006; Friedman *et al.*, 2010). The plasma membrane also undergoes much rearrangement during processes such as endocytosis and cell migration, mostly regulated by actin-associated proteins and phosphoinositides (PIs) (Saarikangas *et al.*, 2010). How ER-PM junctions cope with this ever-changing membranous landscape is yet to be reported in current literature and Video 1.1 depicts two potential mechanisms for the formation of ER-PM junctions in migrating cells investigated during my studies: sliding junctions and saltatory junction formation. Junction sliding would involve the rearrangement of preformed junctions as the cell migrates forwards, to redistribute to new positions. The saltatory formation of junctions would entail the continual formation of new junctions in new locations as the cell migrates, and the dissolution of old junctions as they become physiologically irrelevant.

1.2 Cell migration

1.2.1 Overview

Movement of cells is an essential process, vital during organ development, immunological responses and tissue remodelling. Cell migration also plays a central role in pathophysiological responses; 90% of all cancer deaths are due to an unregulated spread of cells throughout the body ('metastasis'), a process heavily reliant on cells migrating from the primary tumour site to a secondary site elsewhere in the body (Gupta & Massague, 2006).

There are a multitude of interconnected signalling pathways and cascades involved in making a cell move. Essentially a cell must polarise, make projections at the leading edge and form attachments to the substrate, propel itself forwards by these attachments and retract its trailing edge. These forward projections generally take the form of either a broad sheet of cell membrane (lamellipodia), or narrower projections (filopodia), and whilst both these processes involve rearrangement of the actin network, the specific mechanisms involved in making these two structures are different and distinct (Ridley *et al.*, 2003). Migration can be a random process, or can be stimulated by chemicals in the external environment. Migration in response to external stimuli that induces migration towards the source is called chemotaxis; stimulation of migration without provision of directional cues is called chemokinesis (Petrie *et al.*, 2009).

1.2.2 Cell polarity

To migrate, a cell must first become polarised. If chemotaxis is induced by an external stimulus, a concentration gradient of the chemoattractant will form along the length or breadth of the cell, as the side of the cell nearest the source will experience a higher concentration than the opposing side. The

difference in concentration from one side to the other can be relatively small; certain cells have been shown to respond to a < 1% difference in concentration (Mato *et al.*, 1975). Once a cell has detected this difference, changes in morphology and positive feedback loops help to amplify small differences in chemoattractant gradients to promote cell asymmetry (Srinivasan *et al.*, 2003).

1.2.3 Actin polymerisation

The major structural component in cell migration is the actin network, which forms the foundation of filopodia, lamella and lamellipodia (Ingram, 1969; Abercrombie *et al.*, 1970). It also provides the vital framework by which the cell contracts against attachments to allow propulsion. Actin filaments (F-actin) are polarised, dynamic scaffolding structures made up of actin monomers (G-actin), which undergo continuous growth and shrinking phases through polymerisation and depolymerisation respectively. Actin polymerisation itself is a relatively simple process – G-actin binds preferentially to the barbed end of actin filaments. Complexity is introduced however, because there are very many regulatory proteins involved in this process, regulating actin dynamics via processes including capping and cross-linking of actin filaments, coupling of filaments to the external substrate, sequestration of G-actin subunits and modulation of the association and dissociation of actin monomers (Borisy & Svitkina, 2000).

Polymerisation of actin at the cell edge can push against the plasma membrane and create protrusions, in which attachments to the substrate (focal complexes and the more developed and larger focal adhesions) can form. A branched network of actin at the leading edge creates lamellipodia, and is heavily dependent on the Arp2/3 protein complex, which mediates

the formation of actin filament branches protruding off existing filaments at a 70º angle (Mullins *et al.*, 1998). The Arp2/3 protein complex is itself regulated by proteins from the Wiskott-Aldrich syndrome protein (WASP) and WASP family verprolin-homologous (WAVE) protein families (Higgs & Pollard, 2001).

Filopodia are long finger-like projections that protrude from the leading edge of cells. These are formed by long bundles of actin filaments, the production of which is stimulated by the protein Cdc42 (Nobes & Hall, 1995).

1.2.4 Focal adhesions

Structures at the specific sites at which a cell attaches to the extracellular environment were first described in 1971 by Abercrombie et al., who visualised these structures using EM (Abercrombie *et al.*, 1971); the distance between the PM and the substrate at these sites is ~ 10 – 15 nm (Zamir & Geiger, 2001). Attachments are mediated by focal adhesions and focal complexes, a family of protein complexes created from a pool of over 50 proteins (Webb *et al.*, 2002). These attachments provide the anchorage by which the actin network connects to the substrate and a cell can create traction to pull itself forwards.

Integrins mediate the physical attachment of the cell to the outside environment, and consist of a large extracellular domain and a much smaller cytoplasmic domain. Activation of integrins by extracellular substrates induces clustering and initiates the formation of focal complexes (Giancotti & Ruoslahti, 1999). Focal complexes can subsequently either undergo fast turnover (as is often the case during rapid migration) or mature into focal adhesions, which provide a more stable attachment to the extracellular environment (Webb *et al.*, 2002).

1.2.5 Ras GTPases

Several members of the Ras superfamily of proteins are critical in cell migration. This superfamily of GTPases (GTP: guanosine triphosphate) consists of molecular switches that are active when bound to GTP and inactive when bound to guanosine diphosphate (GDP). They are activated by guanine nucleotide exchange factors and inactivated by GTPase-activating proteins. Although there are six main groups of Ras proteins, the Rho family are most important in cell migration – in particular Rho, Rac and Cdc42 (Etienne-Manneville & Hall, 2002).

Both Cdc42 and Rac can be found at the leading edge of cells. Cdc42 is highly active at the very tip of migrating cells; the activity of Rac is highest immediately behind the region of Cdc42 peak activity (Kraynov *et al.*, 2000; Itoh *et al.*, 2002). Rac promotes the formation of actin-rich protrusions by stimulating actin polymerisation and formation of adhesion complexes at the leading edge of cells (Ridley *et al.*, 1992). Cdc42 stimulates the formation of filopodia (Nobes & Hall, 1995) and is heavily involved in the development of polarity, which a cell requires to migrate towards a stimulus. Whilst knockdown of Cdc42 does not prevent migration, it does prevent directionally persistent migration towards a chemoattractant (Allen *et al.*, 1998). Cdc42 also guides the localisation of the microtubule organising centre and Golgi to locations in front of the nucleus in a migrating cell (Ridley *et al.*, 2003). Rho accumulates at the rear ('trailing') edge of a migrating cell, and is responsible for stimulating tail retraction by promoting myosin-mediated contraction (Yamazaki *et al.*, 2005).

1.2.6 Calcium in cell migration

Many of the proteins involved in migration are Ca^{2+}-dependent (Wei *et al.*, 2012). Furthermore, recent studies have demonstrated an importance for both Ca^{2+}, and more specifically SOCE, in cell migration. Ca^{2+} gradients in migrating cells run from low at the leading edges to high at the cell rear (Brundage *et al.*, 1991), whilst Ca^{2+} flicker activity displays the reverse gradient (i.e. increased flicker activity at the front of cells (Wei *et al.*, 2009)). Interestingly, when turning, cells experience a general increase in $[Ca^{2+}]_c$ and a rearrangement of the global Ca^{2+} gradient prior to any visual changes in cell morphology (Brundage *et al.*, 1991). Ca^{2+} flicker activity also increases at the new leading edge and helps to steer cells (Wei *et al.*, 2009). Ca^{2+} pulses at the leading edge of cells cause local actin retraction, and (as a consequence) strengthening of surrounding focal adhesions (Tsai & Meyer, 2012). Schematics showing the distribution of Ca^{2+} gradients, flickers, actin and focal adhesions (in migrating cells and at the leading edge) are shown in Figure 1.2A & 1.2B.

Figure 1.2 Ca^{2+} signalling, actin network and focal adhesions in a migrating cell. A migrating cell has a specific polarity with regards to structural and signalling components. Figure 1.2A shows a general schematic of a migrating cell; Figure 1.2B shows a more detailed schematic of the leading edge of a migrating cell.

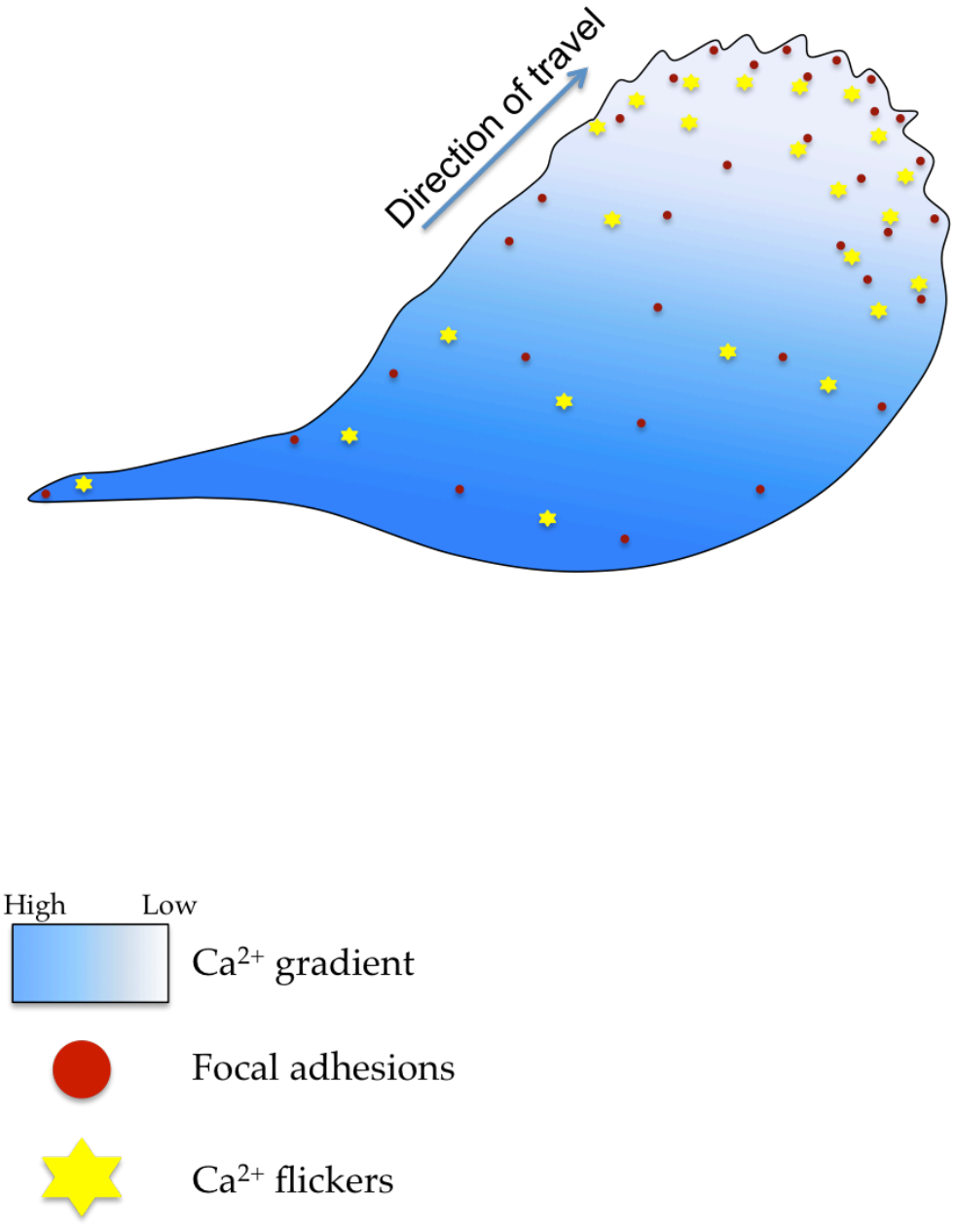

Figure 1.2A Ca^{2+} signalling, actin network and focal adhesions in a migrating cell.

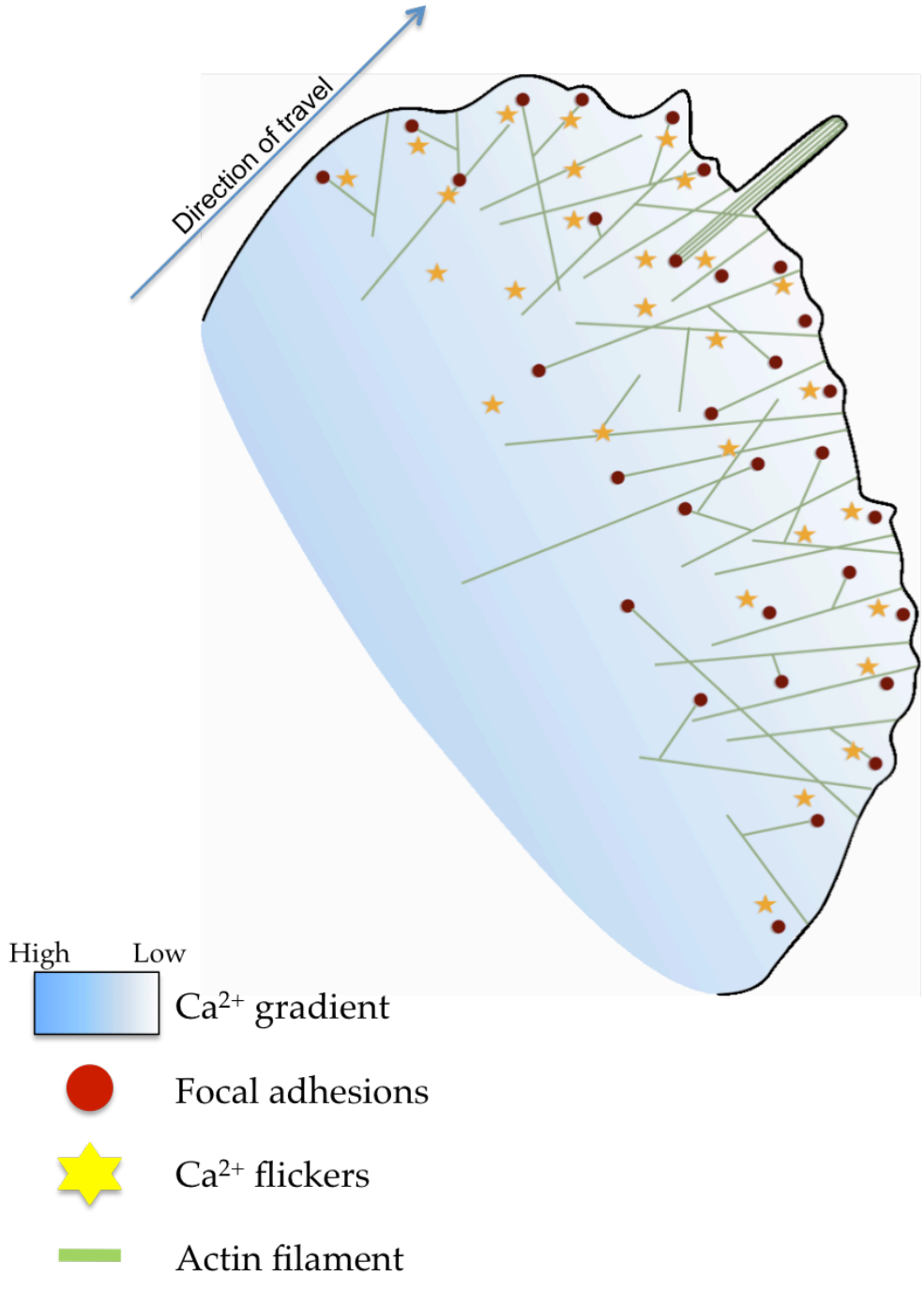

Figure 1.2B Ca^{2+} signalling, actin network and focal adhesions in a migrating cell.

Particularly relevant to this investigation are the findings that inhibition of SOCE can inhibit the migration of cells (Yang *et al.*, 2009), and that knockdown of several of the elements of SOCE can affect migration and focal adhesion turnover (Schafer *et al.*, 2012). An as yet unanswered question however, is how ER-PM junctions (i.e. the sites of SOCE) are actually distributed in migrating cells to mediate these effects, and how this distribution is maintained as the cell migrates.

1.2.7 Caveolae in SOCE and cell migration

Lipid rafts are plasma membrane structures that have long been thought of as platforms for intracellular signalling events, anchoring together proteins to produce signalling microdomains that increase the likelihood of protein-protein interactions. Caveolae are a specific type of lipid raft enriched in the protein caveolin, which manifest as relatively small (50 – 100 nm) invaginations of the plasma membrane (Fujimoto *et al.*, 1998).

Although Orai1 is vital for SOCE, there have also been many reports indicating that TRP channels can form a store-operated channel with STIM1; this complex is suggested to be highly dependent on lipid rafts. STIM1 is reported to localise to lipid raft domains with TRP channels after store depletion and disruption of these domains by reducing cholesterol was shown to diminish SOCE by preventing STIM1 translocation to ER-PM junctions (Lockwich *et al.*, 2000; Alicia *et al.*, 2008; Pani *et al.*, 2008; Pani & Singh, 2009). Expressing an exogenous caveolin with a mutated anchoring domain also reduced SOCE (Brazer *et al.*, 2003).

Caveolin is highly polarised in migrating cells, localising to the cell rear (Beardsley *et al.*, 2005); interactions have also been seen between caveolin and specific subsets of integrins (Wary *et al.*, 1998). Work with caveolin-1

knockout mice has indicated that it is essential for the development of a polarised phenotype, and that cells lacking caveolin-1 are incapable of migrating persistently in one direction. More specifically, they also show an accelerated turnover of focal adhesions (leading to a decrease in their size), effects rescued by expression of a constitutively active Rho protein (Grande-Garcia *et al.*, 2007). Intriguingly, this is opposite to the effects seen when SOCE was inhibited in the same cell type (murine embryonic fibroblasts: MEFs). In those experiments, focal adhesion turnover is drastically slowed (leading to the development of large focal adhesions), an effect that rescued by expression of a constitutively active Ras mutant (Yang *et al.*, 2009).

1.3 Ca^{2+} signalling in pancreatic acinar cells

1.3.1 Overview

The exocrine pancreas is responsible for the secretion of digestive enzymes, the precursors of digestive enzymes and a bicarbonate-rich fluid, all of which travel via the pancreatic duct to the duodenum where they play a vital role in digestion. Pancreatic acinar cells produce these enzymes, their precursors, and a Cl^--rich solution. These cells are present in the exocrine pancreas as clusters of cells called acini. Acini resemble a bunch of grapes, in which every acinar cell of the 'bunch' is connected to a pancreatic duct. Due to the highly catalytic nature of digestive enzymes, the cell packages these and their precursors into zymogen granules, and enzyme activation usually only occurs once they have reached their intended destination (i.e. the duodenum) to prevent autodigestion (Yule, 2010).

1.3.2 Ca^{2+} signalling

Acinar cells are highly polarised cells; zymogen secretion occurs from the apical side (the side connected to the duct), whilst stimulation of secretion occurs at the basal and lateral regions, regions packed with a high density of rough ER (Bolender, 1974). Secretion is tightly regulated by Ca^{2+} signals. These signals are stimulated by activation of PM receptors for acetylcholine or cholecystokinin, which leads to production of IP_3 (in turn stimulating IP_3Rs – IP_3R2 and IP_3R3 are the functionally relevant IP_3Rs in pancreatic acinar cells (Futatsugi *et al.*, 2005)) and release of Ca^{2+} from the ER (Yule, 2010). Notably, if below a certain threshold, cytosolic [Ca^{2+}] transients are apically restricted, even though the PM receptors and sites of IP_3 production are found basolaterally (Ashby *et al.*, 2002). Furthermore, the 'mitochondrial belt' present in pancreatic acinar cells helps to restrict many of the Ca^{2+}

signals apically, preventing global Ca^{2+} waves from traversing the entire cell (though this form of Ca^{2+} signal can also occur)(Tinel *et al.*, 1999). The spatially precise Ca^{2+} signals present in acinar cells are also achieved partially by the localisation of IP_3 receptors, which are located only in the apical ER in this cell type. Ca^{2+} release may also occur from zymogen granules, organelles tightly packed into the apical region (ready for secretion), which contain a high Ca^{2+} concentration (in total ~ 15 mM) and on which IP_3Rs are present (Gerasimenko *et al.*, 1996; Petersen & Tepikin, 2008).

The PMCA in pancreatic acinar cells is highly efficient at extruding Ca^{2+} during Ca^{2+} signalling events and thus the pancreatic acinar cell needs a mechanism whereby Ca^{2+} lost from the ER can be replaced; this is achieved via SOCE. In pancreatic acinar cells, STIM translocation upon store-depletion is specific to the basolateral membrane, providing distinct and discrete regions for Ca^{2+} entry and Ca^{2+} release (Lur *et al.*, 2009).

1.4 Aims

The primary aim of this investigation was to study ER-PM junctions in polarised and migrating pancreatic cancer cells. I aimed to determine both the distribution and dynamics of ER-PM junctions in migrating cells, and their relationship to other proteins integral to migration. I also aimed to further the understanding of the distribution of SOCE-competent ER-PM junctions in pancreatic acinar cells.

Chapter 2: Materials and Methods

Chapter 2: Materials and Methods

2.1 Materials

2.1.1 General reagents and equipment for pancreatic cancer cell culture and transfection

Dulbecco's Modified Eagle Media (DMEM), heat inactivated foetal bovine serum (FBS), PenStrep Glutamine (PSG; 100 x) and 0.05% trypsin ethylenediaminetetraacetic acid (EDTA) were all purchased from Invitrogen (Paisley, UK). Dulbecco's phosphate buffered saline (DPBS) was purchased from Sigma-Aldrich (Gillingham, UK). Cell culture flasks (25 cm^2) were purchased from Corning (Buckinghamshire, UK). The cell culture incubator was purchased from Wolf Laboratories (York, UK) and Promofectin was purchased from Promokine (Heidelberg, Germany).

2.1.2 Constructs

Both the CMV-YFP-STIM1 and mCherry-Orai1 constructs used in this investigation were produced previously by the laboratory in collaboration with L. Haynes (University of Liverpool, UK), as described previously (Chvanov *et al.*, 2008). Orai1 mCherry and myc-tagged Orai1 were inserted into adenoviral vectors by Vector Biolabs (Pennsylvania, USA). LifeAct-TagRFP (RFP: red fluorescent protein) was purchased from Ibidi (Martinsreid, Germany). Several of the constructs used were obtained from the online plasmid repository Addgene. These constructs were amplified upon receipt using a HiSpeed Plasmid Maxi Kit (Qiagen, UK) after recovering the construct via Addgene's instructions. These constructs

included: YFP-STIM1-ΔK (Addgene plasmid 18861), a construct in which a stop codon was inserted prior to the lysine rich polybasic region of STIM1 at its C terminal (stop codon inserted at position 671; (Liou *et al.*, 2007)); and YFP-STIM1(D76A) (Addgene plasmid 18859), in which aspartate 76 in the luminal EF hand of STIM1 was mutated to an alanine (Liou *et al.*, 2005). Other constructs were kind gifts from different sources – T. Balla (NIH, Maryland, USA) kindly provided TK-YFP-STIM1 (a wild-type (WT) STIM1) and the rapamycin-inducible linkers (see Section 2.2.7) (Várnai *et al.*, 2007). The STIM1(NN) mutant was a kind gift from L. Haynes, and was constructed using standard molecular biology procedures and based on the construct described previously (Honnappa *et al.*, 2009) in which isoleucine 644 and proline 645 were both mutated to asparagine residues. A comparison of the different STIM1 mutants used in this investigation is shown in Figure 2.1.

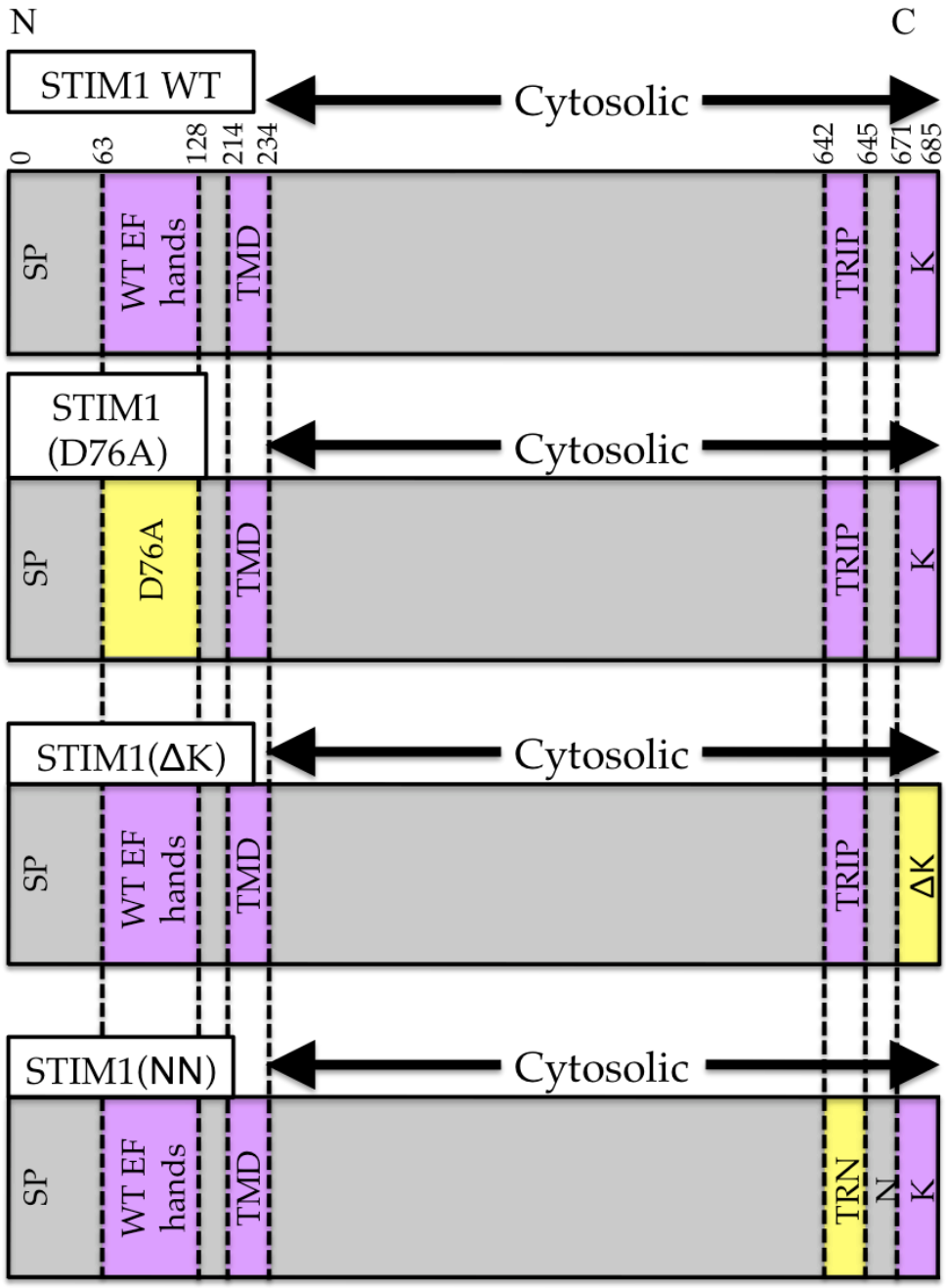

Figure 2.1 Schematic representation of the structure of STIM1 WT and mutated constructs. The different constructs used are shown with the mutated regions highlighted in yellow. K: polybasic region; SP: signal peptide; TMD: transmembrane domain; TRIP: amino acid sequence essential for microtubule binding; WT: wild-type. N and C termini are shown.

2.1.3 Reagents for isolation and overnight maintenance of pancreatic acinar cells

A Na^+-HEPES (4-(2-hydroxyethyl)-1-piperazineethanesulphonic acid)-based solution containing (in mM): 140 NaCl, 4.7 KCl, 10 HEPES, 1 $MgCl_2$, 10 glucose, 1 $CaCl_2$ and adjusted to pH 7.3 using NaOH was used as the extracellular solution. Chromatographically purified collagenase CLSPA was obtained from Worthington Biochemical Corporation (New Jersey, USA). Acinar cell culture media (ACCM) consisted of extracellular solution with added 1 x minimum essential media (MEM) amino acids, 292 μg/ml L-glutamine, 100 units/ml penicillin, 100 μg/ml streptomycin, 1 mg/ml trypsin inhibitor and 2.5 pM sulphated cholecystokinin (CCK)-8 octapeptide (Tocris, Bristol, UK) (the addition of CCK to ACCM is essential for ensuring the continued basal activity of pancreatic acinar cells. The concentration added is marginally higher than the circulating plasma concentration in mice, reported to be approximately 1.2 pM (Tashiro *et al.*, 2004)). This was then adjusted to pH 7.4 using NaOH and sterilised by filtering through a Minisart single use filter unit (Sartorius Stedim Biotech, Aubagne, France) before use. Polycarbonate tubes (15 ml) were purchased from Sarstedt (Leicester, UK) and 70 μm cell strainers were purchased from BD Biosciences (California, USA).

2.1.4 Immunocytochemistry

The antibody against the inositol 1,4,5 trisphosphate receptor type 2 (IP_3R2) (rabbit; against the N terminal) was a kind gift from D. Yule (University of Rochester, Rochester, USA). The antibody against the external epitope of Orai1 (rabbit) was a kind gift from S. Feske (New York University, USA). Anti-caveolin-1 (rabbit) and anti-α-tubulin (clone DM1A; mouse) were purchased from Abcam (Cambridge, UK). Anti-green fluorescent protein

(GFP) (rabbit and chicken) was purchased from Invitrogen. Anti-β-actin (clone AC-15; mouse), anti-calnexin (rabbit) and anti-vinculin (clone hVIN-1; mouse) were purchased from Sigma-Aldrich. All primary antibodies with no clone information were polyclonal. Secondary antibodies were all species-appropriate Alexa Fluor® -conjugated secondary antibodies purchased from Invitrogen.

ProLong Gold, wheat germ agglutinin (WGA) 488 and phalloidin 647 were all purchased from Invitrogen. Paraformaldehyde (PFA) was purchased from Agar Scientific (Essex, UK) and goat serum, bovine serum albumin (BSA), acetylated BSA and Triton-X were all purchased from Sigma-Aldrich. Phosphate buffered saline (PBS) used for immunocytochemistry contained (in mM): 137 NaCl, 2.7 KCl, 10 Na_2PO_4 and 1.8 KH_2PO_4, at pH 7.4.

2.1.5 Chemicals

Thapsigargin (TG) and rapamycin were purchased from Calbiochem (Nottingham, UK). Cyclopiazonic acid (CPA) was purchased from Tocris. All other chemicals were purchased from Sigma-Aldrich unless otherwise stated.

2.2 Methods

2.2.1 Pancreatic cancer cell culture and transfection

PANC-1 cells were obtained from the American Type Culture Collection (ATCC; CRL-1469); these are cells derived from a human pancreatic ductal adenocarcinoma (Lieber *et al.*, 1975). They were cultured in DMEM supplemented with 10% FBS, 100 units/ml penicillin, 100 μg/ml streptomycin and 292 μg/ml glutamine. Cells were passaged 2 – 4 times a week (at ~ 70% confluency) by removing the culture media, rinsing with

DPBS, adding 0.6 ml 0.05% trypsin EDTA and allowing the cells to detach. Detached cells were then resuspended in 10 ml full media, centrifuged and the resulting pellet resuspended in the appropriate volume of media. The cells were then plated into fresh flasks at a ratio of ~ 1:2.

DMEM with no Ca^{2+} (Invitrogen) was used as the basal media for experiments requiring a reduced Ca^{2+} concentration in otherwise full media. For imaging experiments, cells were seeded either into 35 mm glass-bottom dishes (Mattek, Massachusetts, USA), or onto coverslips in 6-well plates (Sarstedt) for 24 hours prior to transfection. Cells were transfected at ~ 50 – 60% confluency using Promofectin, using a protocol optimised from the manufacturer's instructions. Briefly, to 100 μl of antibiotic- and serum-free media, either 6 μl of Promofectin or 2 μg DNA was added. These were then vortexed, centrifuged, and combined, before the resulting mixture was once again vortexed and centrifuged. After 20 minutes incubation at room temperature (RT) the mixture was added to the dishes in a drop-wise fashion.

2.2.2 Isolation of pancreatic acinar cells

Male, 6 – 8 week old CD1 mice (obtained from Charles River, Kent, UK) were used unless otherwise stated. Mice were sacrificed by cervical dislocation in accordance with the Animals (Scientific Procedures) Act 1986 and the pancreas dissected out. Extracellular solution was used to briefly rinse the pancreas before it was injected with 1 ml collagenase and transferred into a 1.5 ml tube, and then placed in a shaking water bath (Grant Instruments, Cambridge, UK) at 37 °C and 120 revolutions per minute (rpm). After 15 minutes, the collagenase solution was removed and the tissue disrupted in extracellular solution by pipetting through a 1 ml pipette tip with the last 5

mm removed. The resultant cloudy supernatant was transferred to a 15 ml polycarbonate tube and the same steps repeated several times with the remaining tissue. The supernatant was then spun at 1000 rpm for 1 minute and the pellet resuspended in extracellular solution. Cells were then filtered through a 70 μm cell strainer and the filtrate washed twice by centrifugation. The resulting pellet was resuspended in extracellular solution and plated onto polylysine coated coverslips or into polylysine coated 35 mm glass-bottom culture dishes.

2.2.3 Viral transfection of pancreatic acinar cells

Freshly isolated cells were resuspended in ACCM and plated into polylysine coated dishes or onto polylysine coated coverslips. Cells were transfected with adenoviral vectors by diluting the appropriate volume of virus into 100 μl of ACCM and adding this mixture in a drop-wise fashion to the cells. Cells were then kept overnight in a cell culture incubator kept at 35 $^{\circ}$C, 5% CO_2 and 95% humidity before experiments.

2.2.4 Immunocytochemistry

After treatment, cells were rinsed once with PBS before fixation. Two fixation methods were used for immunocytochemistry experiments – methanol (MeOH) fixation and paraformaldehyde (PFA) fixation; the optimal fixative for each protein of interest was determined by testing both methods. For experiments using MeOH fixation, cells were treated with ice-cold MeOH in a -20 °C freezer for 10 minutes. For PFA fixation, cells were treated for 30 minutes with 4% PFA (diluted in PBS) at RT, rinsed 3 times with PBS (5 minutes each) and permeabilised by treating with 0.1% Triton-X for 5 minutes at RT. The remaining steps were then identical for both fixation methods. Cells were rinsed three more times using PBS, then a blocking

solution consisting of 10% goat serum and 1% BSA in PBS was added to cells for 1 hour at RT. Primary antibodies were then added at the stated dilution in a PBS-based solution containing 5% goat serum and 0.1% acetylated BSA. After 3 more PBS rinses, the appropriate secondary antibodies, diluted in PBS, were added to cells for 20 minutes, followed by 3 more PBS rinses. Where MeOH fixation was used on cells transfected with a fluorescent construct, an antibody against the fluorophore was used during the primary antibody stage to counter the fluorophore bleaching that occurs during this fixation method. Coverslips were then mounted onto 76 x 26 mm microscope slides (Thermo Scientific, Surrey, UK) using ProLong Gold as a mounting media. Where dishes were used, PBS was left in the dishes for imaging. Slightly different staining protocols were used for both WGA and phalloidin staining. WGA is a plasma membrane stain that was added to live cells at 1:200 dilution for 10 minutes at 37 °C. Afterwards, cells were rinsed twice, then fixation was carried out as normal. Phalloidin is a fluorescently-conjugated toxin that binds F-actin (Lengsfeld *et al.*, 1974). When used, it was added during the secondary antibody stage – instead of the primary and secondary steps, phalloidin was applied to cells after the blocking step in PBS at a dilution of 1:50 for 20 minutes, before rinsing and mounting/imaging.

2.2.5 Confocal microscopy

Several different microscopes were used for the different types of experiments. For imaging of fixed immunocytochemistry experiments a Leica acousto-optical beam splitter (AOBS) microscope was used. Unless otherwise specified, the objective used was a 63 x oil immersion objective (numerical aperture (NA): 1.4) and the pinhole set to ~ 1 airy unit.

For overnight, live imaging of transfected PANC-1 cells, a Zeiss laser-scanning microscope (LSM) 710 with a temperature and CO_2 control unit was used. Cells were seeded into glass-bottom dishes, transfected 24 hours later, and imaged the next day at 37 °C, 5% CO_2 unless otherwise stated. Immediately prior to imaging, the media was removed and replaced with (unless otherwise stated) DMEM (with no Ca^{2+}) supplemented with 15 μM CPA (to inhibit the SERCA pump), 10% FBS, 100 units/ml penicillin, 100 μg/ml streptomycin, 292 μg/ml glutamine and Ca^{2+} at concentrations from 0.5 – 1.2 mM depending on the type and number of constructs transfected. The potential toxicity of this concentration of CPA was investigated for PANC-1 cells previously in the laboratory. Briefly, viability was assessed using a SYTOX® Orange probe and Hoechst 33342 combination. Survival of control cells versus CPA treated cells was 114 out of 117 cells, and 106 out of 111 cells respectively. Objectives used were either 40 x oil or 63 x oil objective (NA of 1.3 or 1.4 respectively) and the pinhole set between 1 – 5 airy units. For total internal refection fluorescence (TIRF) microscopy, an Olympus Till Photonics microscope was used, using a 60 x TIRF objective (NA of 1.4).

Several of the experiments required perfusion of different solutions into the cells. This was achieved using a gravity-fed perfusion system consisting of 6 x 10 ml syringes mounted high above the microscope, connected by tubing to a six-way connector, which was then inserted into a perfusion chamber in which the glass-bottom dish was placed. A suction line connected to the perfusion chamber then extracted the fluid. A switch inserted between the syringes and the connecting tubing allowed control of fluid flow from each syringe.

2.2.6 Migration assays

Cells were seeded in Ibidi 35 mm, high μ-Dishes with single culture-inserts (Ibidi). The insert was removed after 48 hours and the treatment initiated. Dishes were imaged at 0 and 24 hours. The area covered by cells in each image was then analysed using WimScratch software (Wimasis, Munich, Germany) and the change between the cell-covered areas at 0 and 24 hours was calculated. Treated dishes in which the initial cell-covered area was more than 20% different from the controls were discarded.

2.2.7 Rapamycin-inducible linkers

The linker constructs (PM-targeted-long linker-FKBP-mRFP (FKBP: FK506-binding protein; mRFP: monomeric RFP) and CFP-FRB-long linker-ER-targeted (CFP: cyan fluorescent protein; FRB: fragment of mTOR that binds FKBP12) constructs) were a kind gift from T. Balla (NIH, Bethesda)(Várnai *et al.*, 2007). Each of the pair of linkers has three main components – a fluorophore, a membrane targeting sequence (either for the endoplasmic reticulum (ER) or the plasma membrane) and either a FKBP or FRB fragment. As shown in Figure 2.2, prior to rapamycin treatment the two constructs diffuse freely in the separate compartments. Upon addition of rapamycin, heterodimerisation of the two constructs forces colocalisation of the two fluorophores, which can then be seen via confocal microscopy.

2.2.8 Image and statistical analysis

Image acquisition and initial image assessment was performed using either Leica LAS, Zeiss Zen or TILLvisION software. Further analysis was carried out primarily using ImageJ (National Institutes of Health, developed by W. Rasband); any plugins/macros used for further image analysis are described in the accompanying text. All image adjustments were linear. ANOVA and

T-tests were used where stated, and $p < 0.05$ was considered significant. N numbers are given in the text relating to the appropriate figure and represent the number of different dishes unless otherwise stated.

Pre-treatment

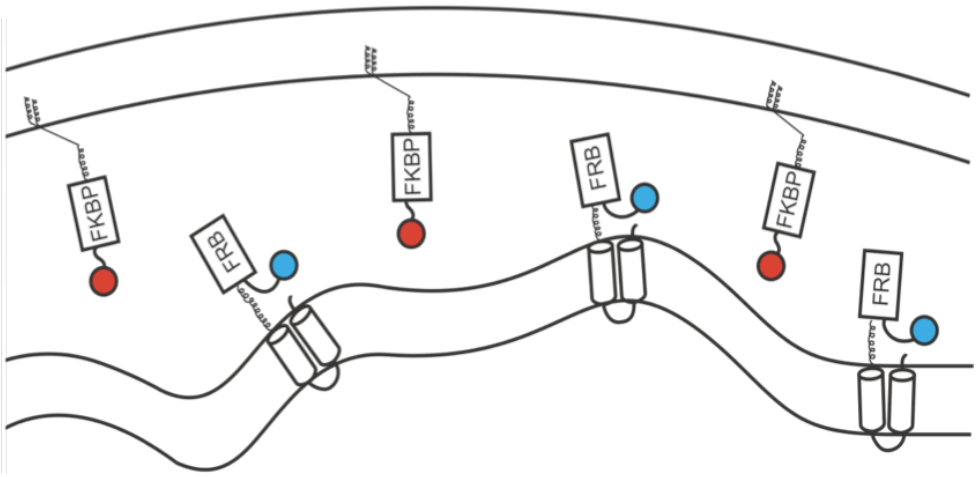

Post-treatment

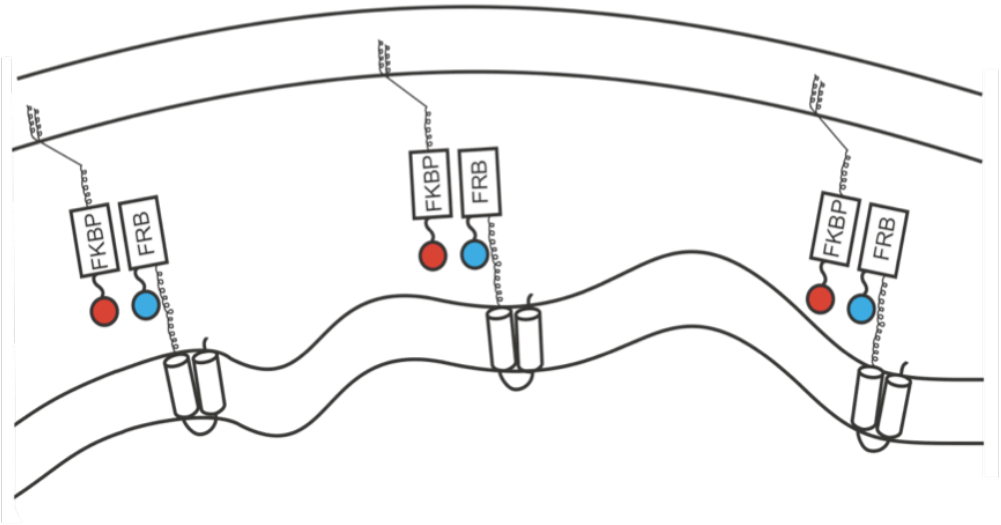

Figure 2.2 Rapamycin induces heterodimerisation of two differentially targeted fragments. Addition of rapamycin induces the formation of a FRB-FKBP complex, which can be identified by co-localisation of the two attached fluorophores. Red circles: monomeric red fluorescent protein; blue circles: cyan fluorescent protein.

Chapter 3: Dynamics of ER-PM Junctions

Chapter 3: Dynamics of ER-PM Junctions

3.1 Overview

STIM1 is a Ca^{2+}-sensing protein found in the ER membrane that travels to ER-PM junctions upon depletion of the ER Ca^{2+}-store. Loss of Ca^{2+} from its EF hand domain (located in the ER lumen) causes the protein to oligomerise and translocate to ER-PM junctions, where SOCE complexes are formed. Here, it activates Orai1 channels located in the plasma membrane, causing influx of Ca^{2+} from the extracellular environment and refilling of the intracellular Ca^{2+} store.

A number of studies have suggested that the sites of the ER-PM junctions that STIM1 translocates to after store-depletion are relatively pre-determined by the cell, indicating that either ER-PM junctions are pre-formed, or that junctions form repeatedly in the same place (Malli *et al.*, 2008; Smyth *et al.*, 2008; Lur *et al.*, 2009; Shen *et al.*, 2011). However, if a cell is migrating the repeated formation of ER-PM junctions at identical sites will (for the most part) not be possible, as the cell membrane of a migrating cell undergoes continuous rearrangement, a process that presumably involves the degradation of junctions between the ER and PM.

The primary aim of this part of the project therefore was to investigate the distribution and dynamics of ER-PM junctions in migrating pancreatic cancer cells. To achieve this, I first needed to develop a method by which ER-PM junctions could be easily identified in live migrating cells. I decided to use a protocol that utilises the translocation of STIM1 to ER-PM junctions after store depletion by employing a fluorescently-tagged STIM1 construct,

depleting internal Ca^{2+} stores, and using the sites of STIM1 puncta as a method for pinpointing ER-PM junctions. Imaging STIM1-transfected store-depleted pancreatic cancer cells over long time periods allowed us to monitor the changing distribution of ER-PM junctions in migrating cells. Faster imaging over shorter time periods allowed us to investigate the dynamics of individual junctions in migrating cells.

Whilst investigating the localisation of ER-PM junctions in migrating cells, I also looked at two possible mechanisms by which ER-PM junctions might be targeted to specific sites in migrating cells: STIM1 binding to phospholipids and the association between STIM1 and microtubules, both of which are introduced below.

3.1.1 The role of phospholipids in the placement of ER-PM junctions

STIM1 contains a C-terminal polybasic lysine-rich region thought to bind negatively charged phospholipids at the PM and encourage translocation of STIM1 oligomers to ER-PM junctions (Huang *et al.*, 2006; Liou *et al.*, 2007; Walsh *et al.*, 2010a). Ca^{2+}-bound STIM1 monomers do not contain enough positively charged amino acids to promote targeting to the PM (Heo *et al.*, 2006; Ercan *et al.*, 2009). Instead, attraction to the PM is achieved by oligomerisation of STIM proteins to induce accumulation of sufficient positive charges; this is only possible after store-depletion and loss of Ca^{2+} from the EF hands of STIM. Deletion of this region is thought to prevent puncta formation of the STIM1 protein, though when expressed in tandem with Orai1, its ability to form puncta reappears (Liou *et al.*, 2007; Park *et al.*, 2009). Phosphoinositides (PIs) are a key constituent of plasma membrane phospholipids and it may be forms of PIs that are required for the membrane targeting of STIM1 after store-depletion, specifically $PI(4,5)P_2$ and $PI(3,4,5)P_3$

(Walsh *et al.*, 2010a; Calloway *et al.*, 2011). These PIs are also well-known for the role they play in cell migration and importantly, are distributed unevenly in polarised migrating cells (Saarikangas *et al.*, 2010). $PI(3,4,5)P_3$ in particular activates (and is activated by) members of the Rho family of GTPases (Srinivasan *et al.*, 2003).

3.1.2 The role of microtubules in the placement of ER-PM junctions

Microtubules are polar structures, consisting of a dynamic 'plus-end' and a more stable minus end. The asymmetrical distribution of microtubules is critical for the development of polarity in migrating cells (Vasiliev *et al.*, 1970; Kaverina & Straube, 2011). Interactions between the ER and microtubules are vital for the reticular distribution of the ER network throughout the cell (Terasaki *et al.*, 1986). One method of ER extension is through tip attachment complexes (TACs), where the ER is extended towards the cell periphery through attachment to a growing microtubule plus-end (i.e. the end of a microtubule undergoing growth through polymerisation (Waterman-Storer *et al.*, 1995)). STIM1 has been shown to play a role in this process through its binding to end-binding 1 protein (EB1) (Grigoriev *et al.*, 2008), an 'adaptor' protein that binds the plus-end of microtubules. In control conditions, STIM1 has been shown to display comet-like dynamics similar to those of EB1; this is abolished after store-depletion as STIM1 translocates into puncta (Baba *et al.*, 2006; Grigoriev *et al.*, 2008; Smyth *et al.*, 2008; Honnappa *et al.*, 2009).

Grigoriev et al. also stated that microtubule dependent ER remodelling might be important for the formation of ER-PM junctions and regulation of SOCE. Nocodazole, an inhibitor of microtubule dynamics can inhibit SOCE, an effect that can be rescued by the overexpression of STIM1. Peculiarly, this

overexpression of STIM1 actually converts nocodazole treatment to an *inducer* of SOCE (Smyth *et al.*, 2007). It seems that at the very least, the two processes – microtubule dynamics and SOCE – are tightly connected and their interaction warrants investigation in the context of cell migration.

3.2 Protocol optimisation

The aim of this investigation was to determine the distribution and dynamics of ER-PM junctions in migrating pancreatic cancer cells. The initial phase of this involved verifying that an exogenously expressed fluorescently-tagged STIM1 protein would function correctly when expressed in a pancreatic cancer cell line. The cell line chosen was the PANC-1 cell line, cells derived from a human pancreatic ductal adenocarcinoma (Lieber *et al.*, 1975). Two main STIM1 constructs were used; the first was a cytomegalovirus (CMV) promoter-driven STIM1 protein tagged with yellow fluorescent protein (YFP) at the C terminus (CMV-STIM1-YFP). This is a convenient construct, as it is extensively tested in this laboratory, but it can only be used for relatively short-term observations (i.e. 2 – 3 hours). I also obtained a construct containing an N-terminally tagged STIM1 protein driven by a thymidine kinase (TK) promoter from Dr Balla's laboratory (TK-YFP-STIM1)(Várnai *et al.*, 2007); this is driven by a slower promoter optimal for prolonged experiments. Complete store-depletion was achieved using either reversible (cyclopiazonic acid; CPA; 30 μM) or irreversible (thapsigargin; TG; 2 μM) inhibitors of the SERCA pumps. These pumps transport Ca^{2+} from the cytosol of the cell back into the ER; when inhibited the constitutive Ca^{2+} leak

from the ER is no longer counterbalanced, and the ER is gradually depleted of its internal Ca^{2+}.

Figure 3.1 shows the distribution of TK-YFP-STIM1 in non-store depleted, and store-depleted conditions. The cell is not store-depleted at time = 0 seconds (start of imaging) and the image shows STIM1 distributed in a reticular fashion throughout the whole cell. After 210 seconds of 2 μM TG treatment, STIM1 had translocated into its characteristic punctate distribution, appearing as small bright spots in the cell. The distribution of the STIM1 protein in both conditions is similar to that shown in previous literature (e.g. (Wu *et al.*, 2006; Liou *et al.*, 2007; Várnai *et al.*, 2007), and so it can be presumed that the TK-YFP-STIM1 construct, when expressed in PANC-1 cells, does indeed function correctly.

Figure 3.1 STIM1 forms puncta in response to store depletion. PANC-1 cells expressing TK-YFP-STIM1 were imaged live whilst being perfused firstly with a standard HEPES-based extracellular solution, then with 2 μM TG in a 0 Ca^{2+}-HEPES-based extracellular solution. TG perfusion was initiated immediately prior to the first image (time = 0s); scale bar represents 10 μm.

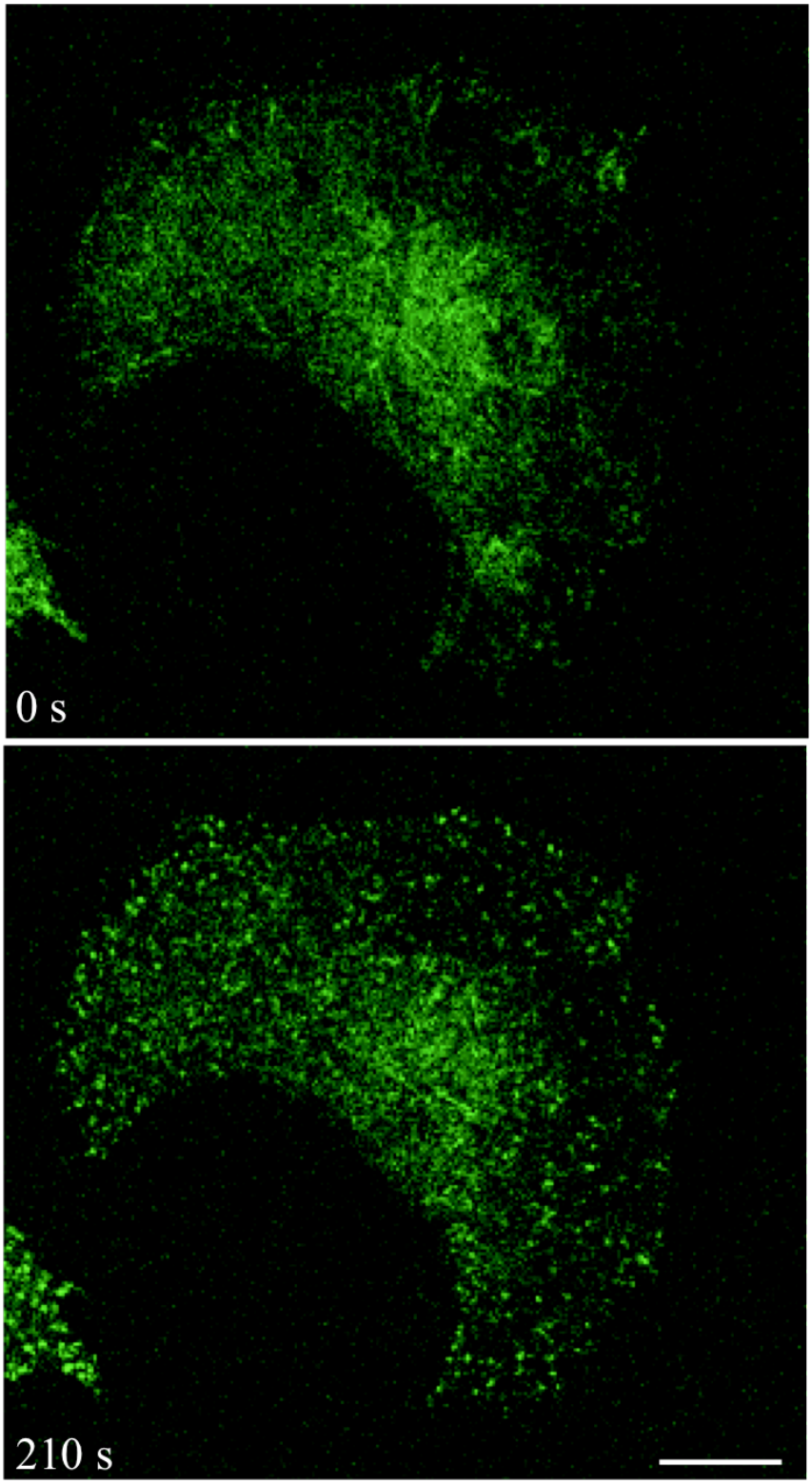

Figure 3.1 STIM1 forms puncta in response to store depletion.

Figure 3.2 shows PANC-1 cells transfected with CMV-STIM1-YFP, treated with 2 μM TG to deplete the ER Ca^{2+} store and imaged live using total internal reflection microscopy (n = 7). With this form of microscopy only cellular structures within 200 nm of the surface of the coverslip can be visualised, whilst those deeper inside the cell are not illuminated (Ambrose, 1956). This figure both verifies the correct functionality of the CMV-STIM1-YFP construct and also illustrates an interesting distribution of STIM1 puncta just behind the cell periphery. Whilst STIM1 puncta can be found throughout a store-depleted cell, in this instance (and many others) there seems to be an accumulation of junctions at the cell periphery, especially concentrated in protrusions at the edge of the cell. This phenomenon was visualised many times throughout this investigation and is discussed further later.

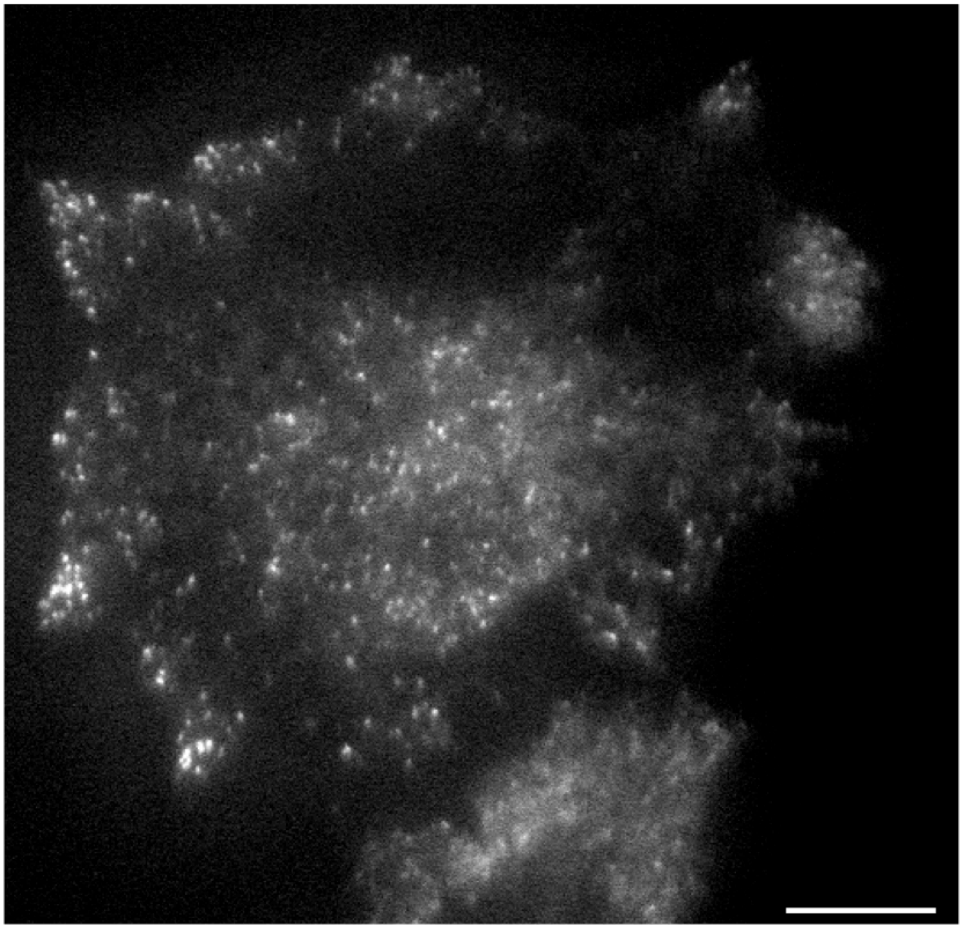

Figure 3.2 Distribution of STIM1 puncta as seen by TIRF microscopy. PANC-1 cells expressing CMV-STIM1-YFP were treated with 2 μM TG in a 0 Ca^{2+}-HEPES-based extracellular solution and imaged live using a TIRF microscope with a 60 x objective. The above image was taken approximately 300 seconds after application of TG.

3.3 Modifying SOCE can inhibit migration of PANC-1 cells

Thus far, I had established that exogenously expressed, fluorescently-tagged STIM1 proteins could form puncta in this cell type. The next step was to determine whether PANC-1 cells were able to migrate in conditions in which STIM1 puncta ordinarily form, i.e. when the internal Ca^{2+} stores were depleted.

A cell migration assay was developed in order to test the effect of different conditions on the migration of PANC-1 cells. The optimised protocol for the assay is shown in Figure 3.3 – 100 μl of freshly resuspended cells were seeded in glass-bottom dishes with specialised inserts (Ibidi) and left for 48 hours to reach confluency. At this time, the insert was removed, leaving a gap of 500 μm +/- 50 μm. The cells were rinsed with PBS and 2 – 3 ml of media (with any additional components being tested) added (Figure 3.3A). Images were taken of the resulting gap (using a 10 x objective) at time 0 and at various further time points (e.g. Figure 3.3B; transmitted images only – cells were not stained with any fluorescent markers). WimScratch software was used to analyse cell migration. This software analyses the cell-covered area (as a percentage of the whole image) in the images obtained (producing images as seen in Figure 3.3C and the values in Figure 3.3D). From this the increase in cell-covered area can be determined and an approximate rate of migration extrapolated.

Figure 3.3 Migration assay protocol. A. Cells were seeded into both sides of the culture insert; 48 hrs later the insert was removed (leaving a gap of 500 μm +/- 50 μm; time = 0 hrs), the cells subjected to different conditions and then the dishes were imaged at 0 and 24 hrs. Pink regions denote where cell media is placed, whilst grey circles show where cells are placed. B. Raw images of control dishes at 0 and 24 hrs. C. Images obtained post-analysis. D. Values obtained of the cell-covered area after analysis of the images in B using WimScratch software.

A.

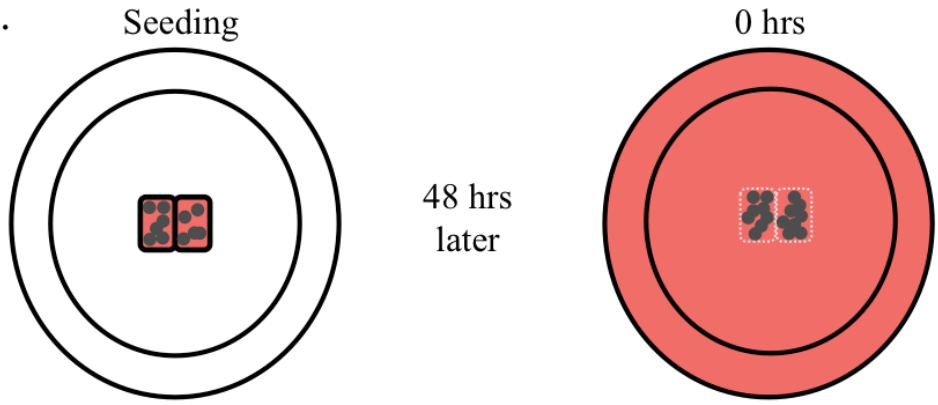

B.

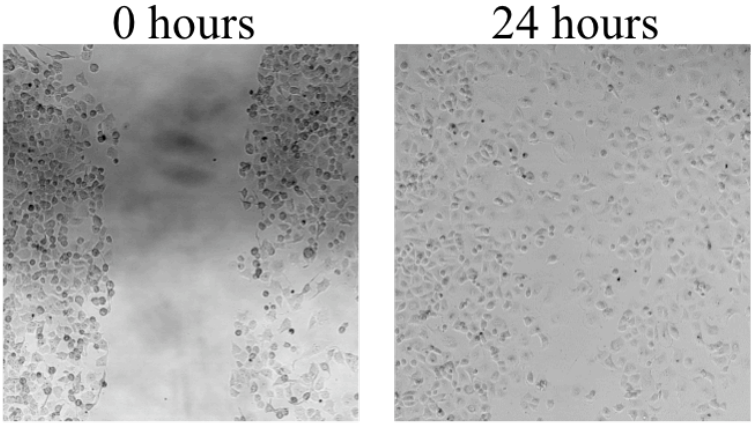

C.

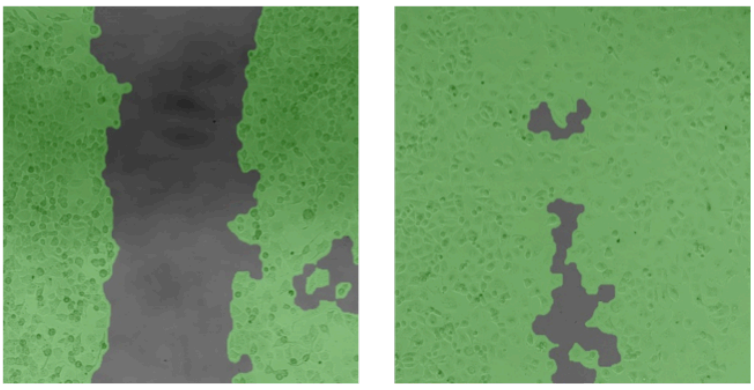

D.

	0 hours	24 hours	Change
Cell-covered area	63.9 %	94 %	30.1 %

Figure 3.3 Migration assay protocol.

Initial optimisation of the migration assay was carried out in a Na^+-HEPES based extracellular solution, however it was found that over longer time periods, PANC-1 cells migrate much better (and seem much healthier – e.g. fewer rounded cells and less cell death) when kept in cell culture media (data not shown).

Store-depletion is ordinarily carried out in nominally Ca^{2+} free conditions, but several previous studies have highlighted the importance of Ca^{2+} for cell migration (Wei *et al.*, 2012), therefore a higher Ca^{2+} concentration than this had to be used to ensure sufficient cell migration. I established that normal DMEM culture media could not be used, as this contains 1.8 mM Ca^{2+}; this level of Ca^{2+} caused Ca^{2+} overload and prevented cell migration in cells that overexpress STIM1 and have continuously active SOCE.

A specialised Ca^{2+}-free DMEM was obtained from Invitrogen as a base for reduced Ca^{2+} conditions to allow us to better control the [Ca^{2+}] used during store-depletion and migration experiments. The addition of 1 mM Ca^{2+} to the basal media was effective in allowing both migration and STIM1 puncta formation in transfected PANC-1 cells, whilst avoiding Ca^{2+} toxicity. As the dishes were placed back in the cell incubator for the duration of the 24 hours after the insert was removed (and only taken out for imaging), additional HEPES-buffering or use of CO_2-independent medias was not required.

Three different time points were tested during optimisation of the protocol: 6, 24 and 48 hours. After 6 hours, little difference could be seen in the percentage cell-covered area, and at 48 hours the cells in the control condition were overconfluent (and the assay therefore saturated). At 24 hours, control cells reached an average of 100% closure (± 5.2%), optimising the range of the assay, so this time point was chosen.

Various conditions were then tested using this protocol (Figure 3.4). As previously shown using murine embryonic fibroblasts (MEFs) (Yang *et al.*, 2009), 50 μM SKF96365 significantly inhibited PANC-1 cell migration compared to control conditions ($p < 0.05$ as determined using two-way ANOVA). Depletion of the intracellular Ca^{2+} store alone (using 30 μm CPA) did not inhibit migration, verifying previous work by Eylenstein et al. which stated that in cells expressing exogenous STIM1 and Orai1, depletion of the intracellular store does not inhibit migration (they actually observed some acceleration of migration)(Eylenstein *et al.*, 2011). Reducing the Ca^{2+} concentration of the media to 1 mM also had little effect on cell migration in cells treated with 30 μM CPA, though the effects of Ca^{2+} overload in non-transfected cells would be much less than in cells overexpressing STIM1/Orai1. The effect of an increased ambient temperature on PANC-1 cell migration was also tested, as this is known to cause translocation of STIM1 to ER-PM junctions (Xiao *et al.*, 2011); migration in these conditions was not found to be significantly different from that of control conditions (for this condition, cells were in identical conditions as the control cells, but were kept at 40 °C instead of 37 °C).

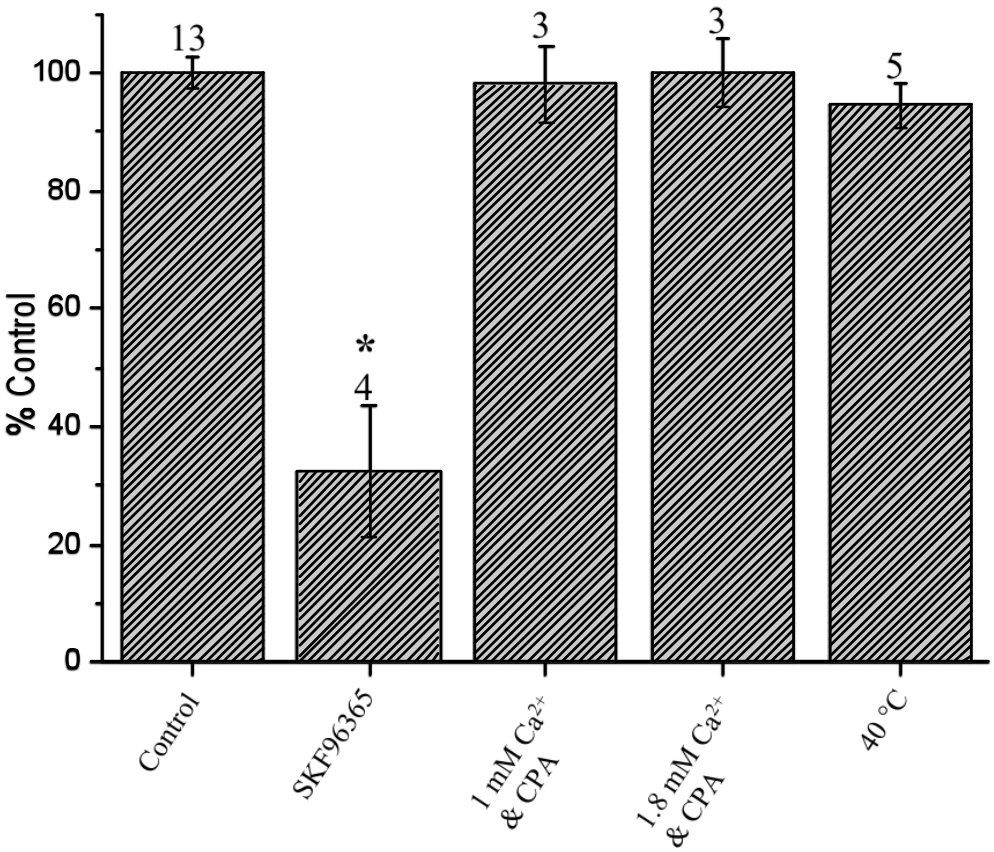

Figure 3.4 Effect of different treatments on the ability of PANC-1 cells to migrate. PANC-1 cells were assessed for their ability to migrate in different conditions using the migration assay protocol described in Figure 3.3. The change in cell-covered area was normalised to that of the average of the controls from the same experimental set. Bars show mean ± standard error of the mean; n numbers are shown above each data set and represent the number of dishes tested for each condition; * = $p < 0.05$.

3.4 ER-PM junctions concentrate at the leading edge of migrating cells

Having established that STIM1 puncta will form in store-depleted PANC-1 cells overexpressing STIM1, and the conditions required to induce this do not impede cell migration, I then further examined the distribution of STIM1 puncta in polarised and/or migrating cells. This was achieved by transfecting cells with the TK-YFP-STIM1 construct, depleting the stores by treating with a reduced concentration of CPA (15 μM) in full media with 1 mM Ca^{2+} and imaging on a confocal microscope overnight (in a chamber with both temperature and CO_2 controlled: 5% CO_2 and 37 °C).

Figure 3.2 has already demonstrated that puncta can accumulate at the periphery of cells; Figure 3.5 demonstrates that this striking phenomenon extends to migrating cells. The four images show a TK-YFP-STIM1 transfected, store-depleted PANC-1 cell at four different time points (with the first image in the series set as time 0), with white arrows showing the direction of movement of the cell at the time of the image. The images show a concentration of STIM1 puncta (i.e. ER-PM junctions) at the leading edge of the cell in each individual image. When a video of all the frames is examined (Video 3.1 on CD), this accumulation of junctions can be seen consistently following the leading edge as the cell migrates.

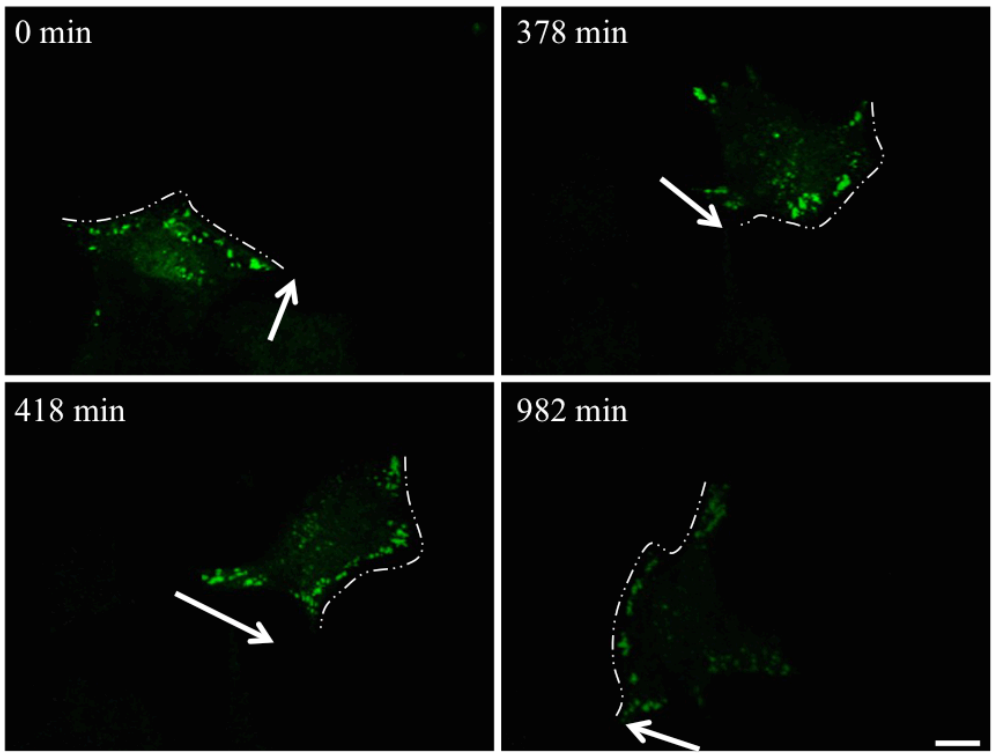

Figure 3.5 There is a concentration of junctions at the cell periphery that follows the leading edge during cell migration. PANC-1 cells expressing TK-YFP-STIM1 were treated with 15 μM CPA to deplete the intracellular Ca^{2+} store, kept in media with reduced Ca^{2+} (1 mM) and imaged on a confocal microscope overnight. Images show the same cell at four different time points (as indicated; relative to start of image series). Arrows show the direction of migration and outlines of the leading edges are highlighted by white dotted lines. Scale bar represents 10 μm. Phenomenon was seen in at least 10 different live imaging experiments.

Another method of demonstrating that the puncta follow the leading edge is by measuring the fluorescence intensity across cellular protrusions as they move forward. Figure 3.6 shows analysis of the puncta dynamics in the cell shown in Figure 3.5. The fluorescent intensity along a line drawn perpendicular to the plasma membrane at the site of a dynamic cellular protrusion (as seen in Figure 3.6B; calculated by using the ImageJ tool 'Plot Profile' and each time point normalised to its maximum intensity) is shown at three different time points. At all three time points the intensity is at background levels outside the cell, sharply increases as it hits the cell periphery, and drops to just over half intensity as it travels into the body of the cell. At 0 minutes, this abrupt increase in fluorescence corresponding to the concentration of puncta just behind the leading edge only starts ~ 7 μm along the line. At subsequent time points, this increase has shifted left, i.e. closer to the start of the line. The sharp drop that occurs as the line enters the main body of the cell also shifts to the left. This indicates that accumulation of puncta at the leading edge is dynamic, i.e. the regions containing a high density of STIM1 puncta have moved.

Figure 3.6 The accumulation of junctions at the cell periphery can be seen moving forward with the leading edge as the cell migrates. PANC-1 cells expressing TK-YFP-STIM1 were treated with 15 μM CPA in media with reduced Ca^{2+} (1 mM) and imaged on a confocal microscope. A. Fluorescent intensity along a line running perpendicular to the cell membrane at three separate time points. B. Images of frames shown in A, with the line used for analysis of fluorescence intensity indicated in white. Scale bar represents 10 μm.

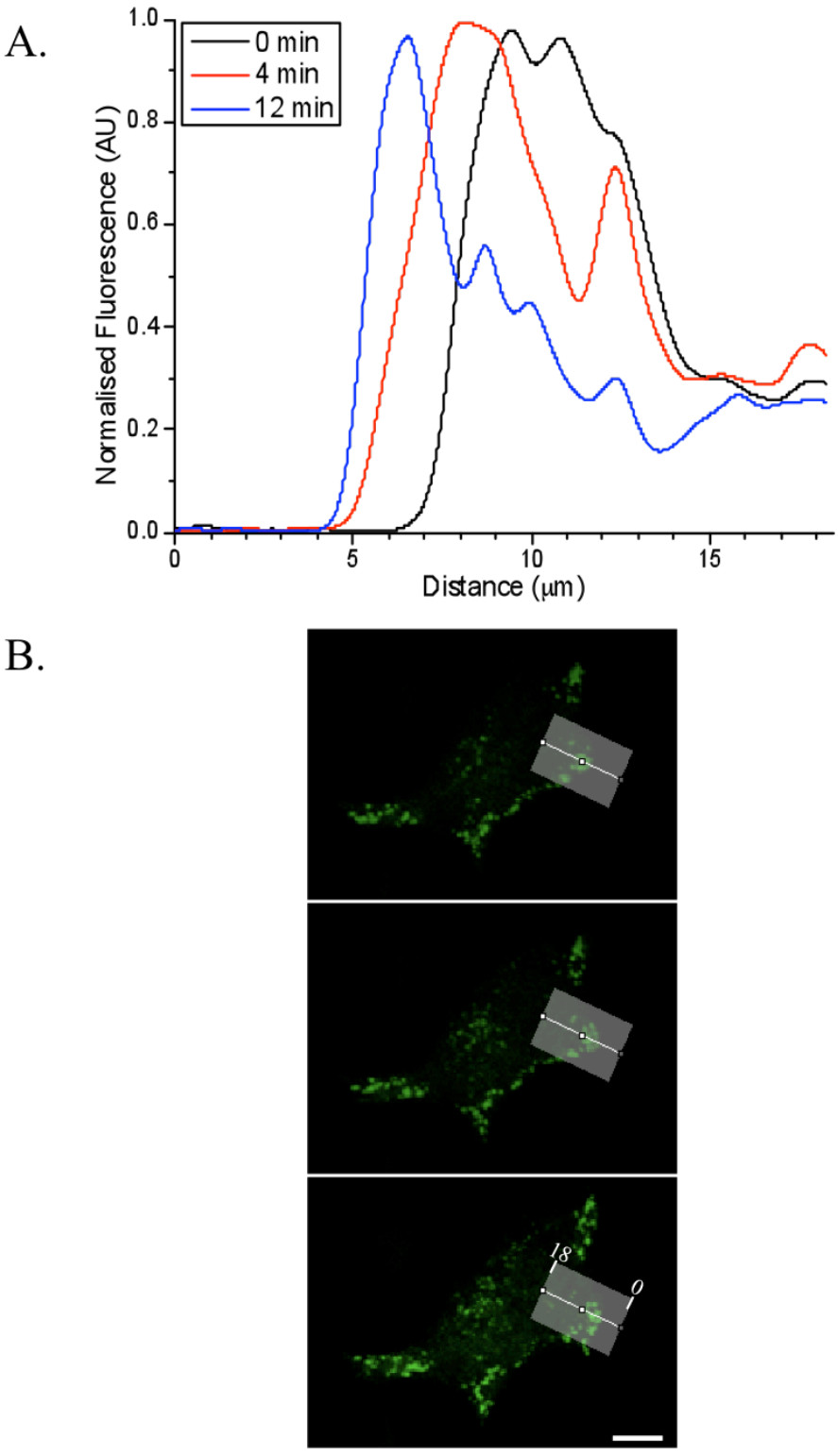

Figure 3.6 The accumulation of junctions at the cell periphery can be seen moving forward with the leading edge as the cell migrates.

Figure 3.7 shows similar analysis performed on another TK-YFP-STIM1 transfected, store-depleted PANC-1 cell imaged on a separate day. Once again, the sharp increase in fluorescent intensity can be seen shifting towards the beginning of the line at the later time point, as seen in the previous figure. This is complemented by Figure 3.7C, which shows an overlay of the images of the cell at 0 (red) and 1205 (green) seconds. In this image, a semi-circle of green, newly formed, puncta can be seen outlining the outer edge of the red, older, puncta, demonstrating the continuously evolving decoration of the leading edge over time.

Figure 3.7 The accumulation of junctions at the leading edge can be seen moving forward as the cell migrates. PANC-1 cells expressing TK-YFP-STIM1 were treated with 15 μM CPA in media with reduced Ca^{2+} (1 mM) and imaged on a confocal microscope. A. Fluorescent intensity along a line spanning the cell membrane at two separate time points. B. Initial image of cell measured in A, with the measured line indicated in white. C. Overlay of the two time points to show development of the leading edge; 0 seconds is shown in red and 1205 seconds shown in green. Scale bar represents 10 μm.

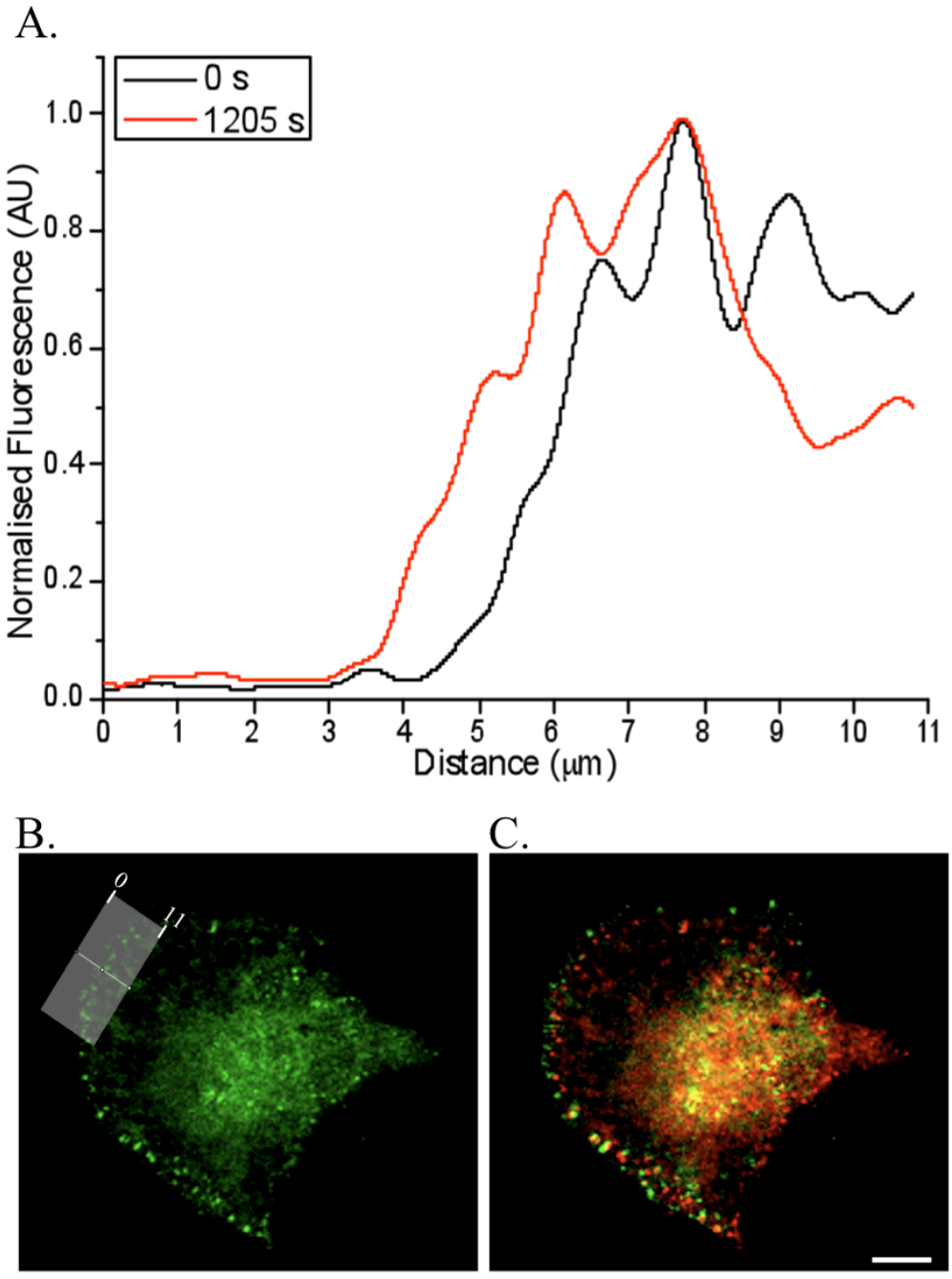

Figure 3.7 The accumulation of junctions at the leading edge can be seen moving forward as the cell migrates.

3.5 Distribution of constitutively active STIM1 mutant in non-store depleted PANC-1 cells

The increased density of STIM1 puncta following the leading edge of migrating PANC-1 cells was an interesting and novel finding. To better understand the mechanism by which STIM1 puncta accumulate at these locations, I investigated whether expressing mutated versions of the STIM1 protein in both control and store-depleted PANC-1 cells could modify the distribution of the puncta in migrating cells.

The first STIM1 mutant construct used was one that contains a mutation in its EF hand domains that prevents Ca^{2+} binding and renders it constitutively punctate and active (Liou *et al.*, 2005). The previous experiments shown all relied upon store-depletion as a mechanism of causing STIM1 to translocate into puncta; this may have caused artefacts in the distribution of puncta due to depletion of the ER Ca^{2+} store. By using this EF hand mutant (YFP-STIM1(D76A)) I could investigate the distribution of STIM1 puncta in non-store-depleted cells and determine if depletion alone affects the distribution of ER-PM junctions. I investigated the distribution of this STIM1 mutant both after fixation and during live imaging, in cells kept in full media. It should be noted that in order to find cells that were healthy enough to image, either low-expressing cells or cells kept in a reduced Ca^{2+}-concentration were used, otherwise the majority of cells were rounded and non-polarised (probably as a consequence of Ca^{2+} toxicity; this effect has been previously shown in S2 cells (Zhang *et al.*, 2005)).

As Figure 3.8 shows, once again cells display a high concentration of STIM1 puncta at the periphery, a high concentration of puncta in the middle of the

cell, and a region of low STIM1 puncta density in the region sitting in between those previously mentioned (n = 4 and 7 for live and fixed experiments respectively).

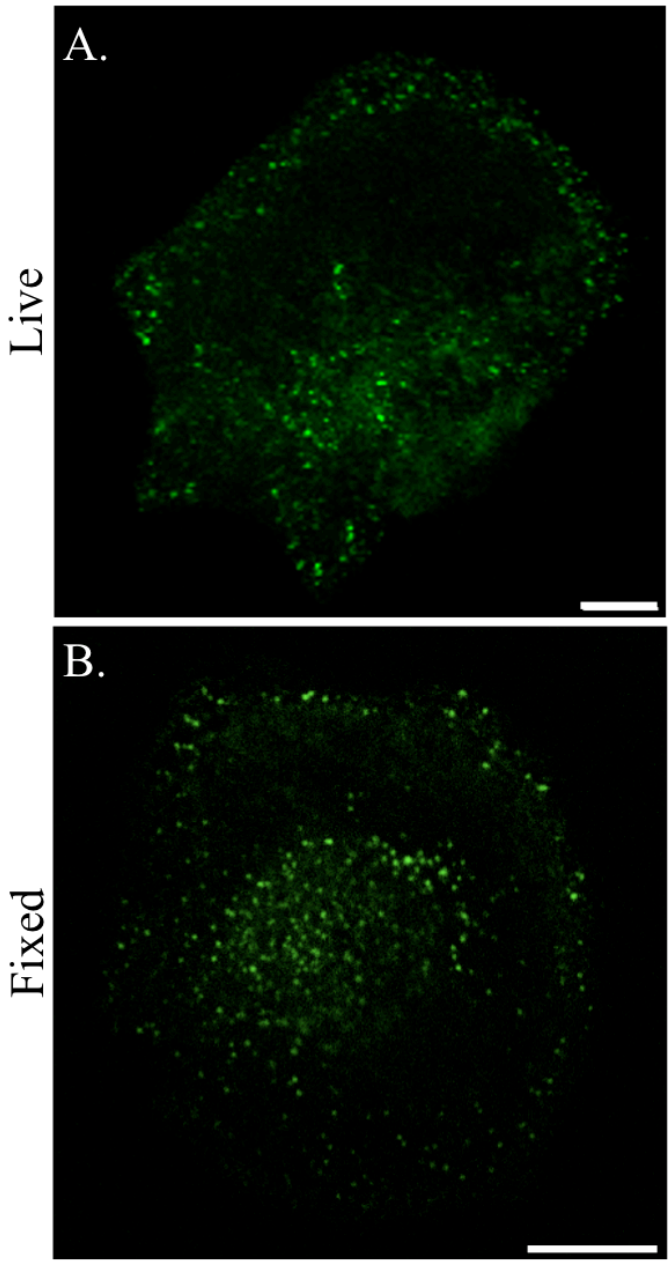

Figure 3.8 The concentration of ER-PM junctions at the edge of cells can be seen in PANC-1 cells expressing a constitutively active STIM1 mutant. PANC-1 cells expressing YFP-STIM1(D76A) were imaged using a confocal microscope either A. live or B. after PFA fixation; scale bars represent 10 µm.

3.6 Effect of deletion of the C-terminal polybasic region of STIM1 on the distribution of STIM1 puncta

Another mutated STIM1 construct of interest to us was the YFP-STIM1(ΔK) construct. This particular form of STIM1 lacks the C-terminal polybasic domain that is likely responsible for binding to phosphoinositides in the plasma membrane and has been reported to be incapable of translocating into puncta upon store-depletion without co-expression of exogenous Orai1 (Liou *et al.*, 2007; Park *et al.*, 2009). Figure 3.9 shows the distribution of this construct in PANC-1 cells in four different conditions. In Figure 3.9A, YFP-STIM1(ΔK) transfected PANC-1 cells were kept in control conditions before fixation, and STIM1 is seen here to be very reticular in distribution (n = 4). In Figure 3.9B, cells were treated with CPA for 30 minutes prior to fixation; the reticular distribution of STIM1 puncta seen here confirms that puncta formation by this mutated STIM1 protein is indeed different from WT-STIM1 (n = 3). Interestingly, YFP-STIM1(ΔK) transfected PANC-1 cells that were store-depleted for a full 60 minutes (C & D) do show a punctate distribution of STIM1 (n = 9). The puncta in these cells seem more homogenous in their distribution, and more are present in the middle of the cell. However, Figure 3.9D shows that peripheral accumulation of these STIM1 puncta is still possible, even if the formation of these puncta does takes a lot longer than their WT-STIM1 counterparts (WT-STIM usually forms puncta in under 10 minutes e.g. Figure 3.1).

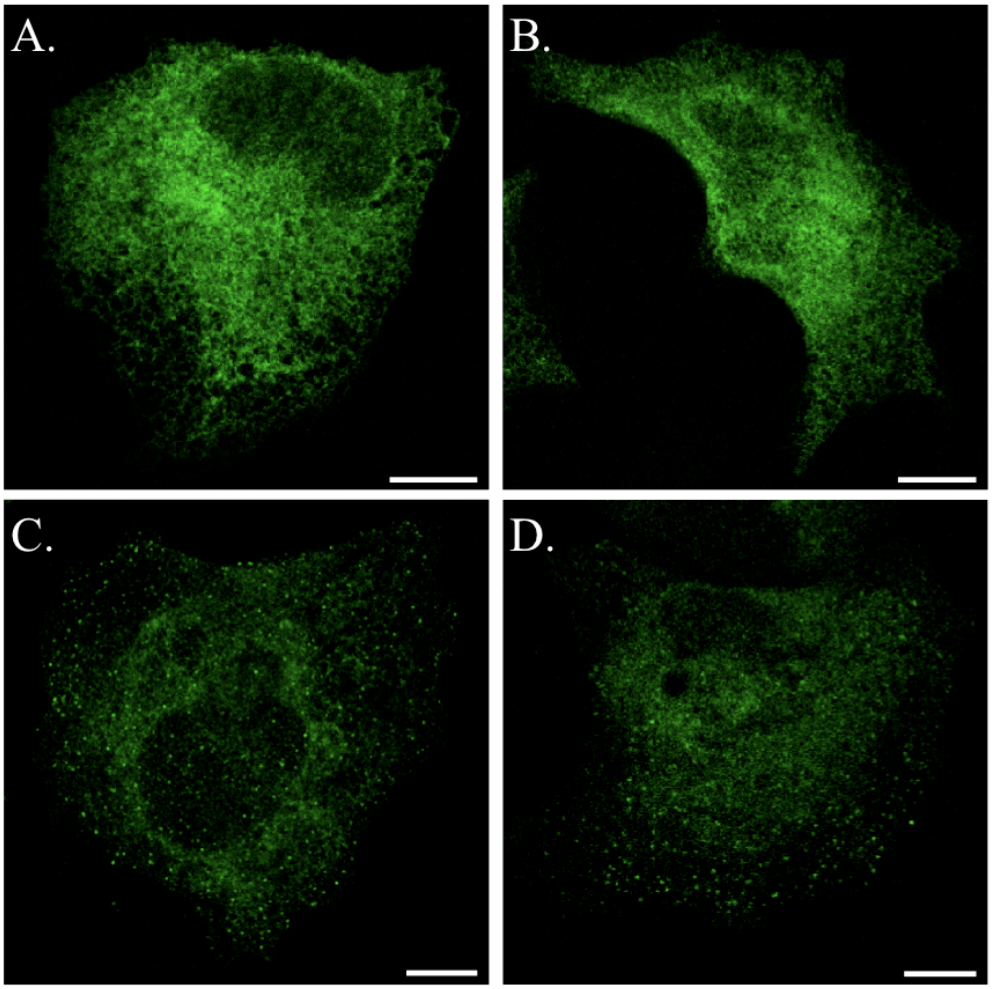

Figure 3.9 STIM1(ΔK) distribution in resting and store-depleted cells. PANC-1 cells were transfected with YFP-STIM1(ΔK) and kept in control conditions (A) or treated with CPA to deplete stores (B: for 30 minutes; C & D: 60 minutes) prior to PFA fixation. Scale bars represent 10 µm.

3.7 Distribution of STIM1(NN) in store-depleted PANC-1 cells

The last construct tested was the CMV-STIM1(NN)-YFP construct, a STIM1 mutant that does not bind to EB1 (Honnappa *et al.*, 2009). Ordinarily ER-located STIM1 can bind polymerising microtubules via the plus-end binding protein EB1, and often displays a very tubular distribution in quiescent cells (an example of which can be seen in Figure 3.10, which shows a PANC-1 cell expressing TK-YFP-STIM1 in control conditions). As microtubules are crucial for the development of cell polarisation and the development of a leading edge I investigated whether disrupting this relationship would prevent the occurrence of peripheral STIM1 puncta distribution that is often seen.

Figure 3.11 shows PANC-1 cells transfected with CMV-STIM1(NN)-YFP in both control and store-depleted conditions. Figure 3.11A shows the expected reticular distribution of STIM1(NN) in control, quiescent PANC-1 cells, however, in this instance, no tubulin-like distribution can be seen (n = 2). Figure 3.11B shows the distribution of STIM1 puncta in store-depleted cells, and demonstrates that STIM1 with disrupted EB1 binding can still form puncta (n = 2), adding to previous reports indicating that neither microtubule disrupting agents nor knockdown of EB1 prevent exogenous STIM1 puncta formation (Smyth *et al.*, 2007; Grigoriev *et al.*, 2008). Not only this, but the cell shown also demonstrates that the STIM1(NN) puncta can still concentrate at the cell periphery, and that binding to microtubules is not necessary for this phenomenon.

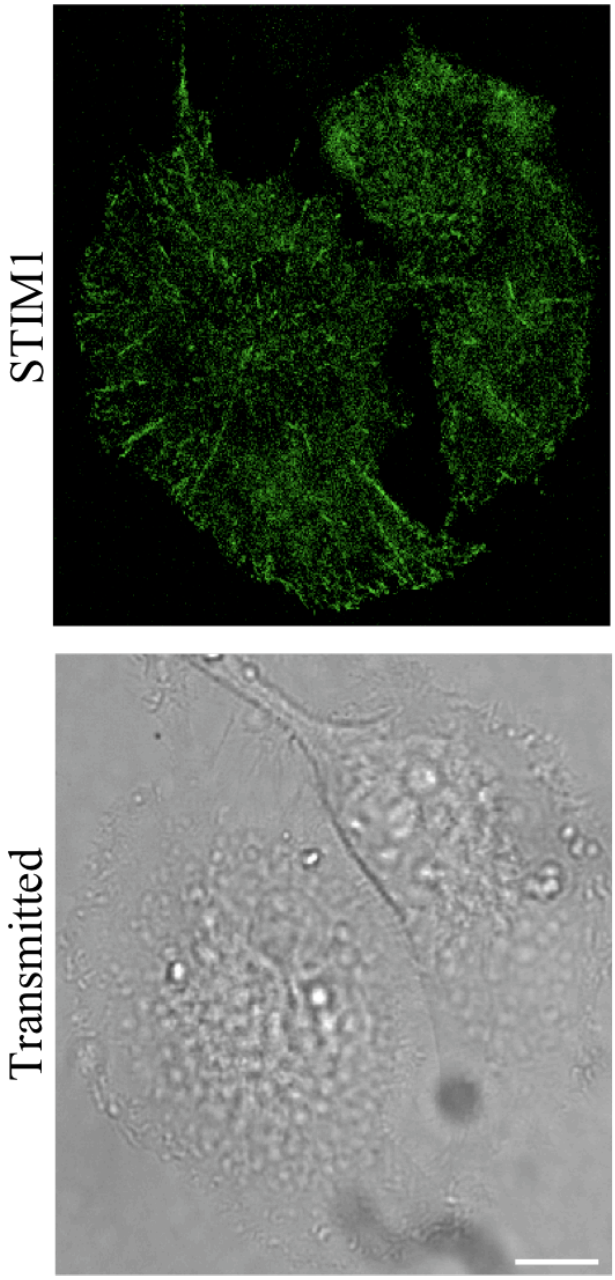

Figure 3.10 TK-YFP-STIM1 distribution is often tubular in resting conditions. An example of the characteristic tubular TK-YFP-STIM1 distribution in PANC-1 cells transfected with this construct and kept in a HEPES-based extracellular solution. Scale bar represents 10 μm.

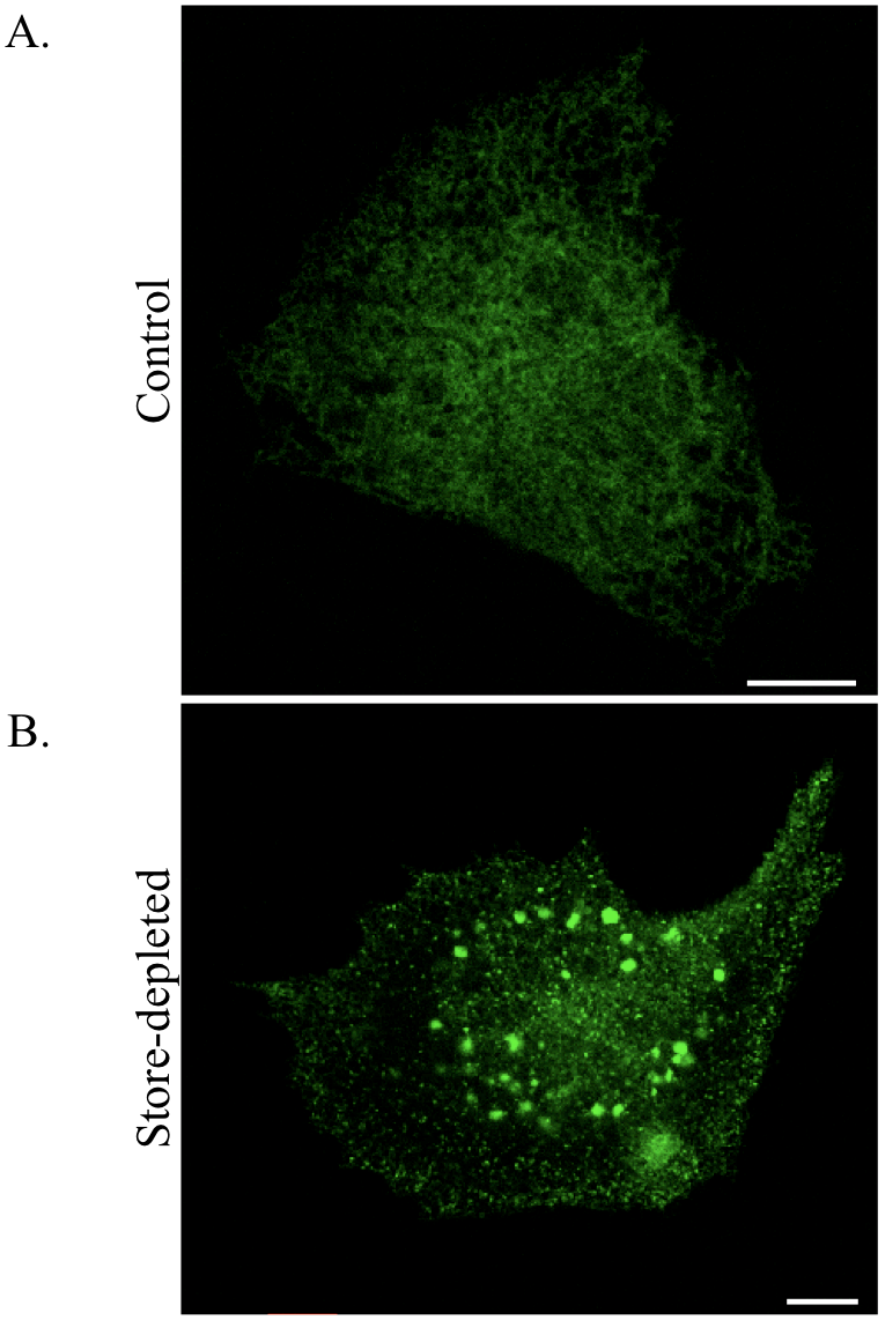

Figure 3.11 STIM1 (NN) has a reticular distribution in quiescent cells, and forms puncta after store-depletion. PANC-1 cells transfected with CMV-STIM1(NN)-EYFP were imaged live in full, CO_2-independent media in either A. control conditions, or B. store-depleted conditions (30 μM CPA). Scale bars represent 10 μm.

Figure 3.12 (and Video 3.2 on the CD) supplements the previous figure, showing a store-depleted, migrating PANC-1 cell transfected with the YFP-STIM1(NN) construct (n = 2). As can be clearly seen in the first frame, there is a strong accumulation of STIM1(NN) puncta at the periphery of the cell. As the frames progress through time, the cell can be seen moving towards the left, and as this occurs the puncta at the leading edge maintain their relative distribution (i.e. the concentration at the leading edge moves forward with the cell). Another interesting observation is that in the middle of the cell a protrusion develops over ~ 3000 seconds. As this protrusion develops, the process of puncta accumulation at a cell protrusion can be seen. Though initially when the protrusion is small (at 620 seconds) there are only a few puncta present, the number of junctions can be seen increasing with the size of the protrusion, accumulating and developing as the protrusion grows.

Figure 3.12 STIM1(NN) puncta can concentrate at the periphery of migrating PANC-1 cells, following the leading edge as the cell migrates. PANC-1 cells expressing CMV-STIM1(NN)-YFP were treated with 10 μM CPA in media with reduced Ca^{2+} (1 mM) and imaged live. Time indicates relative time since start of imaging; scale bar represents 10 μm.

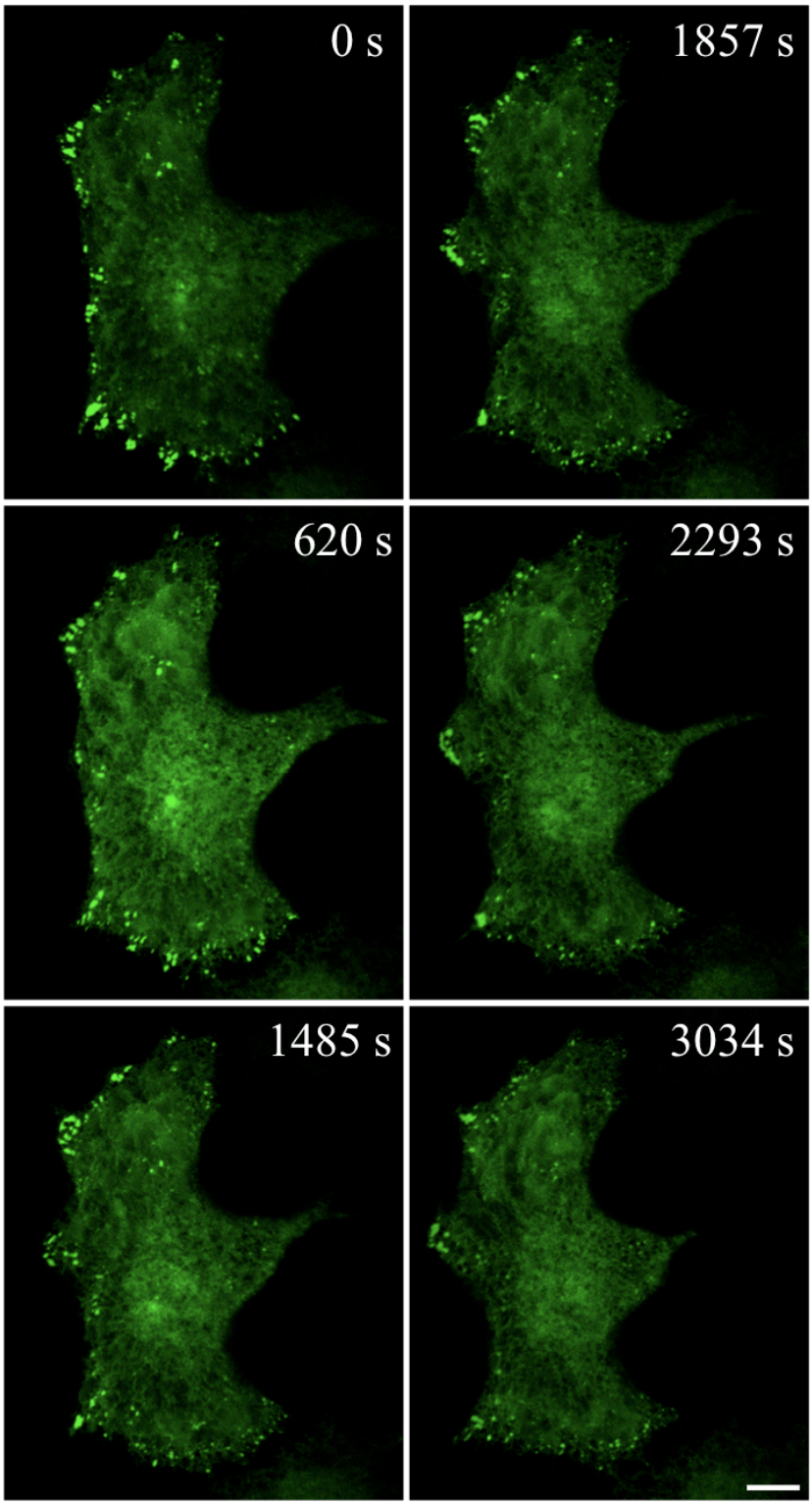

Figure 3.12 STIM1(NN) puncta can concentrate at the periphery of migrating PANC-1 cells, following the leading edge as the cell migrates.

3.8 STIM1 puncta formation at the leading edge of cells is saltatory, and does not involve sliding from the cell interior

Having established that there is a concentration of puncta at the leading edge of migrating cells, I next looked to see how the puncta localise to these sites as cells move forward. Two alternative possibilities were tested, firstly that puncta slide outwards from the body of the cell to reach the cell periphery, or secondly that they form directly at the edge of the cell when new expansion of the cell membrane occurs.

Figure 3.13 shows a store-depleted TK-YFP-STIM1 transfected PANC-1 cell (the same cell as shown in Figure 3.7) displaying a developing extension of the cell edge at the right side of the cell (indicated in Figure 3.13A, which shows the full cell with an arrow highlighting the region of interest). Figure 3.13B shows a set of high magnification images of this area at three separate time points, with an arrow pointing to the punctum of interest (Video 3.3 (CD) shows a video containing the region of interest shown in Figure 3.13B), which appears and disappears during the time course of the recording (two further puncta, highlighted with a white arrow, form during the course of the recording and stabilise). To investigate the mechanism by which the puncta localised to this site, I analysed the changing fluorescence intensities in both the region containing the punctum, and in the regions that span the areas between the punctum and the rest of the cell. If the punctum was sliding outwards towards the cell periphery from the interior of the cell, I would see an increase in fluorescence both in the region containing the punctum and immediately prior to this, an increase in fluorescence in one or more of the other regions as the punctum moves through them. If the punctum appeared in a saltatory fashion then an increase in fluorescence

would only be seen in the region containing the punctum at the time of formation. Figure 3.13C shows that the latter explanation is more likely. The inset shows a magnification of the cell previously shown, focussing on the punctum. The average fluorescence in the four boxes drawn on the inset is shown in the graph (with the layout shown above, i.e. the black line corresponds to Box 1 which corresponds to the top right box, the pink line to Box 2 (bottom right) etc.); data for the graph are from images taken every five seconds. The sharp increase in fluorescence in region 1 (the region containing the punctum) and the constant near-background fluorescence in the other regions suggests saltatory formation of the punctum.

Figure 3.13 Junction formation at the leading edge of migrating cells is saltatory. PANC-1 cells expressing TK-YFP-STIM1 were treated with 15 μM CPA in media with reduced Ca^{2+} (1 mM) and imaged live on a confocal microscope. A. Full-size image of cell with arrow depicting the punctum of interest. Scale bar represents 10 μ m. B. Series of images showing the appearance and disappearance of a punctum in the cell region depicted in A. Yellow arrow shows punctum of interest; white arrow shows a group of puncta that forms and stabilises during the recording. Phenomenon was seen in at least 15 different live imaging experiments.

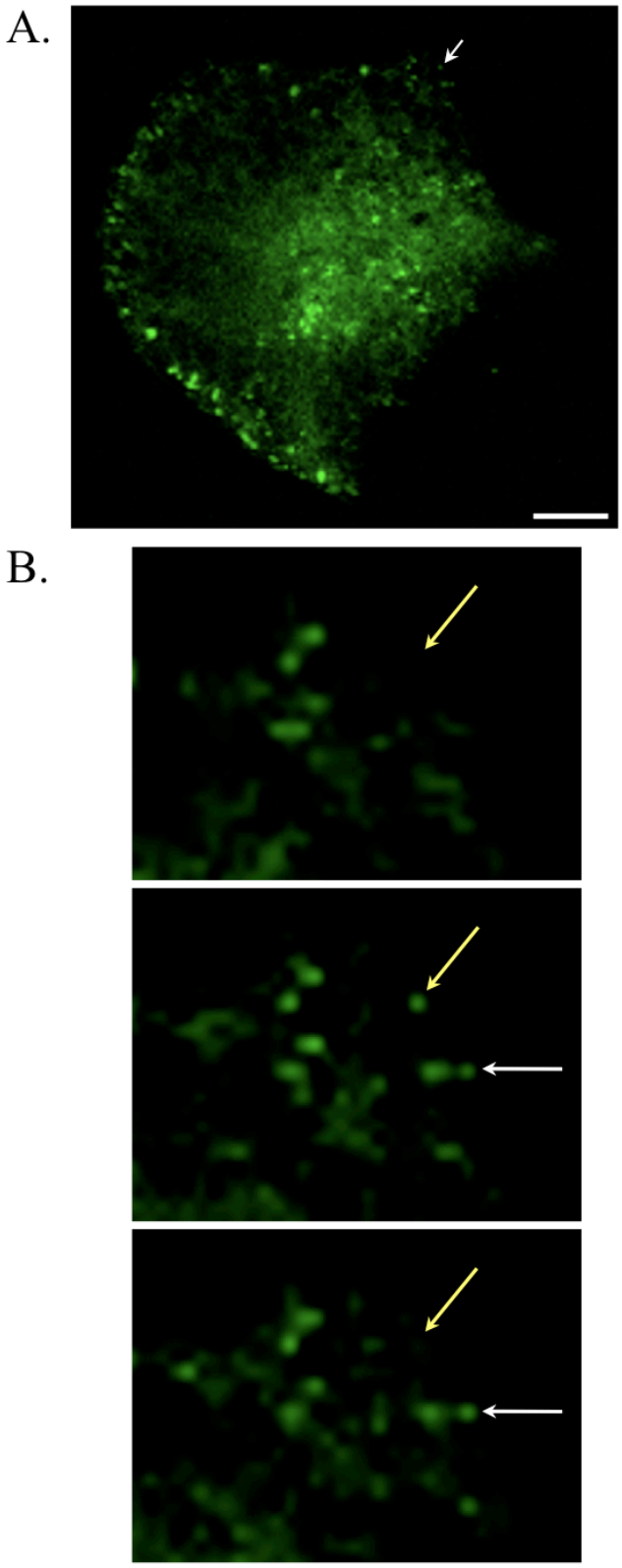

Figure 3.13 Junction formation at the leading edge of migrating cells is saltatory.

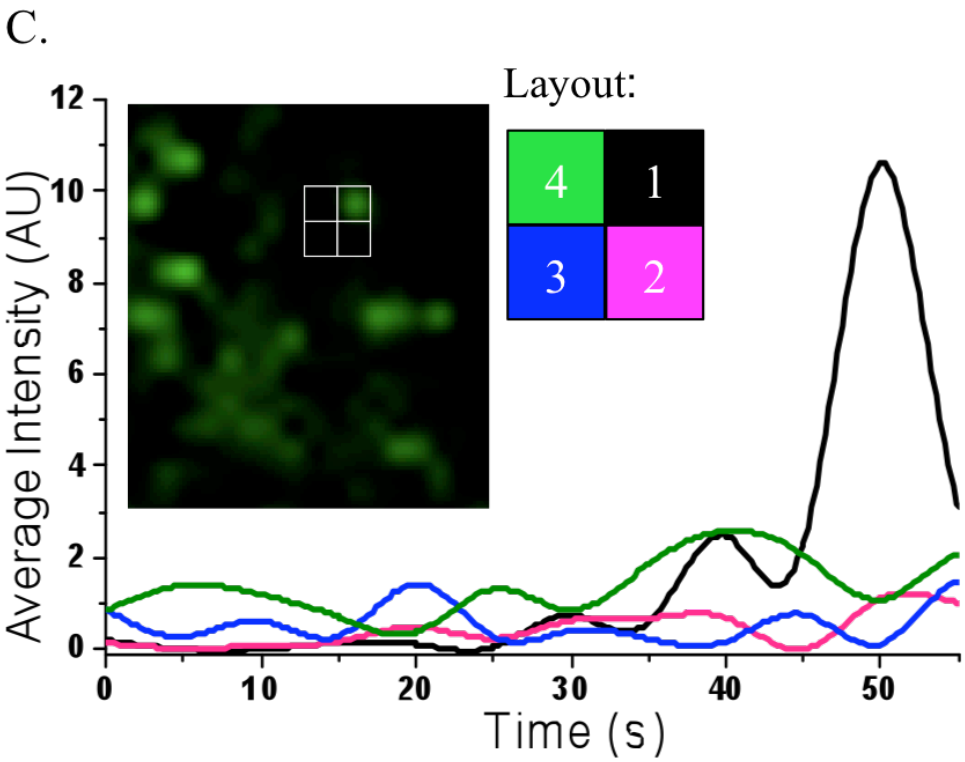

Figure 3.13 (continued) STIM1 puncta at the leading edge form in a saltatory fashion. C. Changing fluorescence intensities in the regions marked by the boxes shown on the inset (with the layout depicted, i.e. the black line corresponds to Box 1 which corresponds to the box in the top right corner, the pink line to Box 2 (bottom right) etc.). Data points are from images taken every five seconds.

Figures 3.14 examines the mechanism of punctum formation at an expanding cell edge in a STIM1-transfected PANC-1 cell, using heat as a mechanism for inducing puncta formation. Increasing the ambient temperature of HeLa cells up to 40 °C has been shown to induce translocation of STIM1 puncta to ER-PM junctions, without stimulating SOCE (Xiao *et al.*, 2011). As this method could be useful for studying ER-PM junction dynamics in migrating cells without depleting the stores or causing Ca^{2+} influx, the ability of this method to induce puncta in TK-YFP-STIM1 transfected PANC-1 cells was also tested and was shown to act as reported. I found that adequate puncta formation in PANC-1 cells could be obtained at 40 °C and therefore examined the dynamics of STIM1 puncta at this temperature.

Figure 3.14 shows a heat-treated TK-YFP-STIM1 transfected PANC-1 cell with an expanding leading edge (Figure 3.14A; expansion shown during Video 3.4 (CD)). A protrusion of the cell edge can be seen between 0 and 840 seconds (Figure 3.14B). A punctum is highlighted at the edge of the cell that is not present at 0 seconds but has appeared by 840 seconds. The graph shown in Figure 3.14C shows the fluorescence intensities of the regions surrounding the punctum compared to that of the region of the punctum itself; again, data for the graph are from images taken every five seconds. Whilst there is a considerable increase in fluorescence that starts at ~ 200 seconds in the region of the punctum, the other three boxes have little to no signal throughout, suggesting that the punctum did not travel through any surrounding regions prior to its appearance at the cell edge.

Figure 3.14 STIM1 puncta at the leading edge form in a saltatory fashion in heat-treated cells. TK-YFP-STIM1 transfected PANC-1 cells were imaged on a confocal microscope at 40 ˚C in full media. A. Full size image of the cell, scale bar represents 10 µm. B. Magnifications of the region highlighted in A, showing formation of puncta at the leading edge (0 s indicates start of imaging). White arrows show the punctum of interest; cell outlines are shown.

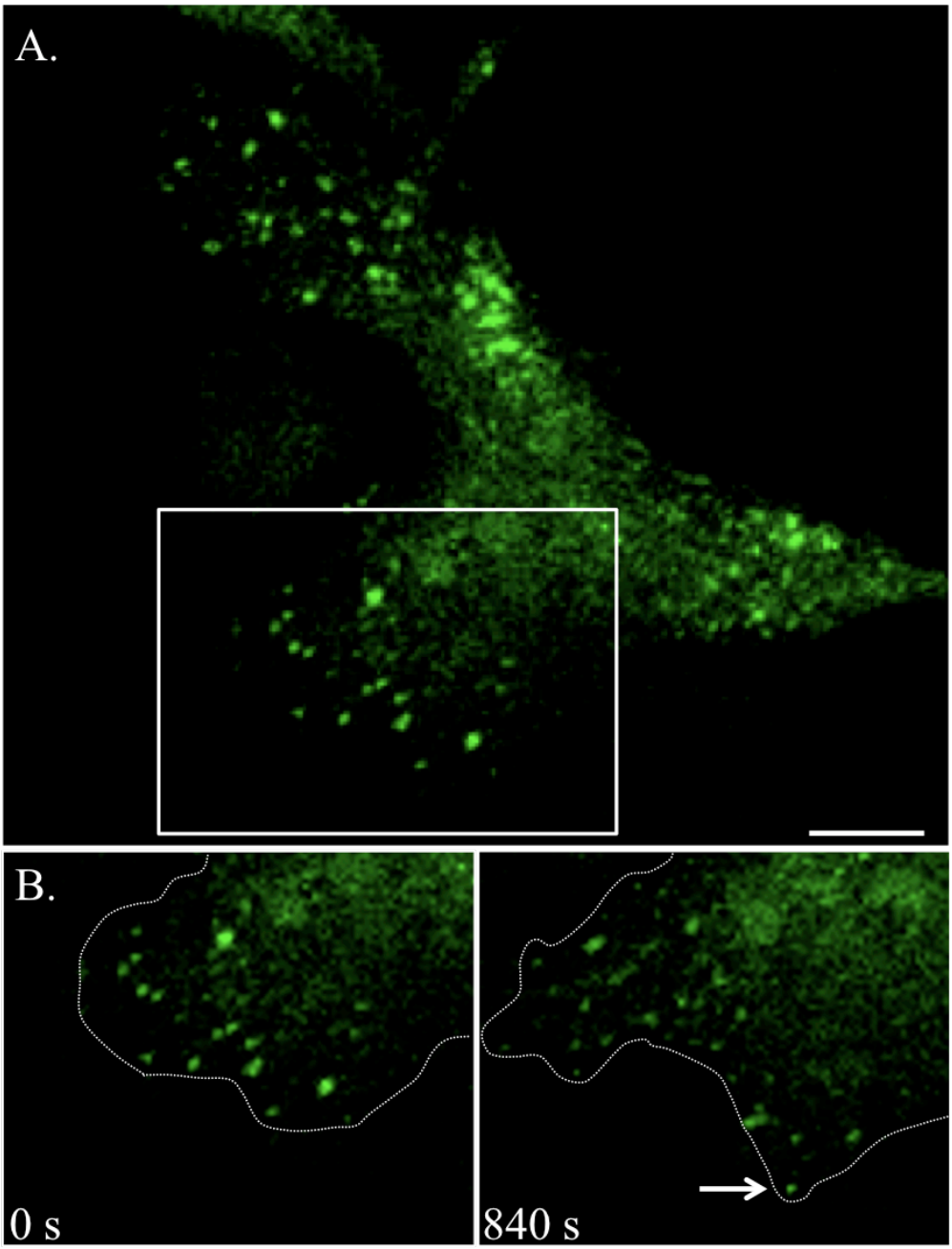

Figure 3.14 STIM1 puncta at the leading edge form in a saltatory fashion in heat-treated cells.

C.

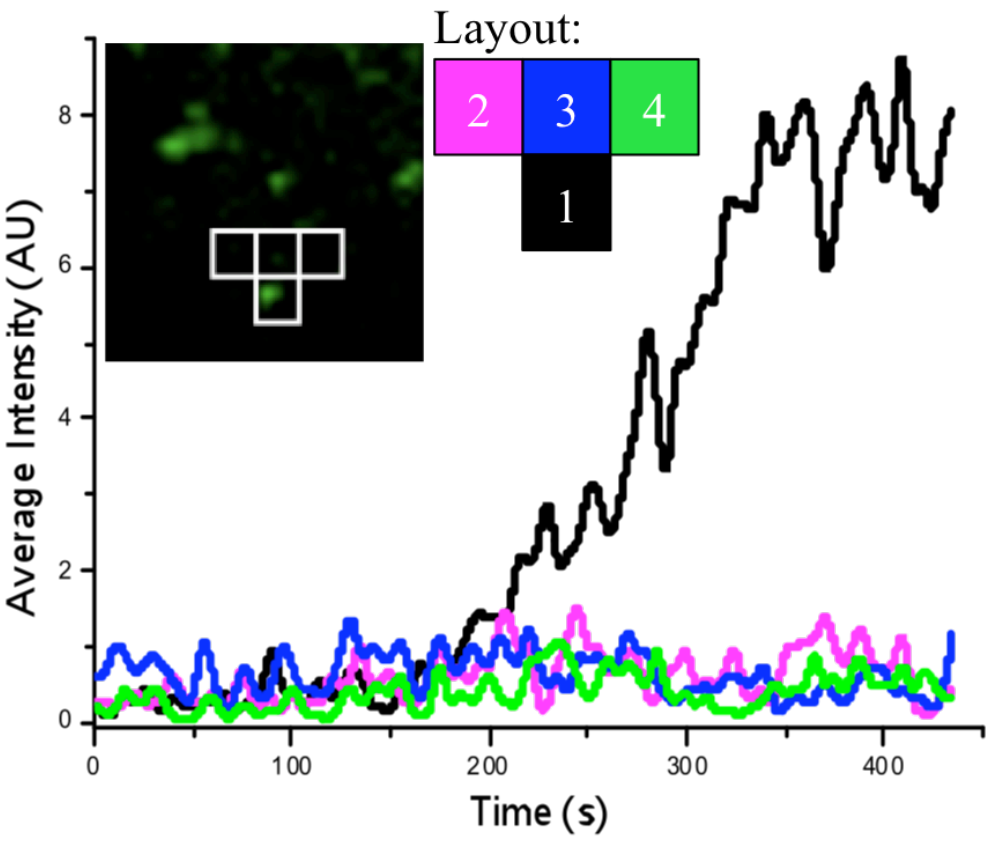

Figure 3.14 (continued) STIM1 puncta at the leading edge form in a saltatory fashion in heat-treated cells. C. Changing fluorescence intensities over time in the regions highlighted by boxes shown on the inset (with the layout depicted). Data points are from images taken every five seconds.

This phenomenon can also be seen in store-depleted PANC-1 cells transfected with CMV-STIM1(NN)-YFP (n = 2). In the store-depleted PANC-1 cell shown in Figure 3.15, a protrusion develops over time as can be seen in both the full images of the cell (Figure 3.15A and Video 3.2) and in the higher magnification images (Figure 3.15B). The white arrow shown in Figure 3.15A shows the protrusion that develops as the cell moves forward. The yellow arrow in Figure 3.15B shows a punctum that appears during the formation of the protrusion and remains relatively stationary as the protrusion develops. The white arrowheads in Figure 3.15B show puncta that appear in a saltatory fashion at the edge of the newly formed protrusion, decorating the leading edge of the cell as it develops.

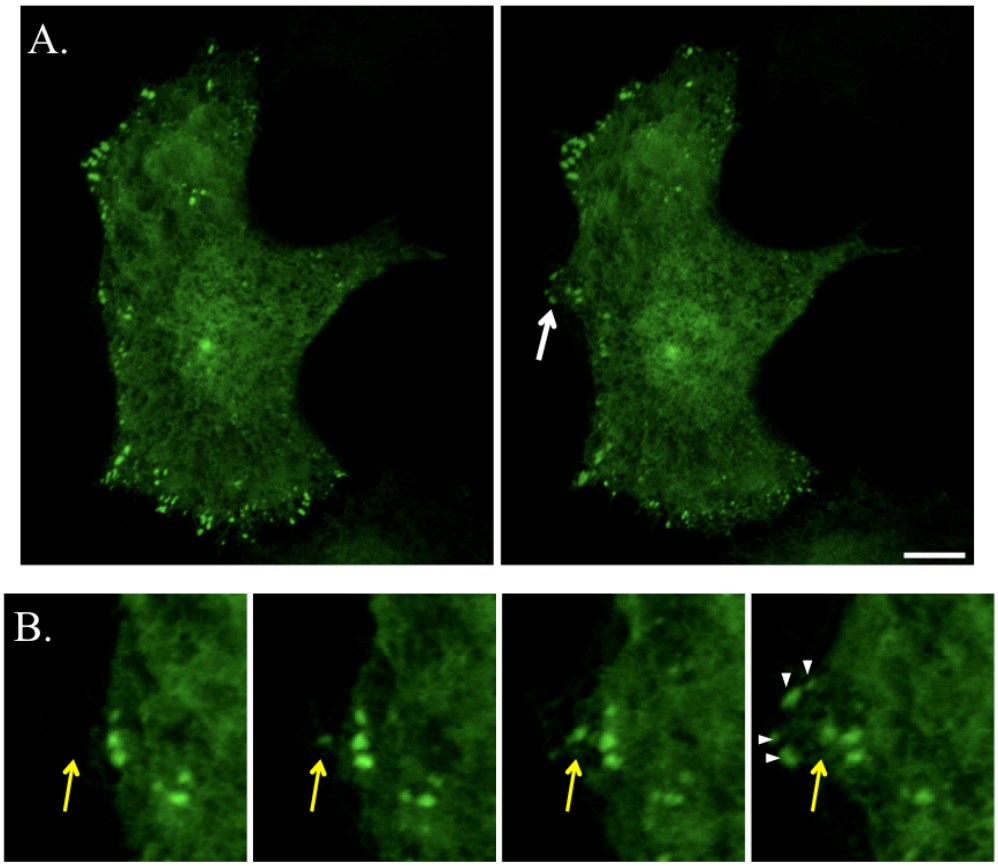

Figure 3.15 STIM1 puncta at the leading edge form in a saltatory fashion in STIM1(NN)-transfected cells. PANC-1 cells transfected with STIM1(NN)-YFP were treated with 10 μM CPA in media with reduced Ca^{2+} (1 mM) and imaged on a confocal microscope. A. Images of a cell at two time points showing development of a protrusion at the leading edge. Scale bar represents 10 μm. B. High magnification images of the cell showing development of the protrusion and saltatory appearance of puncta.

3.9 Puncta can travel long distances during retraction of the cell tail

The saltatory formation of ER-PM junctions in migrating STIM1 transfected PANC-1 cells was one novel form of puncta dynamics discovered during this investigation. Another novel behaviour of the junctions seen was the long distance translocation of puncta during tail retraction.

Figure 3.16 shows an example of a tail retraction event in a store-depleted TK-YFP-STIM1 transfected PANC-1 cell (n = 12), and displays an example of the relatively long cell tails that can often be left trailing as the cell moves forward. In this series of images, puncta are seen remaining in the tip of the cell tail even when this structure is relatively far from the cell body. When the tail is eventually pulled into the cell body (which occurs during this image series), the puncta remain intact as the tail retraction occurs, leading to long distance translocation of puncta.

Figure 3.16 Junctions found in the tail of migrating cells can be seen undergoing long distance translocation during tail retraction. PANC-1 cells expressing TK-YFP-STIM1 were treated with 15 μM CPA in media with reduced Ca^{2+} (1 mM) and imaged on a confocal microscope. The series of images show a tail retraction event. Scale bar represents 10 μm.

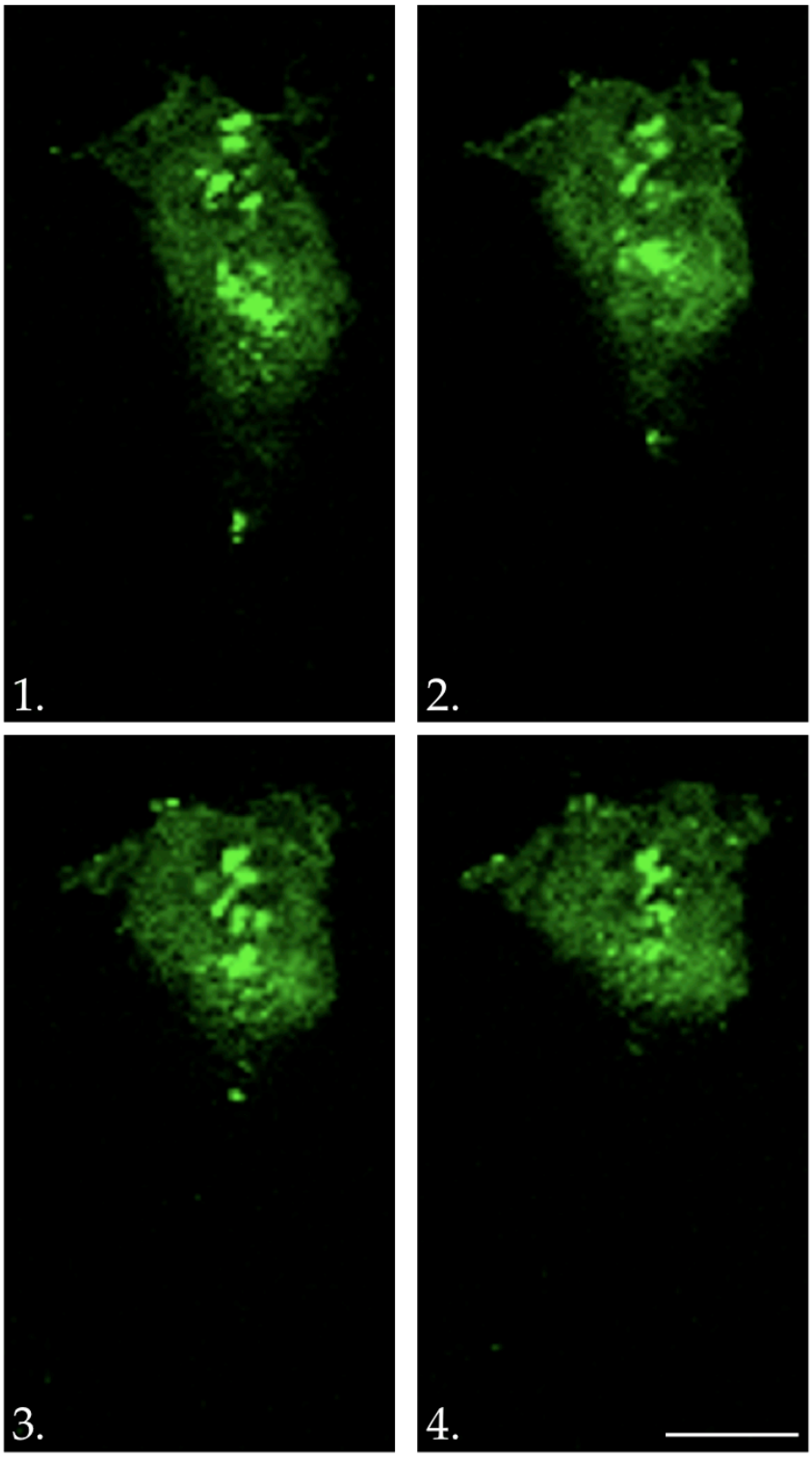

Figure 3.16 Junctions found in the tail of migrating cells can be seen undergoing long distance translocation during tail retraction.

Figure 3.17 shows a tail retraction event occurring in another store-depleted TK-YFP-STIM1 transfected PANC-1 cell. The image series in Figure 3.17A shows the general dynamics of the puncta present in the retracting tail as the cell migrates forwards. Figures 3.17B & C show a kymogram of the tail retraction. Kymography is a method of image analysis that plots a 1D axis (x) against time (in this instance x is shown by the line drawn along the cell tail in Figure 3.17C (with values being the average fluorescence intensity of the line width)). This form of analysis was produced using the MultipleKymograph plugin in ImageJ (produced by J. Rietdorf and A. Seitz, EMBL Heidelberg). At the beginning of the kymogram (i.e. the top or time = 0) there is considerable fluorescence; this indicates the presence of the tail and fluorescent STIM1 puncta along most (~ 2/3) of the line. As time progresses the bright signal seen in the kymogram moves slowly out of the analysis area as both the STIM1 puncta and the tail move towards the cell body.

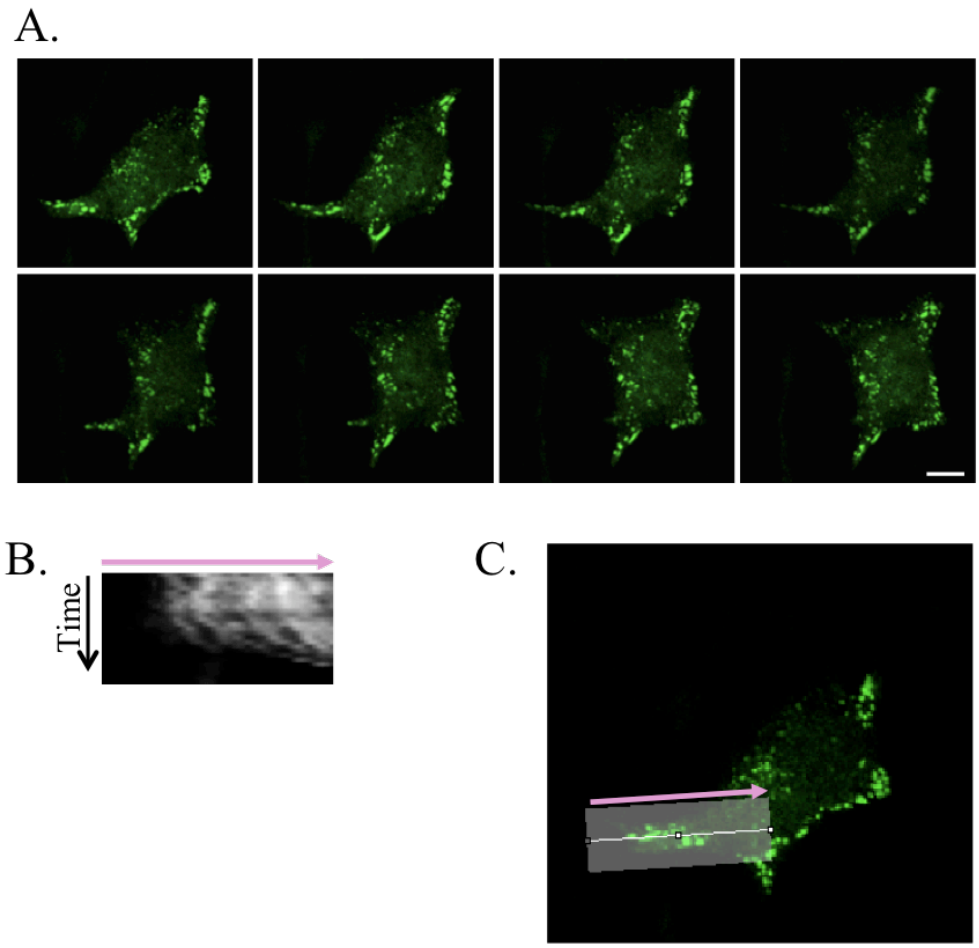

Figure 3.17 Junctions found in the tail of migrating cells can be seen undergoing long distance translocation during tail retraction. PANC-1 cells expressing TK-YFP-STIM1 were treated with 15 μM CPA to deplete the intracellular Ca^{2+} store, kept in media with reduced Ca^{2+} (1 mM Ca^{2+}) and imaged using a confocal microscope. A. Series of images showing a tail retraction. Scale bar represents 10 μm. B. Kymogram showing tail retraction of region indicated in C. C. Arrow indicates kymogram direction.

Figure 3.18 shows another tail retraction event in the same cell. Figure 3.18A (and Video 3.5 on CD) shows the general phenomenon, whereas Figures 3.18B and C show more detailed analysis of the fate of individual puncta during the retraction of the tail. Four individual puncta present in the tail are highlighted in Figure 3.18B and these were tracked during the tail retraction, with the results shown in Figure 3.18C. The relatively long distances that individual puncta can move during a tail retraction event is readily demonstrated by indicating their position in different frames (white dots). Puncta can translocate 10 – 15 μm before they disappear or disassemble (the location of which is indicated by red dots).

Figure 3.18 Puncta found in the tail of migrating cells can travel long distances during tail retraction. PANC-1 cells expressing TK-YFP-STIM1 were treated with 15 μM CPA in media with reduced Ca^{2+} (1 mM) and imaged on a confocal microscope. A. Series of images showing tail retraction at the rear of a migrating cell. B. Images highlighting four puncta (yellow arrowheads), the movements of which are plotted in C. C. Images showing the position of puncta at individual time points (0, 8, 10, 12, 14 and 16 minutes, relative to start of image series), on images from before (left) and after (right) the tail retraction. White dots indicate puncta position, red dots indicate the location at which puncta dissolve. All scale bars represent 10 μm.

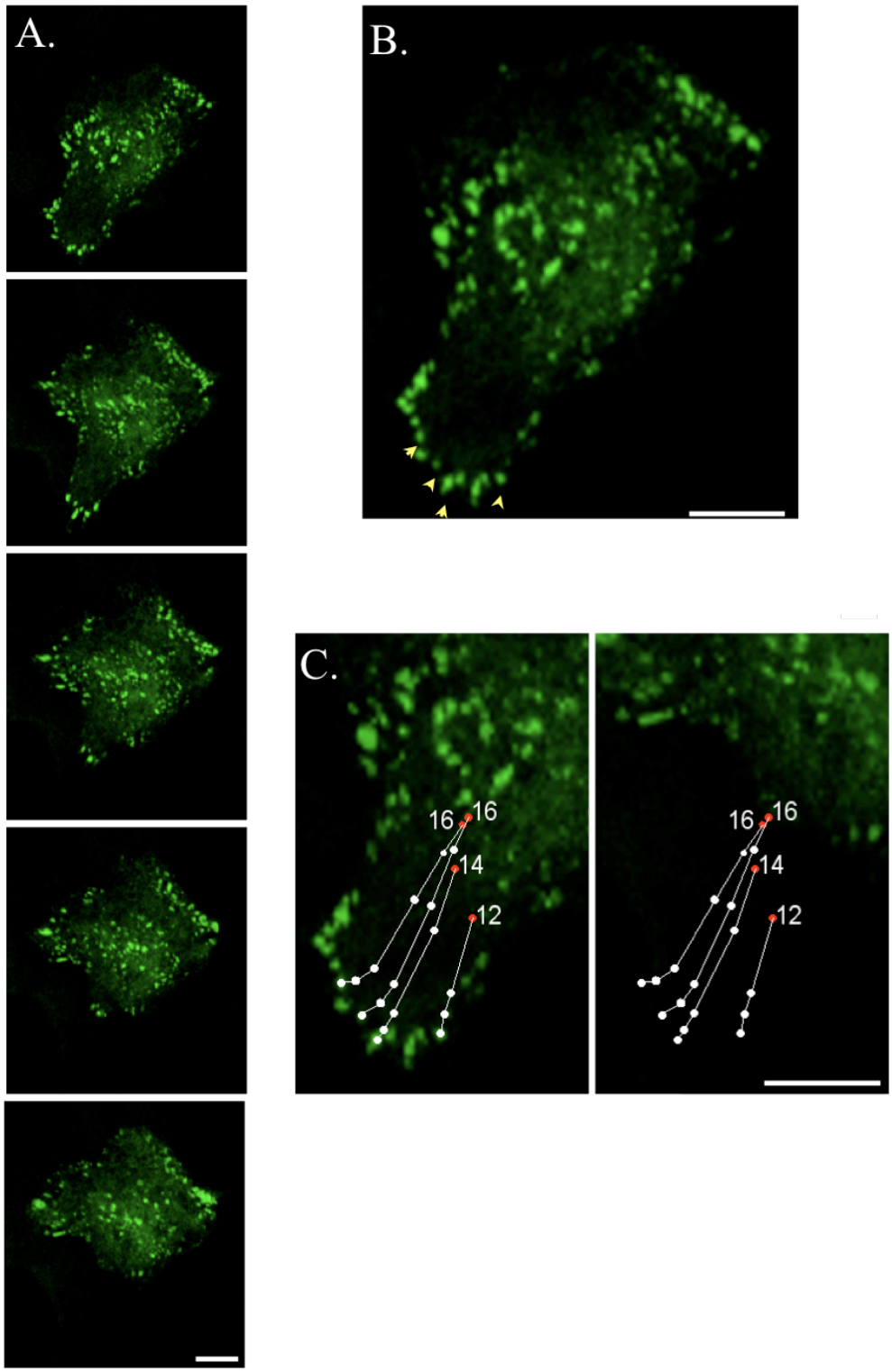

Figure 3.18 Puncta found in the tail of migrating cells can travel long distances during tail retraction.

3.10 STIM1 puncta at the leading edge co-localise with Orai1

The use of a STIM1 construct to highlight ER-PM junctions in migrating PANC-1 cells was a valuable tool for examining the dynamics of these junctions in migrating cells. Upon store depletion, STIM1 oligomerises and translocates into puncta, where it co-localises with Orai1 to form SOCE-competent junctions. Because of the very specific distribution of STIM1 puncta seen in migrating PANC-1 cells, it was of particular interest to determine whether these peripheral puncta were indeed co-localising with Orai1. To test this, I studied migrating store-depleted PANC-1 cells transfected with both CMV-YFP-STIM1 and mCherry-Orai1 (in this instance the Ca^{2+} concentration added to the extracellular media was reduced to 0.8 mM , as two different SOCE-related constructs were transfected). The cell shown in Figure 3.19 shows the characteristic STIM1 puncta localisation at the leading edge (STIM1 shown in green), and also shows that at these locations they co-localise with Orai1 (shown in red).

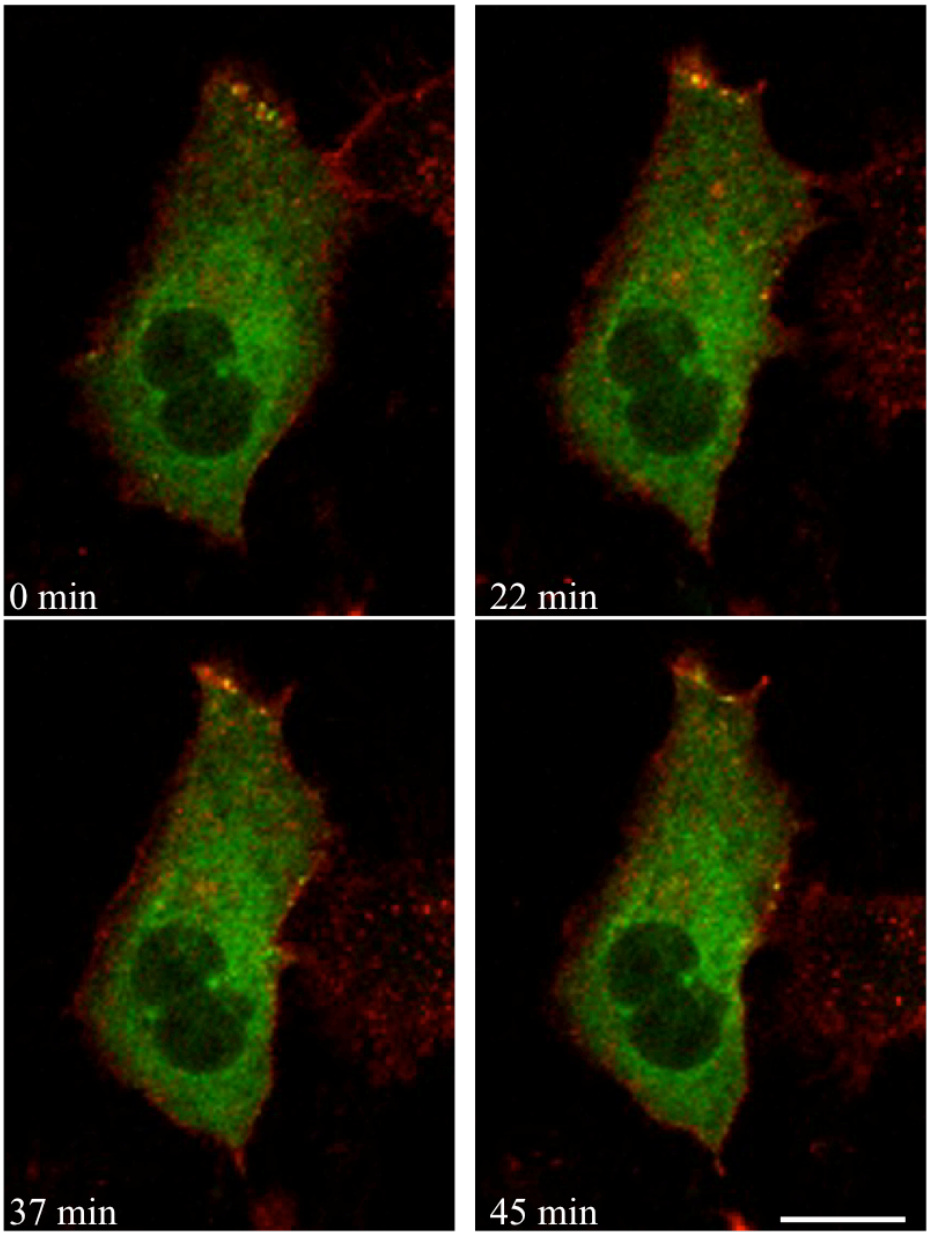

Figure 3.19 STIM1 and Orai1 co-localise at the cell periphery. PANC-1 cell expressing CMV-YFP-STIM1 (green) and mCherryOrai1 (red) were treated with 15 μM CPA in media with reduced Ca^{2+} (0.8 mM) and imaged using a confocal microscope. Images show the same cell at four different time points relative to the first image; scale bar represents 10 μm.

3.11 Summary

3.11.1 Overview

The first part of my investigation established that ER-PM junctions form preferentially at the periphery of migrating cells, especially at the leading edges; this distribution is achieved through saltatory formation of junctions at these locations. I established that this distribution is independent of ER Ca^{2+} content, and is neither critically dependent on STIM1-microtubule associations, nor interactions of STIM1 with membrane phospholipids. I also documented the long distance translocation of puncta during the retraction of tails during cell migration.

3.11.2 Effects of SOCE regulation on cell migration

Migration of PANC-1 cells was significantly inhibited by the SOCE inhibitor SKF96365. Cell were capable however of migrating in the presence of inhibitors of the SERCA pumps (i.e. pumps responsible for maintaining ER Ca^{2+} concentrations) (Figure 3.4). This allowed me to investigate the positioning of STIM1 puncta (i.e. ER-PM junctions) in migrating cells.

The effect of heat on cell migration is somewhat surprising. My experiments in PANC-1 cells (Figure 3.14), and previous research (Xiao *et al.*, 2011) have indicated that increasing the ambient temperature causes formation of puncta. The SOCE complexes formed by temperature induced STIM1 translocation are reported to be inactive until the temperature drops back down to more physiological levels (~ 37 °C), at which Ca^{2+} influx occurs. Theoretically then at 40 °C, STIM1 puncta should be present in PANC-1 cells expressing TK-YFP-STIM1 (as seen), but forming non-functional SOCE complexes, mimicking the effects of SKF96365. However, keeping cells at this

higher temperature had no effect on the rate of migration. This could be because SKF96365 was acting through targets other than SOCE complexes when it was inhibiting migration; more likely, the small, reduced current that does occur at 40 °C (Xiao *et al.*, 2011) allows sufficient Ca^{2+} influx so as not to inhibit migration of PANC-1 cells.

3.11.3 Concentration of STIM1 puncta at the periphery of cells

The first indication that STIM1 puncta (and hence ER-PM junctions) may have a distinctive distribution in certain cells was from experiments carried out using TIRF microscopy (Figure 3.2). Further work demonstrated that STIM1 puncta (and hence ER-PM junctions) are found at high densities at cellular protrusions and are found concentrated at the leading edge of migrating cells (Figures 3.5 – 3.7 and Video 3.1). This striking distribution was seen many times throughout the course of this investigation and is particularly intriguing in the context of several previous studies examining the role of Ca^{2+} in migration. Migrating cells have a Ca^{2+} gradient that runs from the front of the cell to the rear (low at the front, and high at rear of the cell) (Brundage *et al.*, 1991). More recently, it was shown that migrating cells also have a spatial gradient in the degree of Ca^{2+} flicker (small, spatially and temporally restricted Ca^{2+} signals) activity; their occurrence at the leading edge of migrating cells is much higher than at the rear of cells (Wei *et al.*, 2009). Both of these gradients reform in cells changing their direction of migration prior to the actual turning of the cell. When the ER Ca^{2+} store was depleted, the Ca^{2+} flicker activity continued with the same frequency (though with a reduced amplitude), suggesting that it is not release of Ca^{2+} from the ER initiating this signalling (Wei *et al.*, 2009), but instead Ca^{2+} influx across the PM. With this in mind, one could postulate that the observed distribution

of ER-PM junctions in migrating cells mirrors the distribution of the Ca^{2+} channels through which this Ca^{2+} influx occurs, especially as the junctions highlighted by STIM1 puncta do co-localise with Orai1 (Figure 3.19), suggesting that they are sites capable of mediating Ca^{2+} influx.

3.11.4 Mechanism of STIM1 puncta concentration at the periphery of cells

There are several possible mechanisms by which ER-PM junctions may be preferentially formed at these locations. The first studied was that the localisation was an artefact of depleted ER Ca^{2+} stores; this does not seem to be the case, as I observed that the peripheral distribution of STIM1 puncta in PANC-1 cells is unaffected by the status of the ER Ca^{2+} store (Figure 3.8). Whilst WT STIM1 has EF hand domains that bind Ca^{2+} when ER stores are replete (preventing its oligomerisation and translocation to junctions), STIM1(D76A) is a constitutively active STIM1 mutant incapable of binding Ca^{2+}. In cells with full Ca^{2+} stores, there was still a noticeably higher density of STIM1(D76A) puncta seen at the cell edge, indicating that this localisation is not an artefact of depleted ER Ca^{2+} stores.

It also does not seem to be critically dependent on phospholipid distribution. The STIM1(ΔK) mutant (a mutant that lacks the phospholipid binding domain) has been reported to be unable to form puncta in store-depleted cells without the simultaneous co-expression of exogenous Orai1 (Liou *et al.*, 2007; Park *et al.*, 2009). I observed however that, given enough additional time in store-depleted conditions (~ an additional 50 minutes), this construct will translocate into puncta and can distribute peripherally when expressed alone (Figure 3.9, see also Chapter 4). This surprising finding could be due to a number of reasons, primarily that either the STIM1 oligomers are forming

complexes with endogenous Orai1, or that the STIM1(ΔK) mutant was forming dimers with endogenous STIM1, allowing it to travel to ER-PM junctions. If the expression of endogenous STIM1 or Orai1 is higher in PANC-1 cells than in other cell types previously tested, this could explain why puncta formation can be seen where it has not previously been reported with this construct. My finding that STIM1(ΔK) puncta formation takes much longer than for WT STIM1 could also explain why this has not previously been reported in literature; ordinarily puncta formation takes under 10 minutes (e.g. Figure 3.1 and e.g. (Wu *et al.*, 2006; Liou *et al.*, 2007)), and it is possible that other studies did not deplete stores for sufficiently long time periods to see puncta formation.

There is also the possibility that the polybasic region mutated in this construct is only necessary for the interaction of STIM1 with TRPC1 (Huang *et al.*, 2006), and is not required for its interaction with Orai1-containing ER-PM junctions. Interestingly, the polybasic lysine-rich region is missing in the fly and worm homologues of STIM (Huang *et al.*, 2006); understanding STIM translocation to ER-PM junctions in these animals may help to solve this problem.

The interaction between STIM1 and microtubules also does not seem to be of critical importance in the distribution of STIM1 puncta in migrating cells. Several recent publications implicate microtubules as a potentially important mechanism involved in the distribution of ER-PM junctions and STIM1 puncta. The tubulin-like distribution of WT STIM1 (Figure 3.10) arises from the interaction of STIM1 with EB1, a protein that binds the plus-end of microtubules. Work by the Akhmanova lab has suggested that this tubular distribution and comet-like movement is not STIM1 travelling with EB1 as

microtubule polymerisation occurs, but is instead "a traveling wave of diffusion dependent STIM1 concentration in the ER membrane" (Grigoriev *et al.*, 2008).

I used a STIM mutant in which this interaction was disrupted and examined the distribution of STIM1 before and after store-depletion. The lack of a tubular distribution in quiescent cells expressing the STIM1(NN) mutant (e.g. Figure 3.11) was not surprising as when the EB1-STIM1 interaction is specifically inhibited the distribution of STIM1 would be expected to become much more reticular. I also found that even without binding to microtubules STIM1 puncta can still be localised to the leading edges of cells (Figures 3.11 – 3.12 and Video 3.2). Whether this is because the STIM1 in these cells is overexpressed and overriding the necessity for microtubules in the distribution of STIM1 puncta (similar to the rescue of SOCE in nocodazole-treated cells by overexpressing STIM1 (Smyth *et al.*, 2007)) is not known.

One possibility is that microtubular targeting of focal adhesions is a mechanism for directing STIM1 to ER-PM junctions (either pre-existing or newly formed) close to these locations, to promote Ca^{2+} influx at these sites and regulate Ca^{2+}-dependent proteins. Indeed, analysis of integrin distribution and Ca^{2+} flicker activity has shown the two are spatially closely associated (Wei *et al.*, 2009). Focal adhesions can undergo several cycles of interaction with microtubules (Kaverina *et al.*, 1999); this may allow sufficient interaction for the formation of nascent ER-PM junctions and SOCE complexes necessary for Ca^{2+} influx and the formation of Ca^{2+} microdomains at these locations. Further examination into the relationship between microtubules and focal adhesions with WT STIM1 and STIM1(NN) may be a useful avenue for further research.

3.11.5 Saltatory formation of puncta

The formation of puncta at the leading edge of migrating cells was shown to be saltatory in store-depleted cells, in heat-treated cells, and in cells transfected with the STIM1(NN) construct (Figures 3.13 – 3.15 and Videos 3.2 – 3.4). This saltatory formation indicates that the ER-PM junctions are not sliding forwards as the cell migrates, but are instead continually forming new junctions at the leading edge as the cell moves. This is likely to be quite an energy dependent process considering the proteins and specialised structures involved, even though STIM1 translocation to these junctions does not require ATP (Chvanov *et al.*, 2008). Several recent studies have indicated that the ER-PM junctions do not merely consist of STIM1 and Orai1, but are instead a complex of a multitude of different proteins (Srikanth & Gwack, 2012). In several cell types, only specialised forms of rough ER, with the side nearest the plasma membrane stripped of ribosomes, are used to form junctions (Lur *et al.*, 2009). With this in mind, the continued development of new ER-PM junctions at the leading edge of cells is a process that the cell is likely to be expending considerable energy to perform, highlighting its potential importance. The appearance of new focal complexes and adhesions at the leading edges of cells is similar in pattern to the saltatory appearance of ER-PM junctions seen in this investigation (Ballestrem *et al.*, 2001); potentially these junctions are providing the Ca^{2+} required for regulation of actin dynamics by Ca^{2+}-dependent processes.

The presence of local Ca^{2+} transients at the leading edge of cells has already been established, but the source of this Ca^{2+} has not previously been reported, instead only that TG does not abolish it (Wei *et al.*, 2009; Tsai & Meyer, 2012). Taken in addition to my data, this suggests that ER-PM junctions are the sites of Ca^{2+} influx at the leading edge of migrating cells and that Ca^{2+} influx

directly from the extracellular environment is crucial for dynamics at the leading edge. The emphasis on Ca^{2+} influx specifically from the external environment (instead of release of Ca^{2+} from internal stores, the refilling of which is the best known function of SOCE) draws parallels with the activation of certain Ca^{2+}-sensitive adenylyl cyclases by Ca^{2+} microdomains produced specifically by SOCE (Willoughby *et al.*, 2010).

3.11.6 Long distance translocation of STIM1 puncta during tail withdrawal

ER-PM junctions can also be found at the rear of migrating cells, a not surprising phenomenon considering that cells can, in the absence of a chemoattractant, change direction frequently. I observed that ER-PM junctions found in this region remained intact whilst the tail retracts into the cell body. Several junctions were also seen to dissolve either prior to or during tail retraction (Figures 3.16 – 3.18 and Video 3.5). This is interesting when considered in parallel with the effort a migrating cell undergoes to continually form new junctions at its leading edge. Either the cell is not prone to expending unnecessary energy in dissolving these junctions, or these junctions are functionally important. They may be functioning to maintain the increased Ca^{2+} concentration found at the rear of the cell (Brundage *et al.*, 1991), or involved in the dissolution of the remaining focal adhesions at this location. The latter of these is an interesting possibility for several reasons. Firstly, it has previously been suggested that a temporary increase in Ca^{2+} transients at the rear of the cell occurs in elongated fish keratocytes, the elongation activating stretch-activated Ca^{2+} channels and producing Ca^{2+} influx. These Ca^{2+} transients then help promote disassembly of focal adhesions in the cell rear and allow normal forward migration to continue (Lee *et al.*, 1999). Secondly, a similar pattern of sliding in retracting

cell tails has also been shown using fluorescently-tagged integrins and paxillin, suggesting that the sliding of one or more of these structures may be a cause or consequence of the others (Ballestrem *et al.*, 2001; Laukaitis *et al.*, 2001). Finally, it has also been suggested that microtubules may be essential for targeting of focal adhesions in the cell tail to promote their disassembly (Webb *et al.*, 2002; Ezratty *et al.*, 2005); the interaction of STIM with EB1 at the tip of microtubules (Grigoriev *et al.*, 2008) would suggest that this could be a mechanism for targeting ER-PM junctions to this region.

3.11.7 Conclusion

The importance of Ca^{2+} gradients and transients in cell migration has been established by substantial previous research. The findings that ER-PM junctions accumulate at the periphery, and especially at the leading edge of migrating pancreatic cancer cells, suggest that these Ca^{2+} signals are mediated via channels located in ER-PM junctions, most likely SOCE channels. The finding that cells constantly produce new junctions at the leading edge suggests that the cell places some importance on generating new junctions at these locations, especially considering the potential energy requirements of this process. The presence of junctions in the rear of cells suggests that they may play a role in tail retraction and in focal adhesion disassembly.

I found that the peripheral localisation and saltatory formation of junctions is not wholly dependent on any one of the following: the state of the ER Ca^{2+} store; the mechanism of inducing STIM translocation; the interaction of STIM with either microtubules or phospholipids. This suggests either that all these processes combine to contribute to the localisation of ER-PM junctions at the leading edge, or that an entirely different mechanism is responsible. Further

work examining the possibility of modifying the location of ER-PM junctions would help dissect out the mechanisms behind this placement, and may help us to better understand the role of SOCE in pancreatic cell migration and metastasis.

Chapter 4: Distribution of ER-PM Junctions in Relation to Migratory Proteins

Chapter 4: Distribution of ER-PM Junctions in Relation to Migratory Proteins

4.1 Overview

Chapter 3 described the distribution and dynamics of ER-PM junctions in migrating PANC-1 cells, studied using the translocation of STIM1 into puncta to highlight these sites. To rule out that artefacts arising from STIM1 overexpression caused this distribution (and confirm that this technique is a valid method of highlighting ER-PM junctions), I also studied the distribution of junctions using an alternative method to highlight their locations. A set of paired constructs designed to highlight sites of close proximity between the ER and the PM were used. This method involved the use of two constructs, a cyan fluorescent protein (CFP)-tagged construct targeted to the ER and a mRFP-tagged construct targeted to the plasma membrane (Varnai *et al.*, 2006). When rapamycin is added to cells transfected with both constructs, heterodimerisation of the two 'linker' constructs occurs, but only where the distance between the two constructs is sufficiently small (~ 10 nm). As junctions are reported to be ~ 10 – 25 nm in size (Wu *et al.*, 2006; Várnai *et al.*, 2007; Lur *et al.*, 2009), co-localisation should occur at sites of ER-PM junctions.

I also used this method and the STIM1 puncta formation method to examine the novel distribution of ER-PM junctions shown in Chapter 3 in more detail. I did this by studying the relationship between ER-PM junctions and several

different structures central to the process of migration, introduced individually below:

4.1.1 Actin

The intracellular actin network is essential to the process of migration. Polymerisation at the growing end helps to physically expand the cell membrane, creating cellular protrusions to drive migration, and the contractions required for forward movement are dependent on this network of actin filaments. Both major forms of cellular protrusions – lamellipodial and filamentous projections – are created by different forms of the actin network. I was interested to examine the relationship between the actin network and ER-PM junctions because many of the proteins involved in shaping and regulating the actin network are directly or indirectly regulated by Ca^{2+}. These include: gelsolin and villin, proteins that bind to the ends of actin filaments to prevent further disassembly or polymerisation ('capping proteins') and which can also break actin filaments (simultaneously cropping filaments and providing new nucleation sites for further actin polymerisation)(Yin & Stossel, 1979; Northrop *et al.*, 1986; Sun *et al.*, 1999); alpha-actinin, a protein that cross-links actin filaments causing them to bundle together (Burridge & Feramisco, 1981; Noegel *et al.*, 1987).

4.1.2 Focal adhesions

Focal adhesions are a complex of proteins responsible for adhering cells to the extracellular matrix (Webb *et al.*, 2002). The distribution of Ca^{2+} flicker activity that occurs at the leading edge of migrating cells is closely related spatially to the distribution of integrins, proteins that connect cells to the extracellular matrix and promote formation of focal adhesions (Wei *et al.*, 2009). As with the actin network, many of the proteins involved in the

assembly and disassembly of focal adhesions are regulated by Ca^{2+}, so close positioning of Ca^{2+} influx channels near the sites of focal adhesions may be of use to the cell. Vinculin is a protein that connects the actin cytoskeleton to the plasma membrane at sites of focal adhesions (Mierke, 2009) and is used in this investigation as a marker for these structures.

4.1.3 Calnexin

The majority of cellular STIM1 protein is found in the ER membrane, both in control and store-depleted conditions, though in the latter condition it is localised to junctions formed between the ER and plasma membrane. There is a possibility that the accumulation of STIM1 puncta in the peripheral regions of migrating cells (see Chapter 3) may have been as a consequence of increased ER density at these locations. As proteins containing the KDEL targeting sequence have been shown to be excluded from the ER that composes ER-PM junctions (Orci *et al.*, 2009), an ER resident protein without this sequence was chosen to delineate the positioning of the ER in polarised cells. Calnexin is an ER-membrane bound molecular chaperone, which does not contain a KDEL sequence (Shimizu & Hendershot, 2007) and so was suitable for this purpose.

4.1.4 Caveolin

The distribution of caveolin-1 is a reliable method for staining lipid-enriched regions of the plasma membrane ('lipid rafts') – more specifically caveolae, which are small invaginations of the plasma membrane that act as platforms for signalling complexes (Pani & Singh, 2009). Lipid rafts have been implicated in the regulation of SOCE, with modulation of caveolin-1 expression or the lipid raft component of PM affecting this process (Pani *et al.*, 2008). Caveolin-1 and lipid rafts have also been implicated in the

development of cell polarity (Grande-Garcia & del Pozo, 2008), so the relationship between the two structures (ER-PM junctions and caveolae) was studied.

4.2 Use of linker constructs as a mechanism for highlighting junctions

I used the linker constructs to verify the distribution of ER-PM junctions seen previously in polarised PANC-1 cells (n = 7). Figure 4.1 shows the linker constructs expressed in PANC-1 cells imaged live. The left panel shows the distribution in control conditions and the overlay in the bottom row shows no co-localisation of the two constructs. The right panel shows the distribution of the linkers after addition of rapamycin, and here there are large areas of co-localisation between the two separate constructs (seen as yellow in the overlay image). Note the particularly clear co-localisation at the cell periphery. Figure 4.2 shows this in more detail, depicting the development of co-localisation occurring as rapamycin is added. This figure demonstrates that co-localisation starts to occur after ~ 150 seconds, and that the extent of co-localisation drastically increases over time, eventually causing gross morphological changes. Obviously this protocol could not be used during long time scale experiments to image migrating cells (due to these morphological changes). The junctions highlighted in the images from 150 – 270 seconds however are small and are likely to depict existing junctions prior to the 'zipping up' of junctions between the PM and ER membranes seen in the later images.

Figure 4.1 Relative distribution of endoplasmic reticulum (ER) and plasma membrane (PM) linker constructs before and after the addition of rapamycin. PANC-1 cells transfected with both CFP-FRB-LL-ER-targeted and PM-targeted-LL-FKBP-mRFP constructs were imaged using a confocal microscope before and during rapamycin treatment (450 seconds after addition of 100 nM rapamycin). Scale bar represents 10 μm.

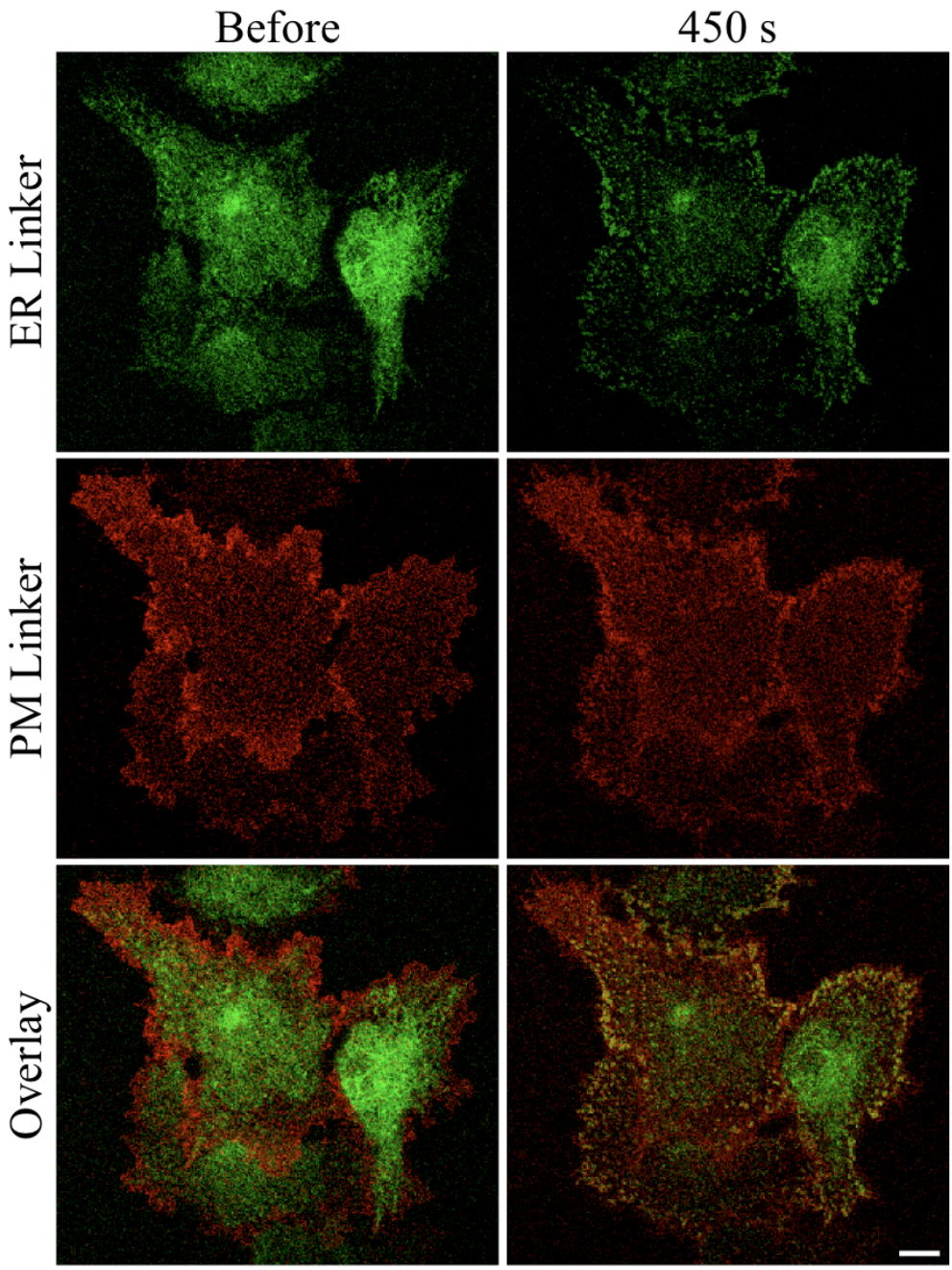

Figure 4.1 Relative distribution of endoplasmic reticulum (ER) and plasma membrane (PM) linker constructs before and after the addition of rapamycin.

Figure 4.2 Development of linker co-localisation after addition of rapamycin. PANC-1 cells transfected with the linker constructs were imaged on a confocal microscope before and during rapamycin treatment (100 nM) and the overlay of both channels is shown. Time elapsed since addition of rapamycin is indicated; scale bar represents 10 μm.

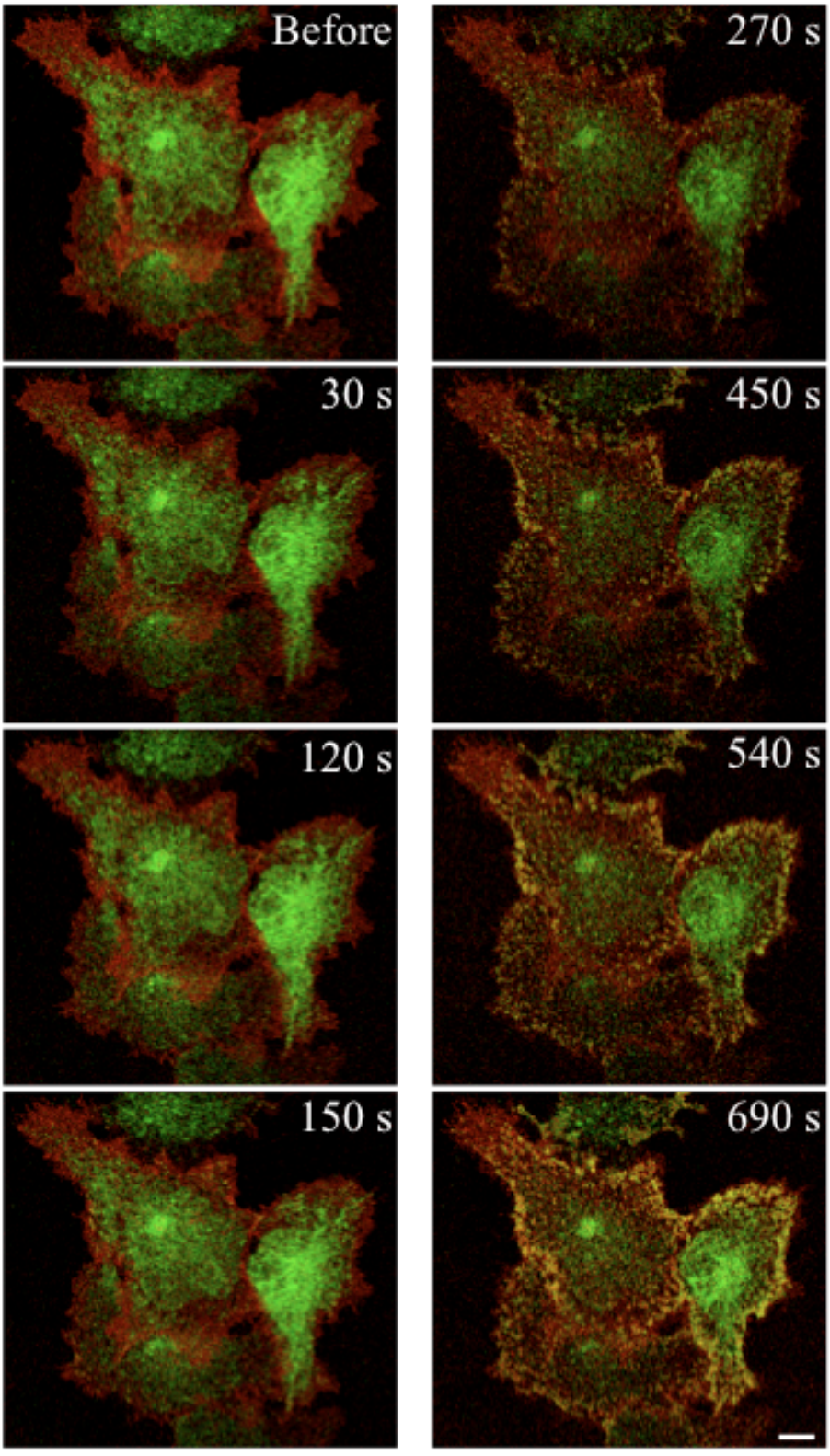

Figure 4.2 Development of linker co-localisation after addition of rapamycin.

To further validate the use of STIM1 puncta to highlight junctions (as used in Chapter 3), I then expressed all three constructs in PANC-1 cells simultaneously (i.e. TK-YFP-STIM1 and the two linker constructs) to monitor the relative distribution of the constructs in different conditions. Figure 4.3A shows PANC-1 cells expressing all three constructs that were treated with both CPA and rapamycin to induce STIM1 puncta formation and reveal the junctions (n = 3). Co-localisation of STIM1 puncta and linkers was observed (particularly at the cell periphery). To further probe the relationship between the three constructs, a line was drawn on the image of the STIM1 construct, connecting sites of puncta (drawn blind, i.e. without comparison to the linker images). This line was then overlaid onto the images of the linker constructs and the fluorescence intensity along this line was measured for all three constructs (using the ImageJ 'Plot Profile' tool). The results of this are shown in Figures 4.3B & C; the line measured (running from top to bottom) is shown in B and the resulting graph in C. The graph shows that at places where there is a high fluorescence of both the ER and PM linker constructs (indicating co-localisation, i.e. an ER-PM junction) there is also an increase in STIM1 fluorescence (indicating a puncta, and hence an ER-PM junction).

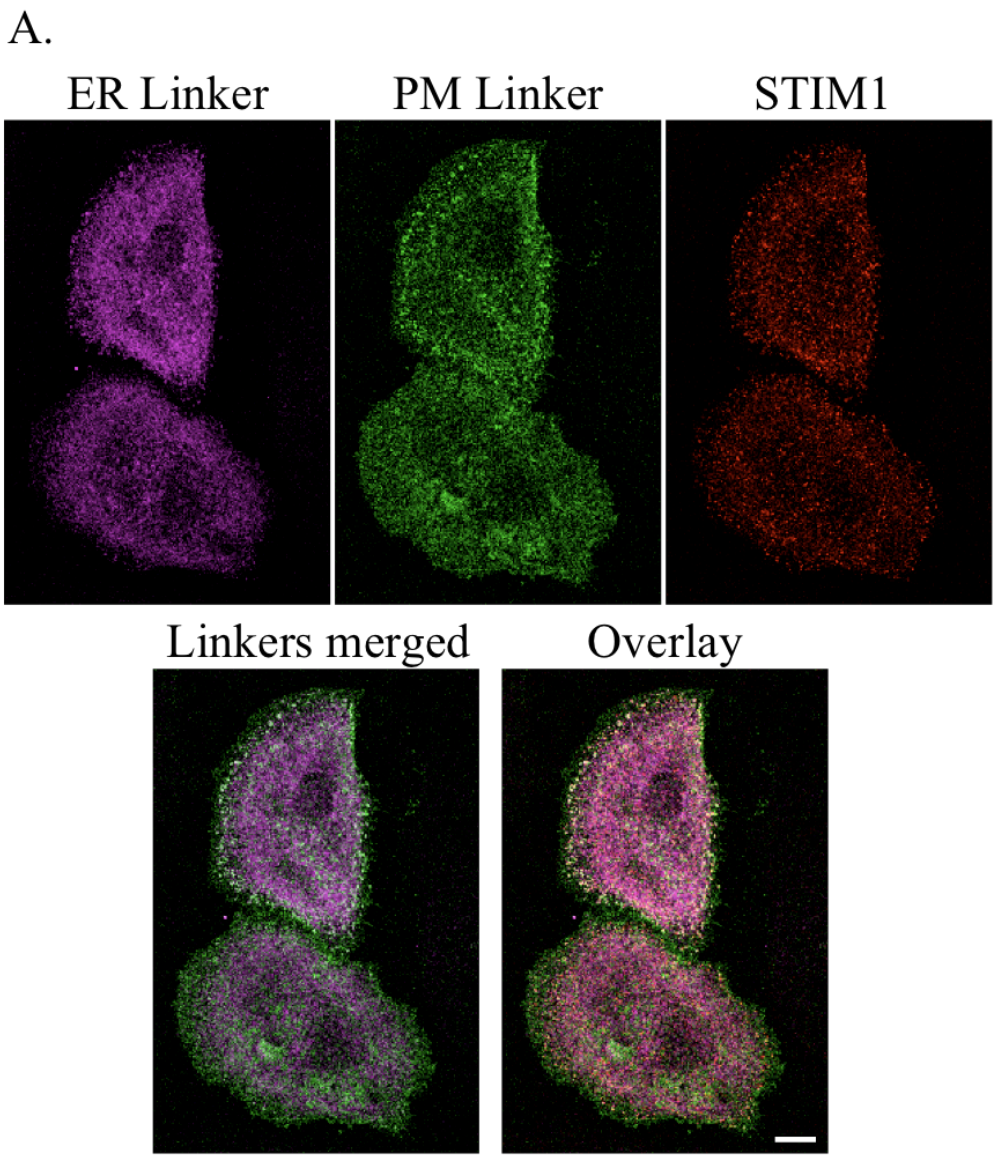

Figure 4.3 Junctions can be highlighted by linker co-localisation and by STIM1 puncta formation. PANC-1 cells transfected with the linker constructs and TK-YFP-STIM1 were treated with 15 µM CPA in 0 Ca^{2+}-media for 30 minutes before treatment with 100 nM rapamycin and 15 µM CPA in 0 Ca^{2+}-media for 4 minutes and fixation with PFA. Scale bar represents 10 µm.

Figure 4.3 (continued) Junctions can be highlighted by linker co-localisation and by STIM1 puncta formation. B. A line connecting several STIM1 puncta was overlaid onto the ER and PM channels separately. C. The fluorescence intensities of each of the three channels along the line shown in B (running from top to bottom) are shown. Scale bar represents 10 μm.

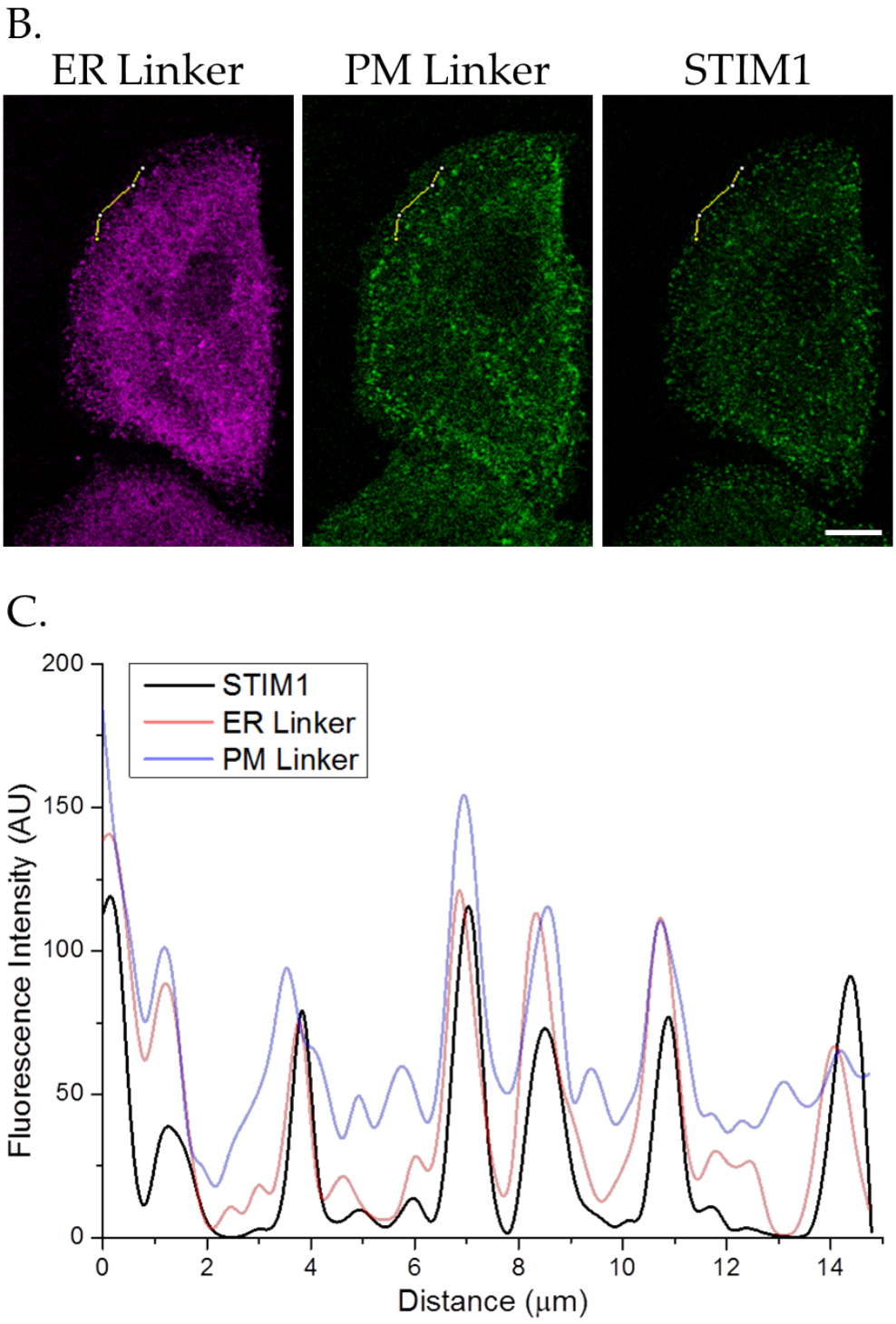

Figure 4.3 (continued) Junctions can be highlighted by linker co-localisation and by STIM1 puncta formation.

4.3 Distribution of ER-PM junctions in relation to actin

Having verified that these two methods are capable of highlighting ER-PM junctions, I then used them to study the relationship between the distribution of ER-PM junctions and proteins involved in migration. The first of these was actin, and Figure 4.4 shows the relative distribution of the ER-PM junctions and actin in PANC-1 cells (n = 4). The cells shown were expressing the linker constructs, treated with rapamycin (for 4 minutes), fixed using PFA and stained for actin using a fluorescently-conjugated phalloidin (here and elsewhere used at a dilution of 1:50). Whilst Figure 4.4A shows the original images, there were difficulties in differentiating the separate structures when all three channels were overlaid; to circumvent this problem, and to clearly display the distribution of ER-PM junctions (using the linkers) and actin simultaneously, I used the method illustrated in Figure 4.4B. Here, the two linker channels have been overlaid and a new image created showing just the pixels with above-background signals in both channels (the 'Mask'). This was achieved using the RG2B Colocalization ImageJ plugin developed by C.P. Mauer (Northwestern). When the mask and the actin channels are shown together, the relationship between the ER-PM junctions and the actin distribution can be seen much more clearly; the combined image shows that the ER-PM junctions concentrate immediately behind the actin-enriched regions of the cell (Figure 4.4).

Figure 4.4 Linker-highlighted junctions can be seen concentrated directly behind actin-rich regions in PANC-1 cells. PANC-1 cells expressing the linker constructs were treated with 100 nM rapamycin for 4 minutes in 1.8 mM Ca^{2+}-HEPES-based extracellular solution, fixed using PFA and stained for actin using fluorescently-conjugated phalloidin. Scale bar represents 10 μm.

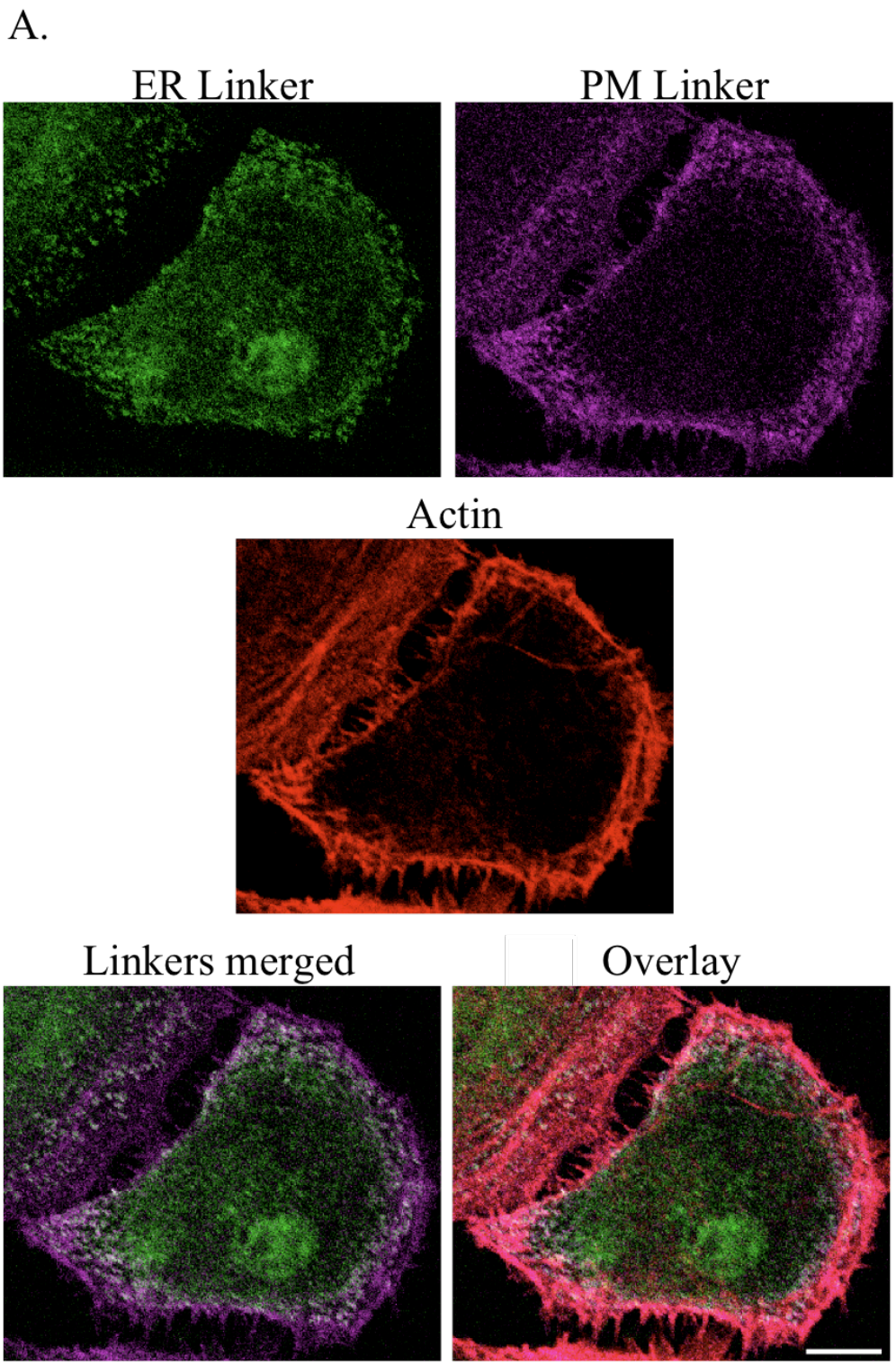

Figure 4.4 Linker-highlighted junctions can be seen concentrated directly behind actin-rich regions in PANC-1 cells.

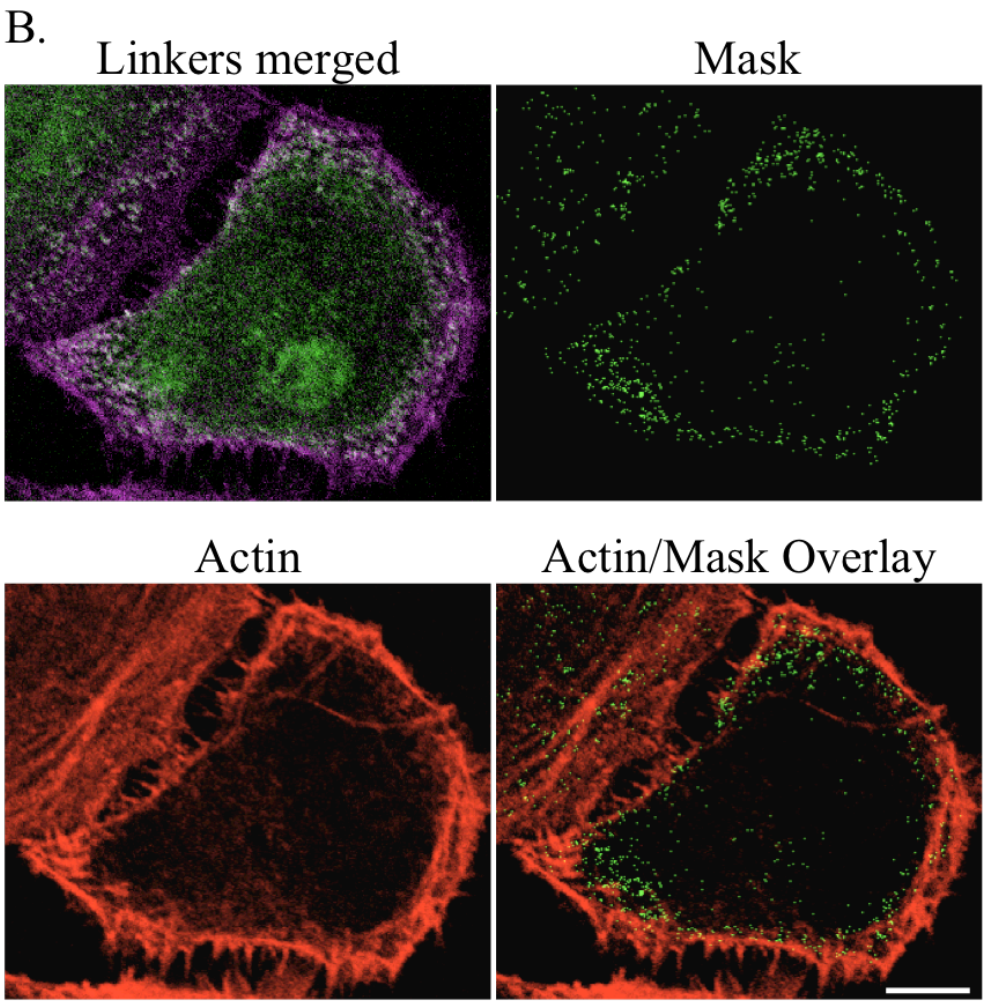

Figure 4.4 (continued) Linker-highlighted junctions are seen concentrated immediately behind actin-rich regions in PANC-1 cells. PANC-1 cells expressing the linker constructs were treated with 100 nM rapamycin and stained for actin using fluorescently-conjugated phalloidin. An image depicting just the regions of co-localisation of the two linkers (Mask) is shown overlaid onto the actin image to show the relationship between linker-highlighted junctions and actin. Scale bar represents 10 μm.

The same relationship was investigated using the distribution of STIM1 puncta (n = 5 and 2 for fixed and live images respectively). Figure 4.5 shows store-depleted PANC-1 cells expressing CMV-STIM1-YFP that were fixed with MeOH, then stained for YFP and actin (an antibody against the STIM1-conjugated fluorophore had to be used as MeOH fixation bleaches YFP fluorescence; here and elsewhere the antibody against the fluorophore was used at a 1:200 dilution). The F-actin-enriched area clearly seen at the left-hand side of the cell was more than likely the leading edge of the cell (though this cannot be known for certain as the cell was fixed). Immediately behind this area, a cluster of STIM1 puncta line the inside actin edge, followed by a region sparsely decorated with puncta, and a return to high puncta density in the cell body. A similar distribution can be seen in live cells. Figure 4.6 shows a polarised store-depleted PANC-1 cell transfected with both TK-YFP-STIM1 and LifeAct-TagRFP, a fluorescent actin construct. Here, STIM1 puncta can once again be seen sitting behind the actin-rich protrusions at the edge of the cell.

Figure 4.5 STIM1 puncta concentrate immediately behind actin-enriched regions at the leading edge of PANC-1 cells. CMV-YFP-STIM1 transfected PANC-1 cells were treated with 2 μM TG in 0 Ca^{2+}-HEPES-based extracellular solution, then fixed with MeOH and stained for actin and the STIM1-conjugated fluorophore. Scale bar represents 10 μm.

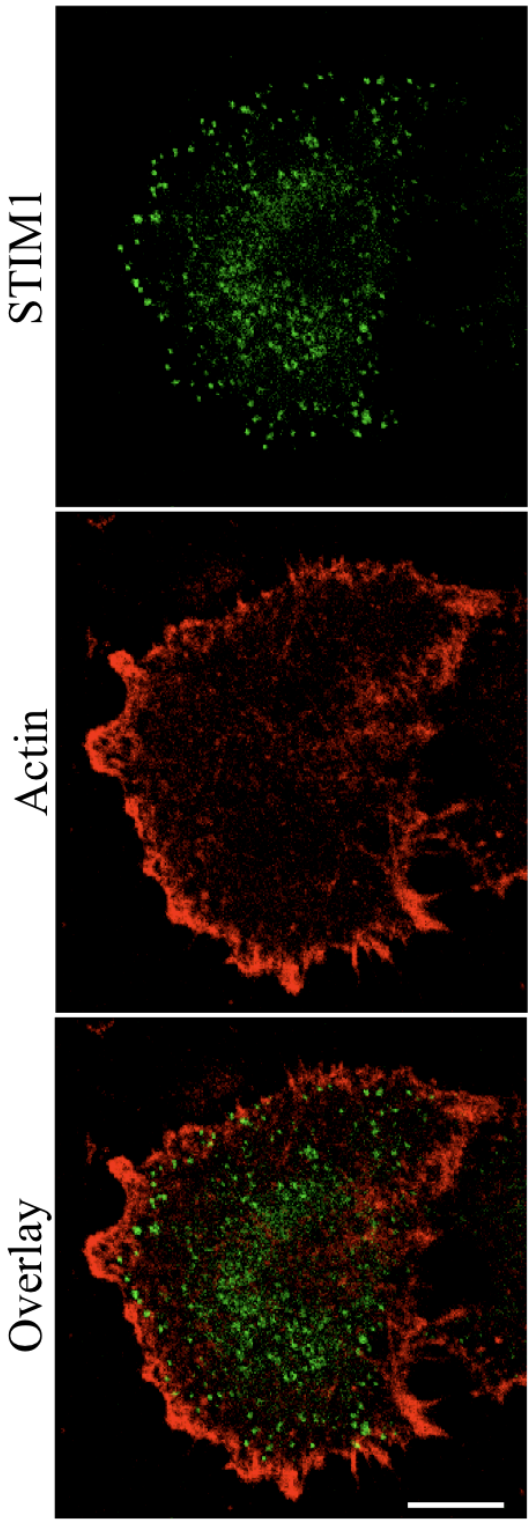

Figure 4.5 STIM1 puncta concentrate immediately behind actin-enriched regions at the leading edge of PANC-1 cells.

Figure 4.6 STIM1 puncta concentrate immediately behind actin-enriched regions at the edge of PANC-1 cells. PANC-1 cells transfected with RFP-LifeAct and TK-YFP-STIM1 were treated with 20 μM CPA in media with reduced Ca^{2+} (0.8 mM) and imaged live using a confocal microscope. Scale bar represents 10 μm.

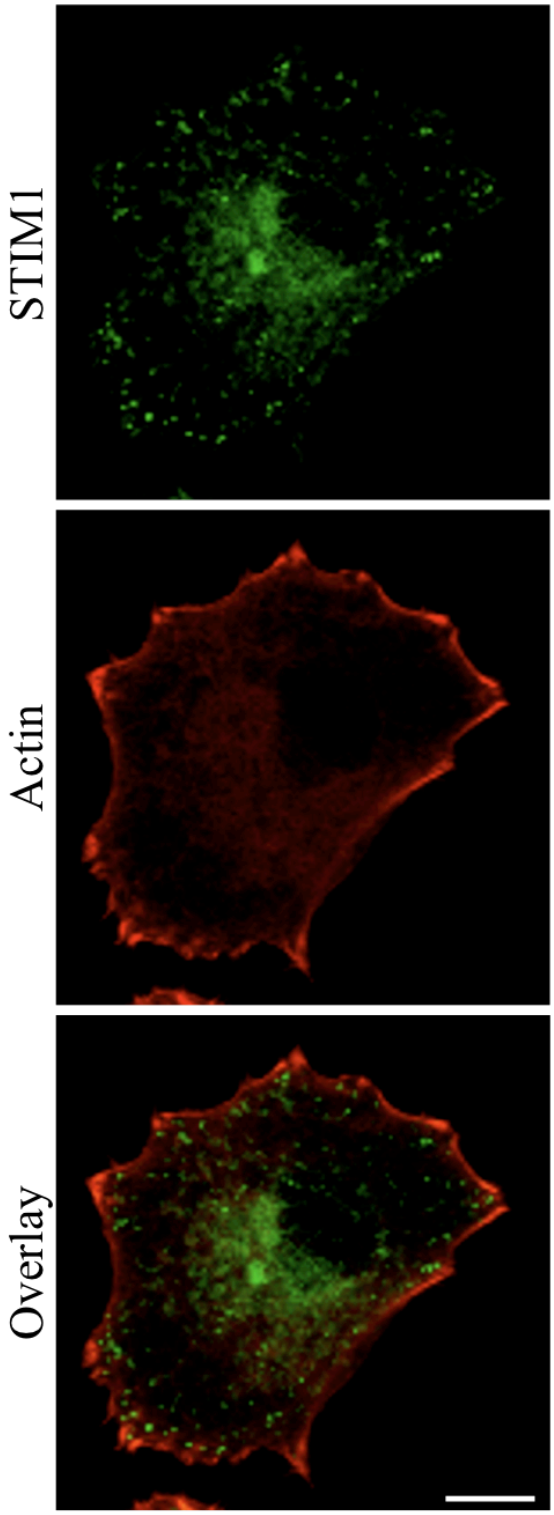

Figure 4.6 STIM1 puncta concentrate immediately behind actin-enriched regions at the edge of PANC-1 cells.

This relationship was examined further by measuring the distances between the peripheral STIM1 puncta (i.e. those found within 4 μm of the inside edge of actin staining) and the inside and outside edge of actin staining (Figures 4.7 and 4.8; n = 99 puncta in 9 cells). Whilst puncta can be found at distances between 0 and 4 μm from the inside edge (Figure 4.7), the majority of puncta (60.6%) in this range are located within 0.5 μm of the inner actin edge. When the distances to the outside edge of the actin staining were measured (Figure 4.8) the results were more wide-ranging, though distances above 7 μm were much less common (~ 2%) than those below this distance.

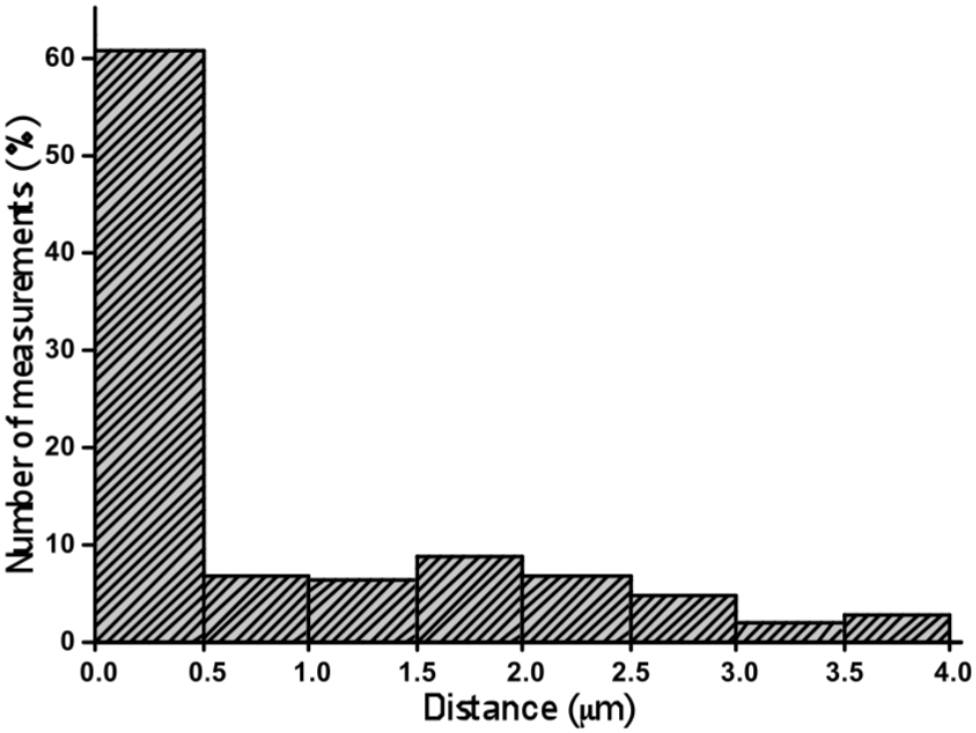

Figure 4.7 Dimensions of the STIM1 puncta-actin relationship. Distances between STIM1 puncta and the inside edge of actin staining in store-depleted PANC-1 cells transfected with TK-YFP-STIM1, fixed using PFA and stained for actin. Only puncta within 4 μm of the inside actin edge were included in the analysis.

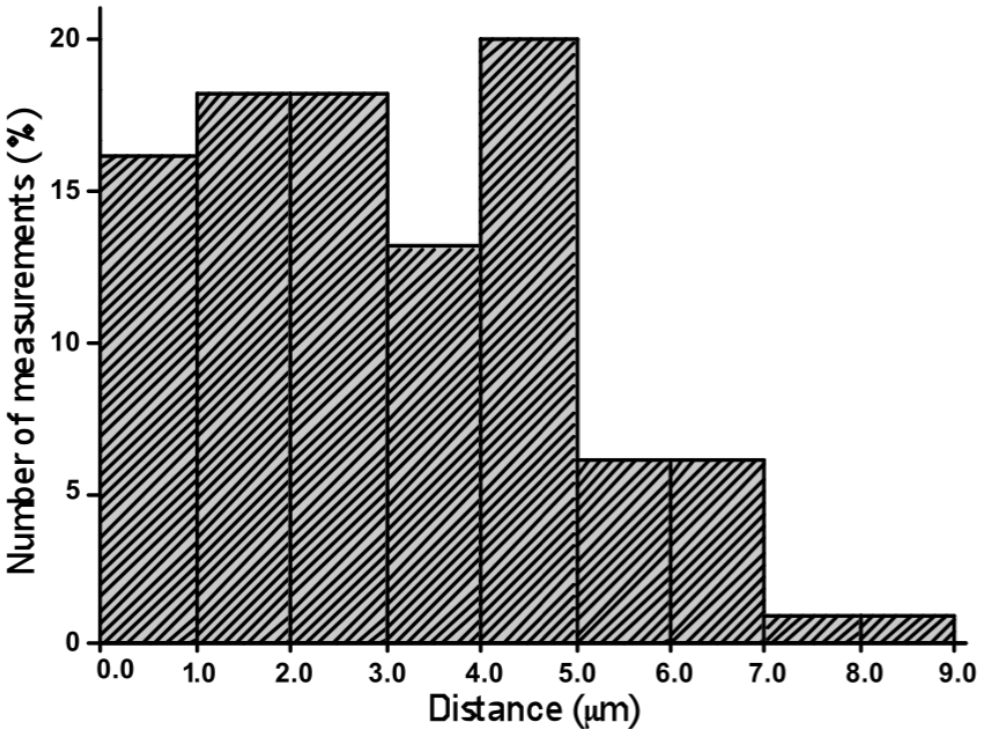

Figure 4.8 Dimensions of the STIM1 puncta-actin relationship. Distances between STIM1 puncta and the outside edge of actin staining in store-depleted PANC-1 cells transfected with TK-YFP-STIM1, fixed using PFA and stained for actin. Only puncta within 4 μm of the inside actin edge were included (with measurements taken to the outside actin edge).

Because of the close relationship between actin polymerisation and polyphosphoinositides (Saarikangas *et al.*, 2010), I studied the distribution of actin and STIM1 puncta formed by STIM1(ΔK). As shown in Chapter 3, this construct will form puncta in store-depleted PANC-1 cells if treated with a SERCA inhibitor for at least 60 minutes. With this in mind, PANC-1 cells were transfected with YFP-STIM1(ΔK) and treated with CPA in media with 0 Ca^{2+} for 60 minutes, before fixation with PFA and staining for actin using fluorescently-conjugated phalloidin (n = 2). The cell shown in Figure 4.9 displays regions of puncta closely behind actin-enriched protrusions, similarly to WT STIM1, though some internal puncta can also be observed.

Figure 4.9 STIM1(ΔK) puncta can form with a similar distribution to WT STIM1 (i.e. concentrating behind actin-enriched regions at the leading edge of cells). PANC-1 cells transfected with CMV-STIM1(ΔK)-EYFP were treated with 30 μM CPA for 60 minutes in media with 0 Ca^{2+}, before fixation with PFA and staining for actin using fluorescently-conjugated phalloidin. B is a magnification of A; scale bars represent 10 μm.

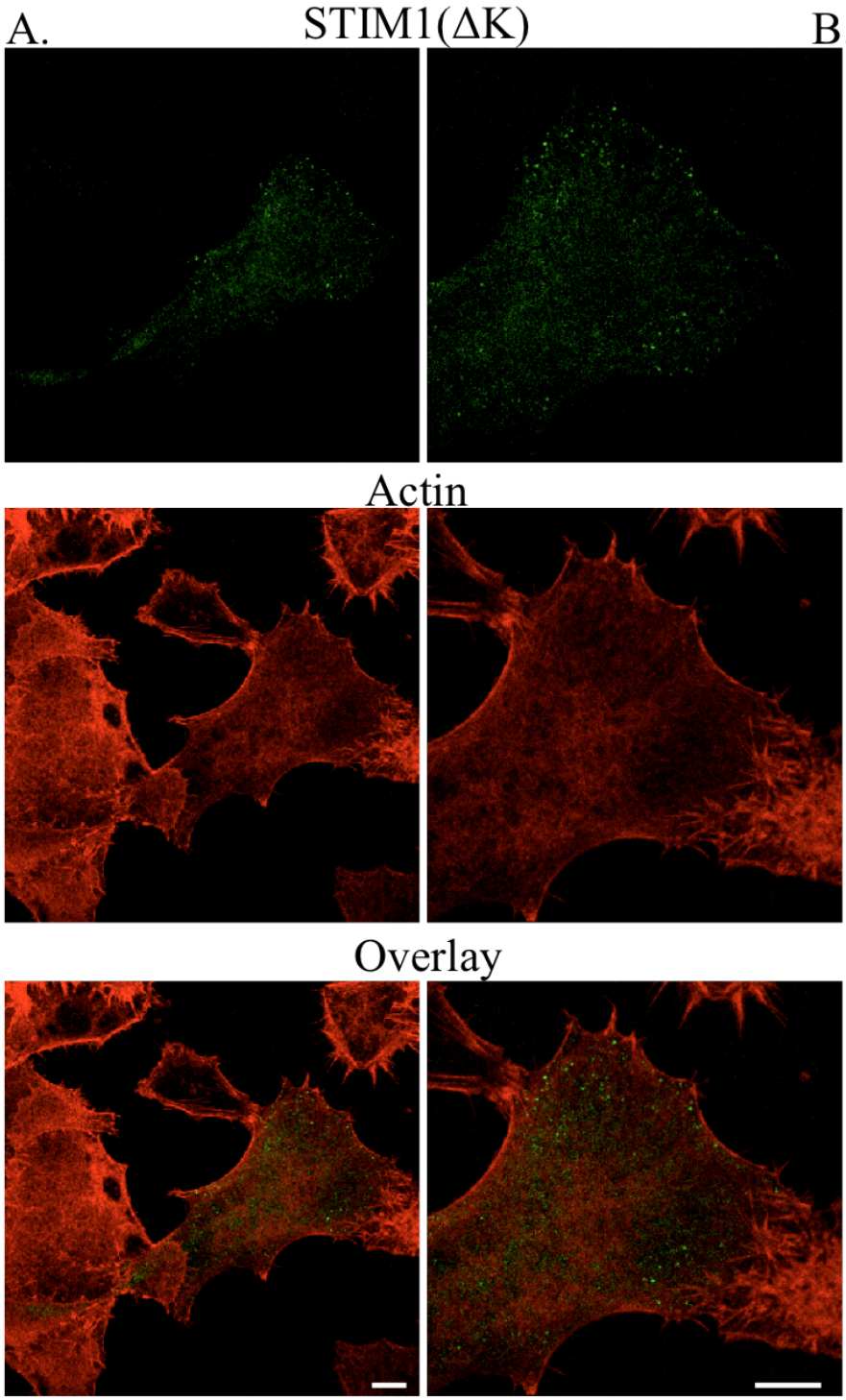

Figure 4.9 STIM1(ΔK) puncta can form with a similar distribution to WT STIM1 (i.e. concentrating behind actin-enriched regions at the leading edge of cells).

4.4 Distribution of ER-PM junctions in relation to vinculin

Vinculin is a protein that connects the actin cytoskeleton to the plasma membrane at sites of focal adhesions (Mierke, 2009); it was of interest therefore to examine if there was a distinctive relationship between vinculin and distribution of ER-PM junctions. Figure 4.10 shows store-depleted PANC-1 cells expressing TK-YFP-STIM1 fixed using PFA and stained for vinculin (n = 4; here and elsewhere the antibody against vinculin was used at a 1:200 dilution). The vinculin distribution is similar to that reported in the literature (e.g. (Chen *et al.*, 2005)); the distribution of STIM1 puncta is similar to that shown previously, though it shows a slightly more tubular distribution in the centre of the cell than some of the previously shown store-depleted cells. At the cell periphery many of the vinculin complexes seem to be closely associated with STIM1 puncta, a phenomenon further highlighted in Figure 4.10B which shows a magnification of the cell periphery. The distances between vinculin-containing focal adhesions and the closest STIM1 puncta were examined (Figure 4.11; n = 84 puncta in 7 cells) and shown to be usually less than 0.5 μm (77%), though larger distances are also seen.

Figure 4.10 STIM1 puncta can be found close to vinculin-rich regions in PANC-1 cells. TK-YFP-STIM1 transfected PANC-1 cells were treated with 15 μM CPA in full media with reduced Ca^{2+} (0.8 mM), then fixed using PFA and stained for vinculin. A. Scale bar represents 10 μm. B. A magnification of the images in A; scale bar represents 5 μm.

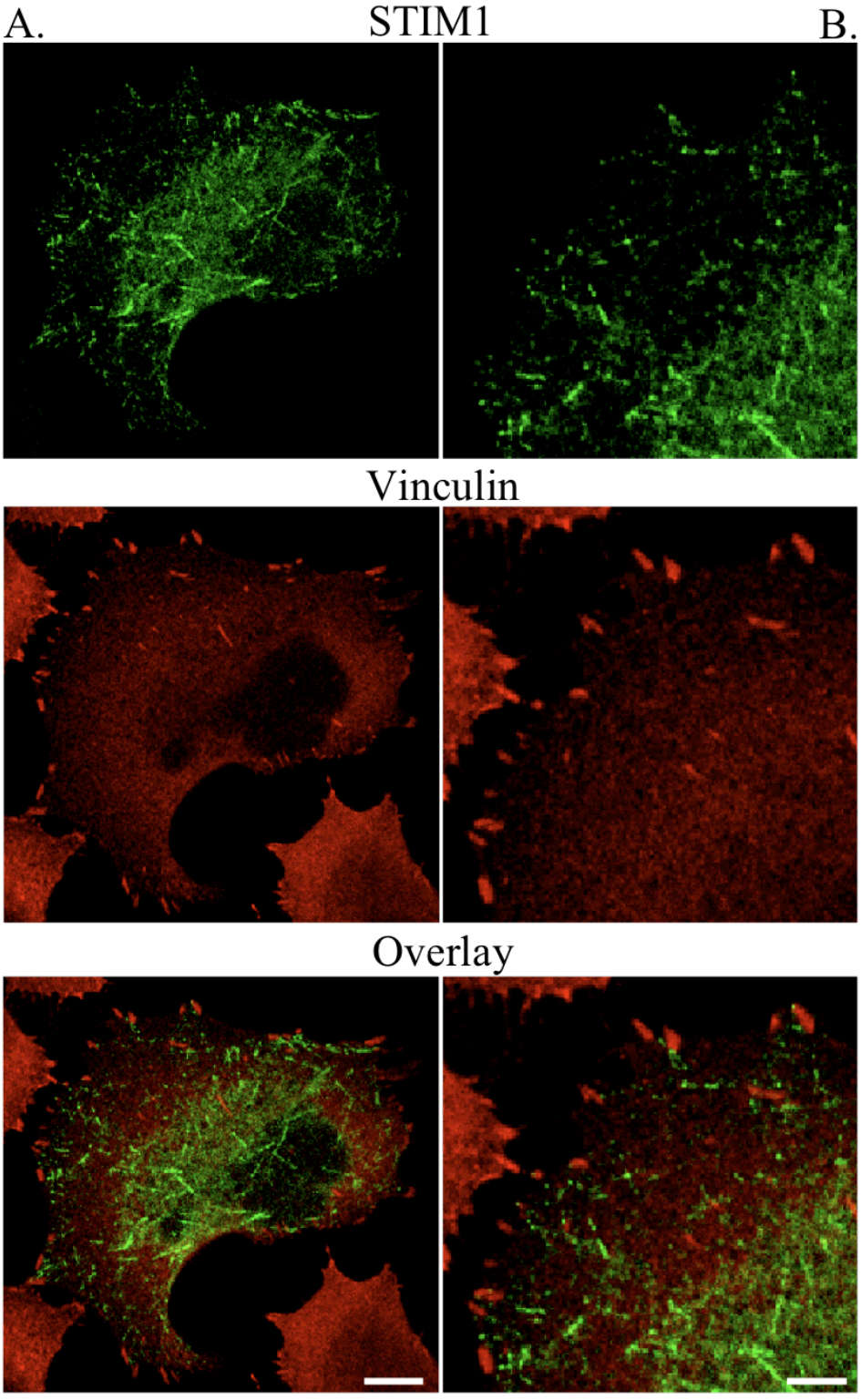

Figure 4.10 STIM1 puncta can be found close to vinculin-rich regions in PANC-1 cells.

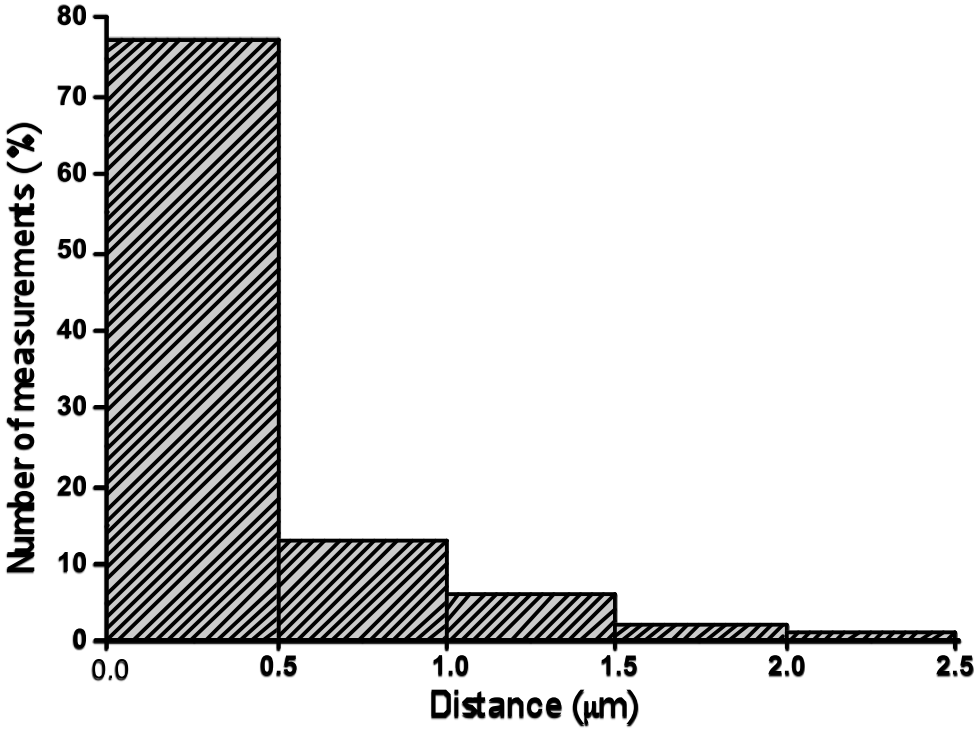

Figure 4.11 Dimensions of the STIM1 puncta-vinculin relationship. Distances between vinculin and the nearest STIM1 puncta in STIM1-transfected PANC-1 cells were measured. PANC-1 cells were fixed and stained for vinculin.

Figure 4.12 shows four high magnification images (n = 4) of sites of vinculin / STIM1 puncta association, emphasising the extremely small distances between the two structures (often below the limits of the resolution of the confocal microscope).

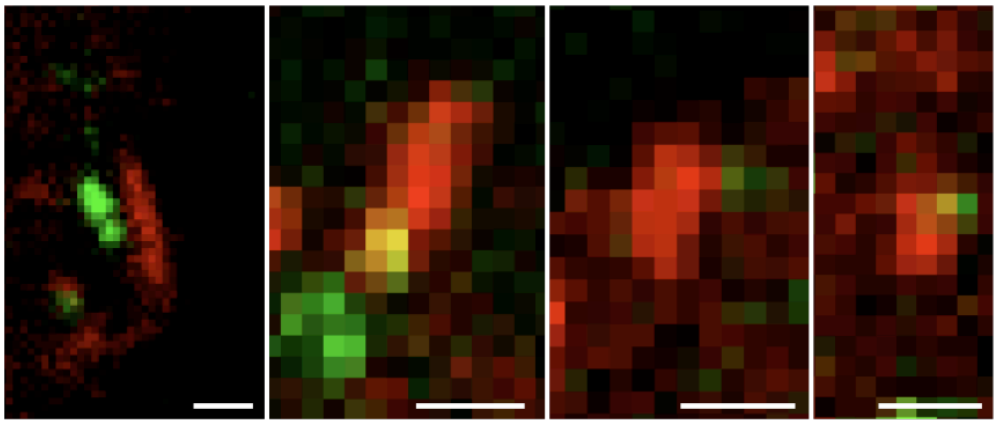

Figure 4.12 High magnification images show the spatial relationship between focal adhesions and STIM1 puncta. High magnification images of closely apposed vinculin (red; used as a marker for focal adhesions) and STIM1 puncta (green) in store-depleted PANC-1 cells expressing fluorescently-tagged STIM1, fixed, and stained for vinculin. Scale bars represent 1 μm.

4.5 The concentration of STIM1 puncta at the leading edge of cells is not due to an increased density of ER

To determine whether the increased STIM1 puncta density at the periphery of PANC-1 cells was due to an increased presence of ER, I studied the positioning of calnexin (an ER membrane protein) relative to STIM1 in both control and store-depleted conditions. Figure 4.13 shows a reticular distribution of both calnexin and STIM1 in untreated CMV-STIM1-YFP transfected PANC-1 cells (n = 2; here and elsewhere the antibody against calnexin was used at a 1:100 dilution), with a large amount of co-localisation between the two proteins seen as expected (similar experiments were carried out by a colleague in the laboratory – E. Okeke – which confirmed the findings from these experiments). Towards the edge of the cell there is a gradual reduction in both STIM1 and calnexin. Figure 4.14 shows the same proteins in a store-depleted STIM1 transfected PANC-1 cell (n = 2); the distribution of calnexin is mainly unchanged (high staining in central regions and low at the periphery). STIM1 has a punctate distribution and the peripheral puncta are located in the region with the decreased density of calnexin (again similar experiments were carried out by E. Okeke and confirmed the findings from these experiments).

Figure 4.13 STIM1 relationship to ER distribution in untreated PANC-1 cells. PANC-1 cells expressing CMV-YFP-STIM1 in control conditions (i.e. not store-depleted) were fixed with PFA and stained for calnexin. Scale bar represents 10 μm.

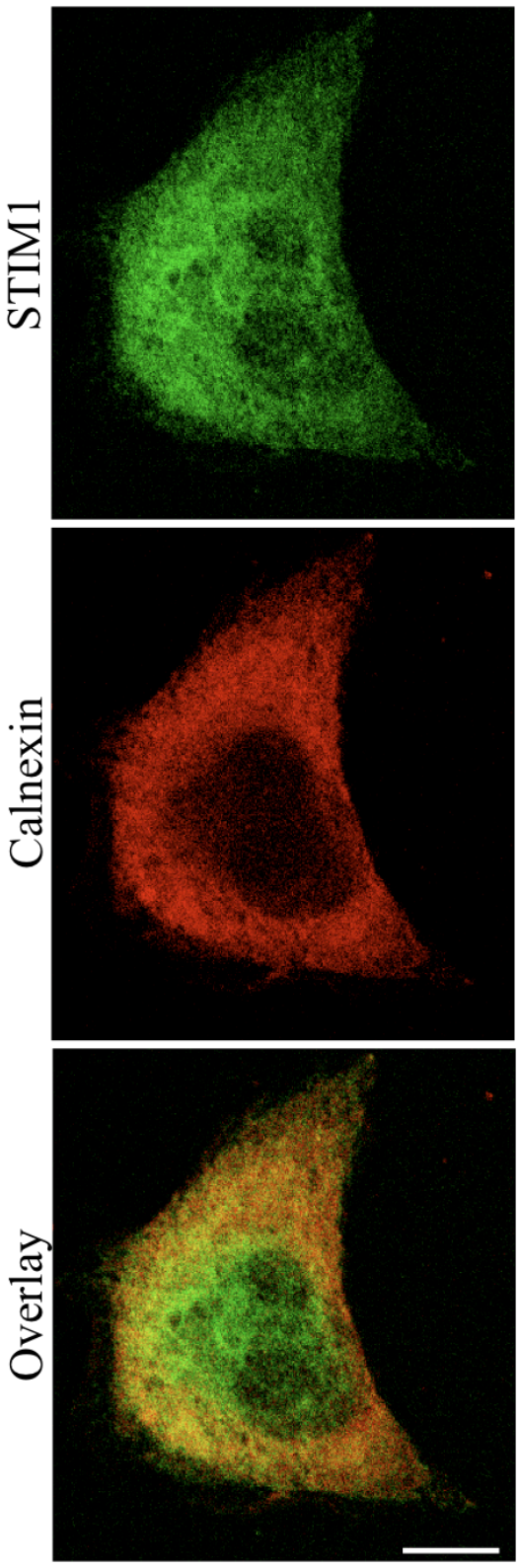

Figure 4.13 STIM1 relationship to ER distribution in untreated PANC-1 cells.

Figure 4.14 STIM1 puncta localisation in relation to ER distribution. PANC-1 cells expressing CMV-YFP-STIM1 were treated with 2 μM TG in a 0 Ca^{2+}-HEPES-based extracellular solution, fixed with PFA and stained for calnexin. Scale bar represents 10 μm.

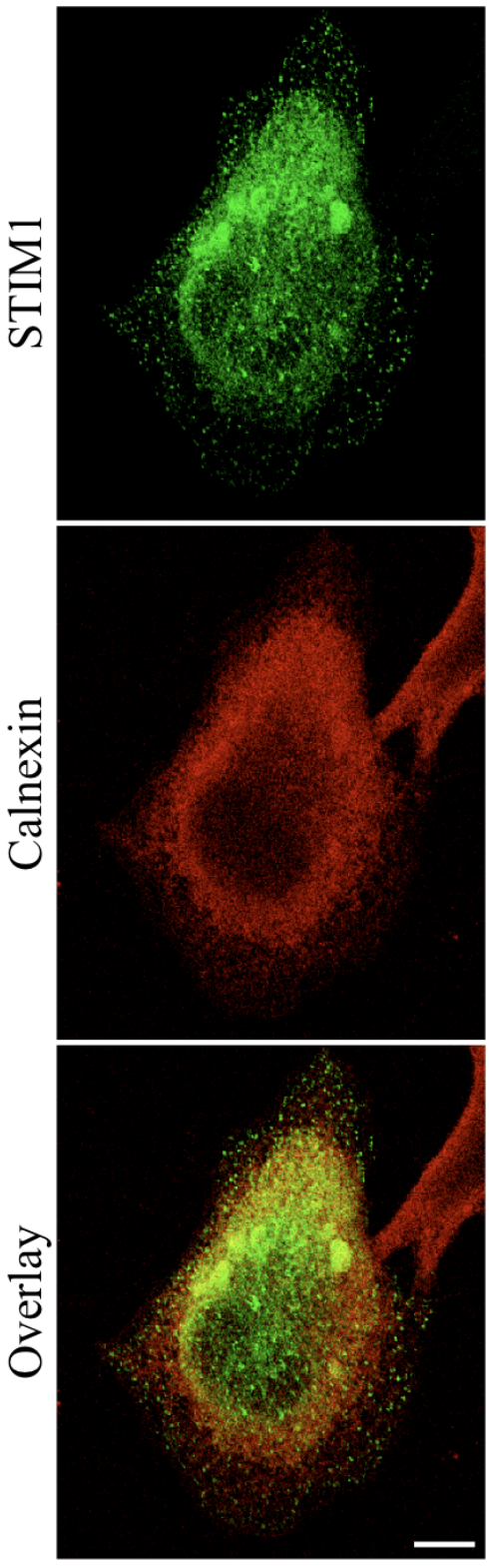

Figure 4.14 STIM1 puncta localisation in relation to ER distribution.

4.6 Localisation of caveolin in relation to STIM1 puncta

Caveolin, a key component of caveolae, is found concentrated in lipid-rich regions of the PM, regions potentially involved in the regulation of SOCE and the distribution of ER-PM junctions (Pani & Singh, 2009). I therefore investigated the distribution of caveolin-1 in PANC-1 cells. Figure 4.15 shows the intriguing distribution of caveolin in control and store-depleted PANC-1 cells (n = 4 for both; here and elsewhere the antibody against caveolin was used at a 1:100 dilution). The localisation is similar in both conditions; it is interesting that caveolin seems to be preferentially concentrated at the rear of the cell in each instance (the presumed rears of cells shown are indicated by white arrows). This rear positioning can also be seen in Figure 4.16, which shows a PANC-1 cell transfected with CMV-STIM1-YFP and kept in control conditions before fixation and staining.

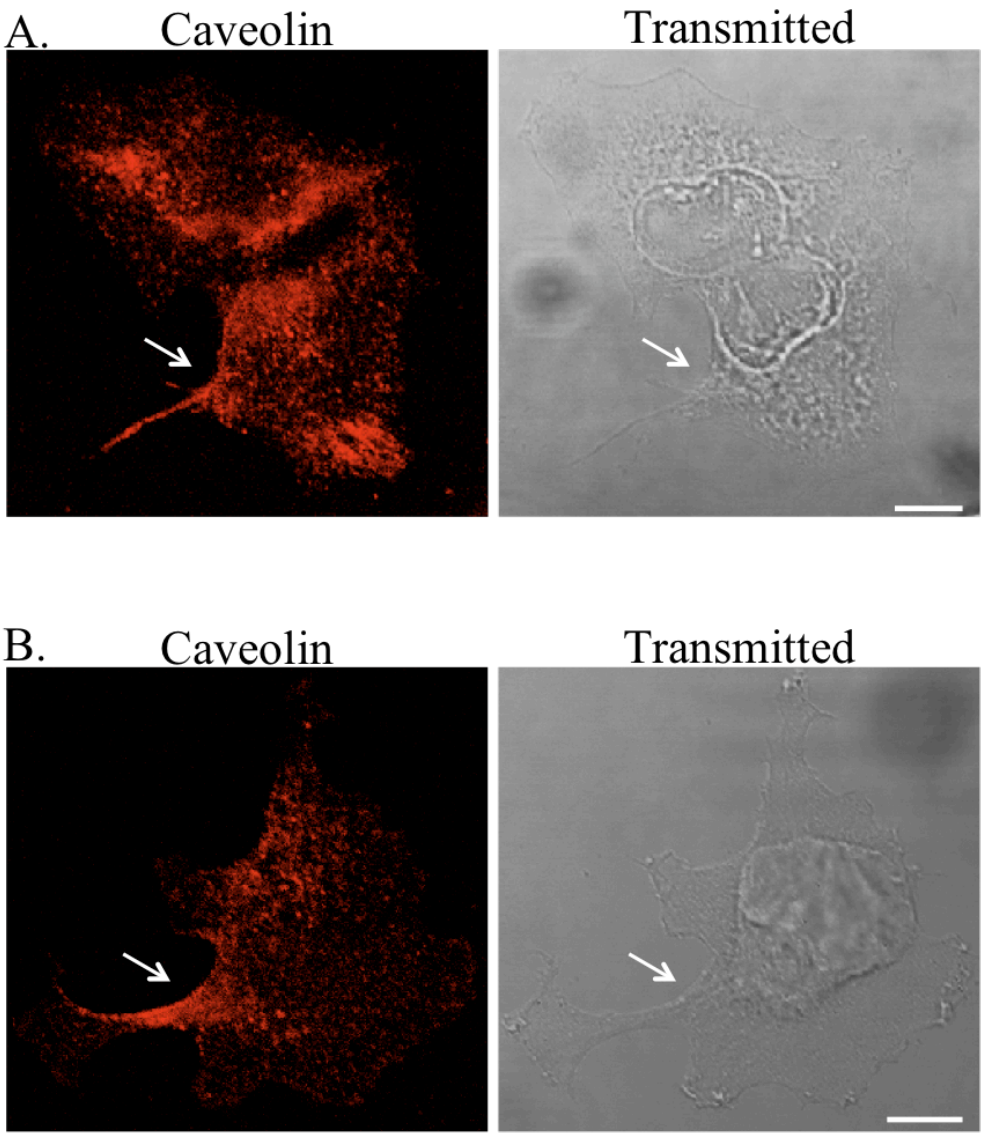

Figure 4.15 Caveolin distribution in non-transfected PANC-1 cells. Non-transfected PANC-1 cells were A. kept in control conditions or B. treated with 2 μM TG in 0 Ca^{2+}-HEPES-based extracellular solution, before fixation with MeOH and staining for caveolin. Arrows indicate presumed cell rear; scale bars represent 10 μm.

Figures 4.16 and 4.17 show the relative distribution of caveolin-1 and STIM1 in both control and store-depleted conditions. Both figures show PANC-1 cells transfected with CMV-YFP-STIM1, fixed and stained for the STIM1-conjugated fluorophore and caveolin-1. Figure 4.16 shows a typical reticular distribution of STIM1 in control PANC-1 cells (n = 2). Figure 4.17 shows a store-depleted PANC-1 cell (n = 2); the distribution of STIM1 is fairly typical, and there are many peripheral puncta. Both figures show no apparent co-localisation of STIM1 and caveolin.

Figure 4.16 STIM1 localisation in relation to caveolin distribution. PANC-1 cells expressing CMV-YFP-STIM1 were kept in control conditions (i.e. not store-depleted), then fixed with a 1:1 MeOH/EtOH mix and stained for caveolin and the STIM1-conjugated fluorophore. Scale bar represents 10 μm.

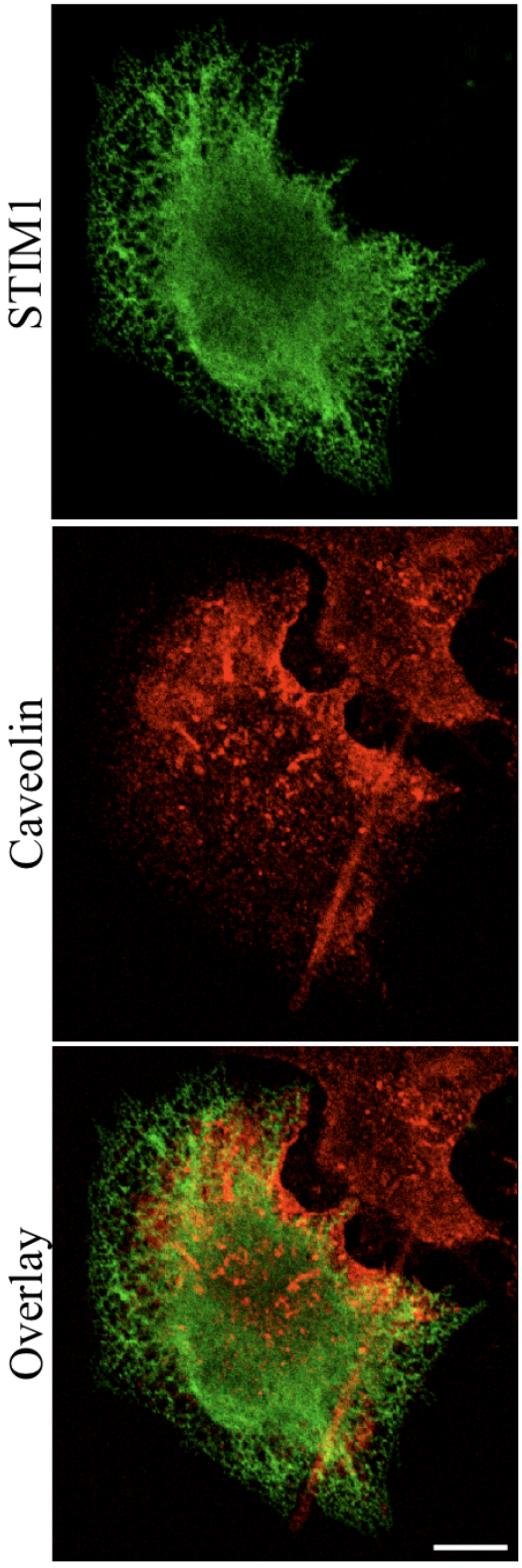

Figure 4.16 STIM1 localisation in relation to caveolin distribution.

Figure 4.17 STIM1 puncta distribution in relation to caveolin. PANC-1 cells expressing CMV-YFP-STIM1 were treated with 2 μm TG in 0 Ca^{2+}-HEPES-based extracellular solution, fixed with MeOH and stained for caveolin and the STIM1-conjugated fluorophore. Scale bar represents 10 μm.

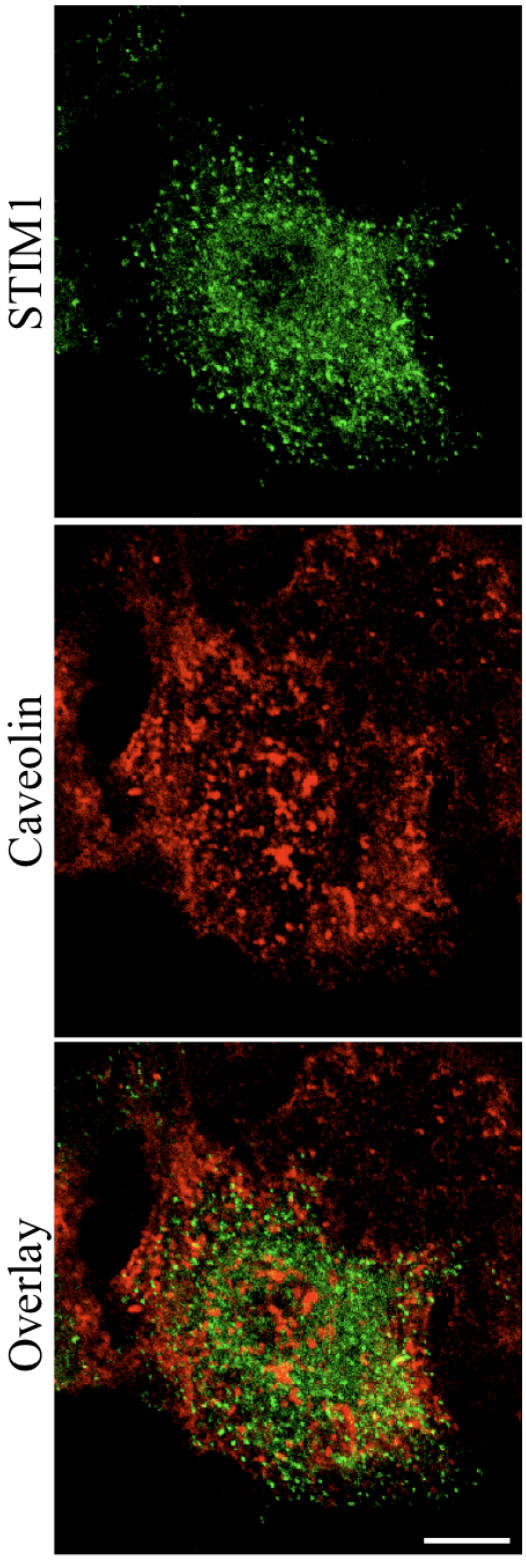

Figure 4.17 STIM1 puncta distribution in relation to caveolin.

4.7 Summary

4.7.1 Overview

The second part of my investigation showed that the peripheral distribution of ER-PM junctions previously shown could also be displayed using an alternative method of highlighting junctions. I found that ER-PM junctions are found in close proximity to actin-enriched regions and sites of vinculin-containing complexes, and that the peripheral distribution of STIM1 puncta is independent of ER density. I also found no co-localisation between ER-PM junctions and caveolin, in either control or store-depleted conditions, despite previous reports to the contrary.

4.7.2 Verification of ER-PM junction distribution in polarised PANC-1 cells

A set of linker constructs designed to co-localise upon addition of rapamycin were used to investigate the distribution of ER-PM junctions in polarised cells. These contain a FRB / FKBP fragment split between two constructs. Upon addition of rapamycin, the two fragments combine, provided the space between them is sufficiently small to allow this (~ 10 nm)(Várnai *et al.*, 2007). As the two constructs were targeted to the PM or ER, they should only combine at sites where the ER and PM are close enough together, i.e. ER-PM junctions. Data from experiments using these constructs confirmed the distribution of junctions as seen in Chapter 3, showing peripheral localisation of junctions (Figures 4.1 – 4.2). Figure 4.2 demonstrates why this method of highlighting junctions cannot be used in long time-scale experiments, as over time, the conjoining of the two constructs causes the junctions to spread along the ER-PM contact sites, grossly affecting the membrane interface.

4.7.3 Relationship between ER-PM junctions and actin

Polymerisation of actin is a process integral to cell migration, so I studied the relationship between ER-PM junctions and actin staining in polarised PANC-1 cells (Figures 4.4 – 4.8). Using two separate approaches (i.e. both linkers and STIM1 puncta) to highlight junctions, I found that junctions were located in the close vicinity of actin-enriched regions, likely to represent regions of high actin dynamics. I examined this in more detail by studying the dimensions of this relationship in STIM1-transfected, store-depleted PANC-1 cells, looking at the distances between STIM1 puncta and both the inside and outside edge of actin staining. When compared to the inside edge of actin, most peripheral STIM1 puncta were located in close proximity (closer than 0.5 μm) to the actin staining (though larger distances were seen). The distances to the outside actin edge were both much larger, and more evenly distributed. This likely indicates that whilst there are differences in the thickness of actin-enriched regions at the periphery of PANC-1 cells, the actual minimal distance between actin and STIM1 is relatively small. It also suggests that it is the positioning of STIM1 puncta just behind the actin-enriched regions that is tightly regulated by the cell, and not the positioning of STIM1 puncta in relation to the absolute edge of actin staining.

A similar STIM1 puncta-actin relationship was seen in store-depleted cells expressing the STIM1(ΔK) mutant construct (Figure 4.9), indicating that the relationship is not due to STIM1 interacting with an increased concentration of certain types of phospholipids that can often be found at the leading edge of migrating cells (Saarikangas *et al.*, 2010).

4.7.4 Relationship between ER-PM junctions and focal adhesions

I also examined the spatial relationship between vinculin and STIM1 puncta (Figures 4.10 – 4.12). Vinculin is an integral part of newly formed focal complexes, connecting the actin network to the plasma membrane. Previous studies have indicated that Ca^{2+} flicker events are closely associated with the distribution of integrins (indicative of sites of focal adhesions)(Wei *et al.*, 2009); I saw a similar distribution between vinculin and STIM1. There was a close association of vinculin complexes with STIM1 puncta / ER-PM junctions. The majority of vinculin complexes at the cell periphery were within ~ 0.5 μm of the nearest STIM1 puncta or less (indeed overlaps between the two structures can be seen in high magnification images). Together with literature suggesting that Ca^{2+} influx at the leading edges of cells helps strengthen focal adhesion complexes (Tsai & Meyer, 2012), this again suggests that there is an increased occurrence of Ca^{2+} flickers at the leading edges of cell, and that this is conducted by SOCE channels.

4.7.5 Relative distribution of calnexin

The distribution of an ER-resident protein, calnexin, was examined in relation to the distribution of STIM1 in both control and store-depleted PANC-1 cells (Figures 4.13 – 4.14). The calnexin staining gradually disappears towards the cell edge in cells from both conditions. The distribution of STIM1 however is markedly different in the two separate conditions. Whilst it shows the same reticular distribution as calnexin in control conditions (as expected for an ER-resident protein), it has a very different distribution to calnexin in store-depleted conditions. At the periphery of the cell, there is a high density of STIM1 puncta in regions where the calnexin (i.e. ER density) is minimal. This suggests that not only is

STIM1 puncta concentrating at the cell periphery of polarised cells, it is doing this on a background of low calnexin density, making the ratio between STIM1 puncta and ER density highest at the cell edge, and suggesting that the properties of the ER and PM in this region are particularly conducive for junction formation.

4.7.6 Caveolin and ER-PM junctions in migrating cells

The role of caveolin and plasma membrane lipid rafts in the formation of SOCE-competent ER-PM junctions is controversial. Literature seems to suggest that although cholesterol depletion and disruption of lipid rafts inhibits SOCE, the main role of lipid rafts is to aid the colocalisation of TRP channels and STIM1 after store-depletion (Lockwich *et al.*, 2000; Alicia *et al.*, 2008; Pani *et al.*, 2008; Pani & Singh, 2009). Caveolin-1 also plays a role in cell migration (Beardsley *et al.*, 2005). My work has shown that caveolin-1 is polarised in PANC-1 cells, displaying strong staining at the rear of the cell as reported (Beardsley *et al.*, 2005), and that there is minimal co-localisation of STIM1 with caveolin upon store-depletion in this cell type.

Whilst for the most part it is the alternative store-dependent TRP Ca^{2+} influx channels that are reported to be found in caveolin-dense lipid domains, Orai1 is also found associated with caveolin during meiosis, where caveolin-dependent Orai1 internalisation inhibits SOCE during this process (Yu *et al.*, 2010). Further work would involve over-expressing Orai1 and caveolin to help determine the specific distribution of STIM1 and caveolin-1 in polarised pancreatic cancer cells.

The lack of co-localisation of STIM1 with caveolin in store-depleted PANC-1 cells contradicts suggestions by Yang et al that TRP channels mediate the Ca^{2+} influx steering cell migration. SOCE-competent TRP channels have been

shown several times to localise to lipid raft domains, particularly caveolin-containing lipid raft domains. If in PANC-1 cells, STIM1 is not co-localising with these domains, then SOCE in these cells is unlikely to be mediated by TRP channels, and is more likely to be mediated by the STIM1-Orai1 complexes.

4.7.7 Conclusion

This chapter describes the distribution of peripheral ER-PM junctions in pancreatic cancer cells in relation to several other proteins / structures integral to cell migration. My findings strongly suggest that the Ca^{2+} flickers that have been previously reported to be critical during cell migration are probably mediated by SOCE channels, at least in this cell type. A separate approach to examining the distribution of ER-PM junctions (that circumvented the need for store-depletion or over-expression of the STIM protein) confirmed the distribution described previously in Chapter 3, suggesting that my findings may well be physiologically relevant. The close relationship seen between ER-PM junctions and regions of high actin dynamics and sites of focal adhesions suggest that Ca^{2+}-dependent processes occurring here can be regulated by SOCE, and may not require Ca^{2+} release from the ER. This may be of importance considering the intracellular Ca^{2+} concentration at the front of cells is much lower compared to that at the rear, and the $[Ca^{2+}]_{ER}$ may also be diminished in this region. Further investigation into the distribution of Ca^{2+}-dependent migration proteins in relation to SOCE complexes, and modification of focal adhesion turnover may be a useful research direction for the future.

Chapter 5: Localisation of Orai1 in Pancreatic Acinar Cells

Chapter 5: Localisation of Orai1 in Pancreatic Acinar Cells

5.1 Overview

Previous studies into SOCE complexes in pancreatic acinar cells have yielded intriguing results; STIM1 has been shown to only translocate to ER-PM junctions found at the basolateral region of the pancreatic acinar cell upon store-depletion, segregating Ca^{2+} influx sites from IP_3R release sites (Lur *et al.*, 2009). The distribution of Orai1 however has been reported to be both at the basolateral membrane (where it co-localises with STIM puncta), and much more strongly, in the apical region of the acinar cell, a region in which ER-PM junctions have not previously been seen. This has thrown up some interesting questions as to the function of apical Orai1 if it is not co-localising with its usual partner, STIM. Additionally, there is strong co-localisation of apical Orai1 with the IP_3Rs, a distribution unaffected by the state of the ER Ca^{2+} stores (Lur *et al.*, 2011). The apical region of pancreatic acinar cells is heavily packed with zymogen granules (which do contain IP_3Rs), and contains little ER with which to form ER-PM junctions, in which Orai1 channels would ordinarily be found in store-depleted conditions.

The hypothesis investigated here is that this apical Orai1 is not located in the plasma membrane, but is instead in a separate sub-plasmalemmal structure in which it interacts with IP_3Rs.

5.2 Apical IP_3R2 and Orai1 in pancreatic acinar cells

Figure 5.1 shows the localisation of IP_3R2s in a cluster of rat pancreatic acinar cells (n = 6). Cells were freshly isolated, fixed using MeOH and stained for the IP_3R2 with an antibody against the N-terminal (at a dilution of 1:50). The top panel shows a single confocal section and the bottom panel shows a maximum projection of the cell cluster. The strong apical staining is very characteristic for pancreatic acinar cells (Lur *et al.*, 2011).

Figure 5.2 shows the distribution of Orai1 seen in mouse pancreatic acinar cells virally transfected with a fluorescently-tagged Orai1 (n = 2; the same experiments were carried out by a laboratory colleague – G. Lur – and achieved similar results); viral transfection is required to transfect isolated pancreatic acinar cells as ordinary constructs cannot be transfected into these cells (Padfield *et al.*, 1998; Nicke *et al.*, 1999). The figure shows a maximum projection of a single cell cluster. The cells have very bright apical staining and much weaker basolateral plasma membrane staining, but it is not possible from this image to determine if the apical fluorescence is due to Orai1 located in the plasma membrane or solely in regions beneath it.

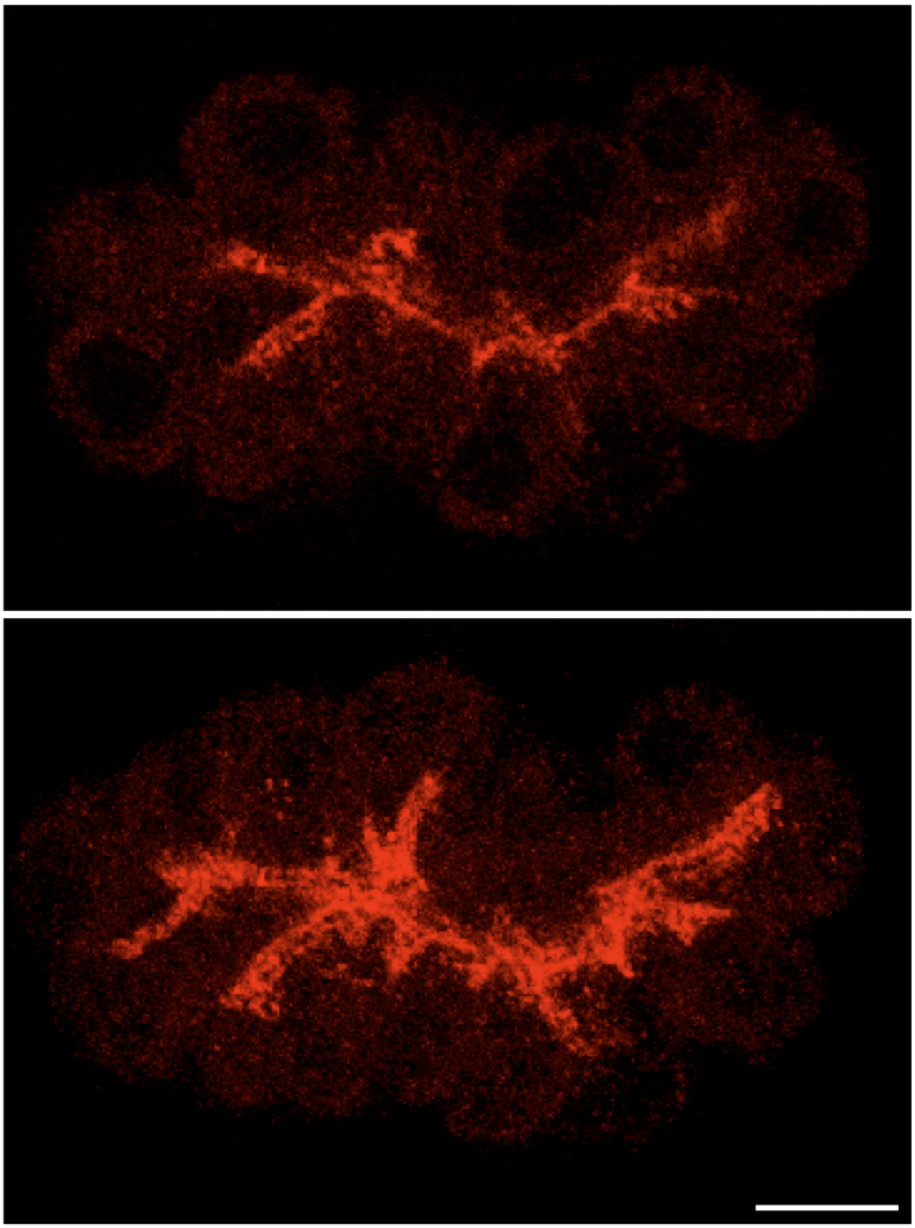

Figure 5.1 Distribution of IP_3R2 in rat acinar cells. Isolated rat pancreatic acinar cells were fixed using MeOH, then stained with an antibody against the N-terminal of the IP_3R2. A. A single confocal section; B. Maximum projection of the same cell cluster; scale bar represents 10 μm.

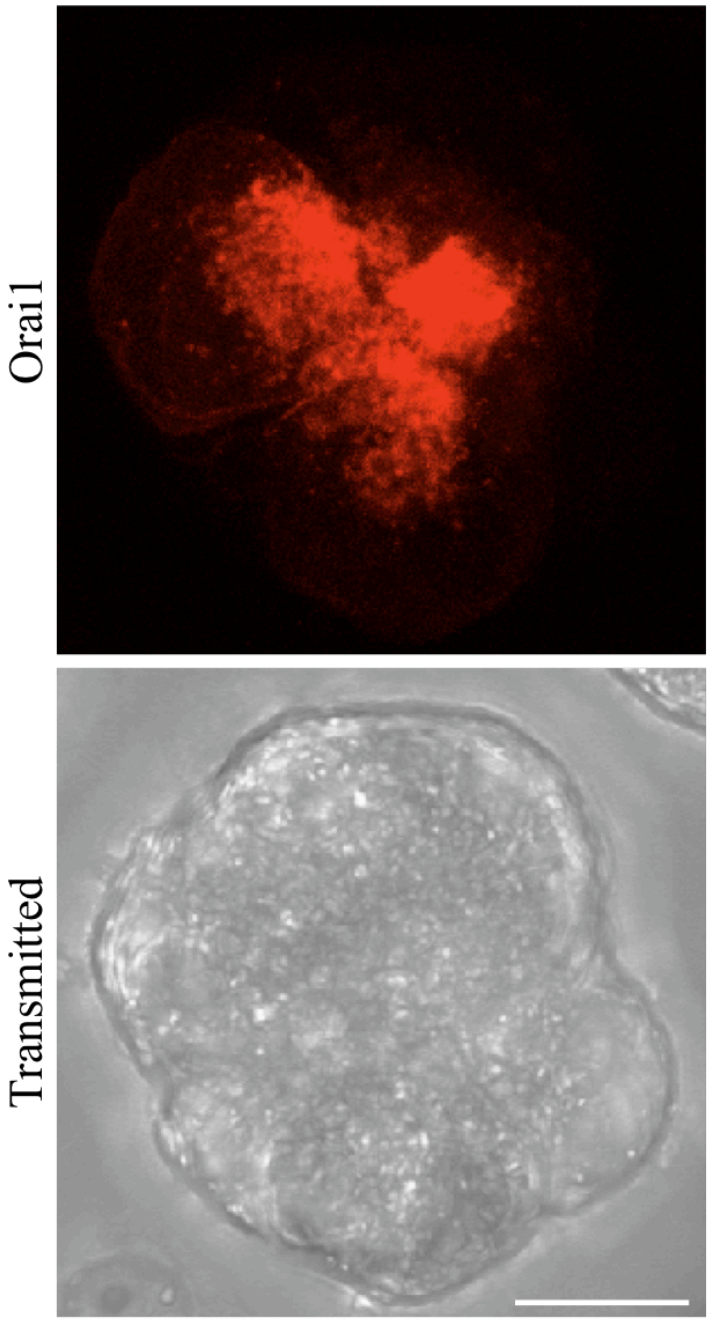

Figure 5.2 Orai1 distribution in virally transfected mouse acinar cells. Isolated mouse pancreatic acinar cells were transfected with mCherryOrai1 overnight, before fixation with PFA. A maximum projection is shown; scale bar represents 10 μm.

5.3 Testing the localisation of Orai1 in pancreatic acinar cells

One method used to delve into this problem was by using an antibody against an extracellular epitope of Orai1 (a kind gift from S. Feske, New York University, USA) to stain for the protein in both permeabilised and non-permeabilised cells. Without permeabilisation, antibodies (which are relatively large proteins) cannot enter a cell and stain internal structures, and are therefore restricted to binding epitopes present extracellularly.

Figure 5.3 shows the staining obtained when isolated mouse pancreatic acinar cells were fixed and stained for endogenous Orai1 (using an antibody against the external epitope used at a 1:50 dilution) without a permeabilisation step (n = 4). Fixation was carried out using PFA, as MeOH fixation simultaneously fixes and permeabilises cells whereas PFA does not. By carrying out immunofluorescence in this way, only Orai1 correctly orientated at the plasma membrane will be picked up, as this will be the only protein with the extracellular epitope exposed to the extracellular space and hence available for antibody binding. The image shows staining at the basolateral membrane (similar to the small amount of basolateral fluorescence seen in Figure 5.2) and an absence of staining in the apical region.

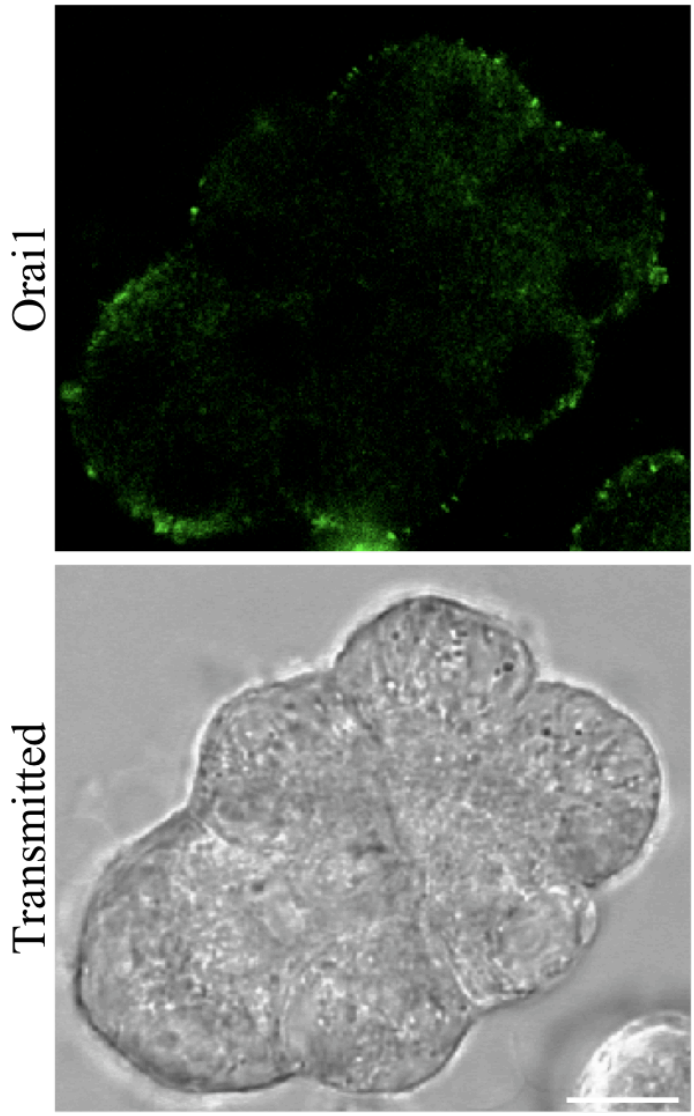

Figure 5.3 The distribution of endogenous Orai1 in mouse pancreatic acinar cells discernible without permeabilisation. Isolated mouse pancreatic acinar cells were fixed using PFA, and (without a permeabilisation step) stained with an antibody against an extracellular epitope of Orai1. Scale bar represents 10 μm.

Figure 5.4 shows endogenous Orai1 staining in pancreatic acinar cells that were permeabilised before staining with the Orai1 antibody (allowing the antibody to bind to intracellular proteins)(n = 3). The image shows a large amount of endogenous Orai1 in the apical region, in addition to the previously seen staining at the basolateral plasma membrane.

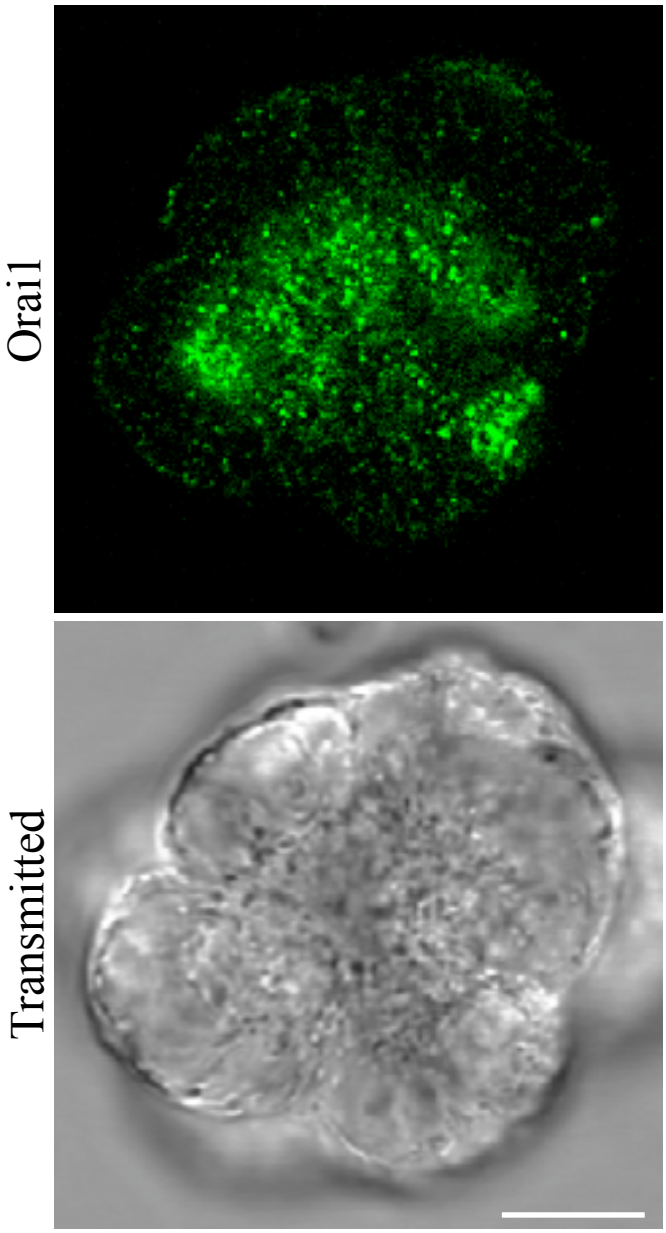

Figure 5.4 The distribution of endogenous Orai1 in mouse pancreatic acinar cells discernible after permeabilisation. Isolated mouse pancreatic acinar cells were fixed using PFA, permeabilised and stained with an antibody against an extracellular epitope of Orai1. Scale bar represents 10 μm.

Another method of examining the localisation of apical Orai1 was by the use of a viral myc-tagged Orai1 construct. This construct is similar to the fluorescently-tagged Orai1 construct, however the fluorescent tag is replaced by a small epitope easily recognisable by an antibody – the myc epitope. Figure 5.5 shows isolated mouse pancreatic acinar cells virally transfected with myc-tagged Orai1, incubated with a fluorescently-tagged wheat germ agglutinin (WGA) to stain the plasma membrane (at a dilution of 1:200), fixed using PFA and (without permeabilisation) stained for the myc epitope (n = 5; antibody against the myc epitope used at a dilution of 1:200). Whilst the myc antibody tends to give slightly less clean staining (i.e. more non-specific binding), the images clearly show a lack of apical staining for the myc antibody. The use of WGA to stain the plasma membrane shows that the apical plasma membrane is visible in the confocal section shown (and is accessible to fluorophores), but does not show staining for the myc-tagged Orai1.

Figure 5.5 The distribution of myc-tagged Orai1 in virally transfected mouse pancreatic acinar cells discernible without permeabilisation. Isolated mouse pancreatic acinar cells were virally transfected with myc-tagged Orai1 overnight before incubation with WGA to stain the plasma membrane. Cells were then fixed with PFA, and (with no permeabilisation step) stained with an antibody against the myc epitope. White arrow indicates apical region of indicated cell; scale bar represents 10 μm.

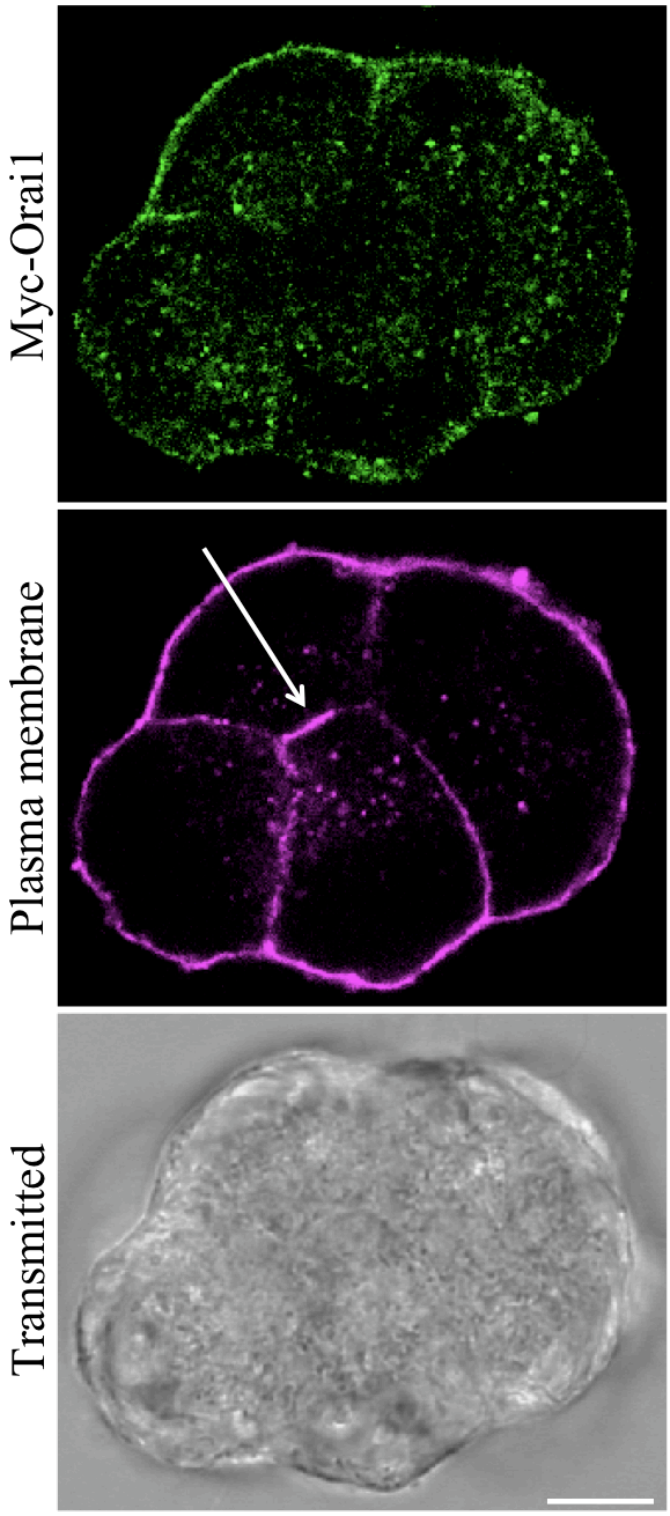

Figure 5.5 The distribution of myc-tagged Orai1 in virally transfected mouse pancreatic acinar cells discernible without permeabilisation.

Again, this can be compared to staining seen in permeabilised cells to see the difference in localisation. Figure 5.6 shows pancreatic acinar cells virally transfected with myc-tagged Orai1, fixed using PFA, permeabilised and stained for the myc epitope (n = 4). Once again, a strong apical staining can be seen, along with the much weaker basolateral plasma membrane staining, indicating that the distribution of the myc-tagged Orai1, the mCherry-tagged Orai1, and endogenous Orai1 are all relatively similar.

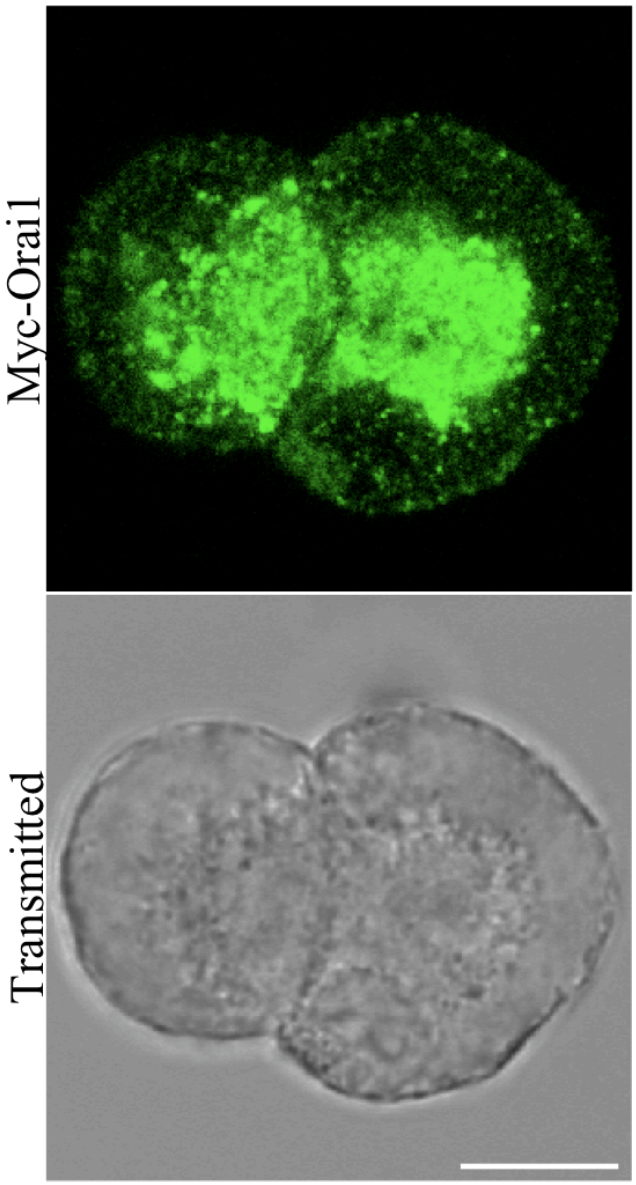

Figure 5.6 Distribution of myc-tagged Orai1 in virally transfected mouse pancreatic acinar cells discernible after permeabilisation. Isolated mouse pancreatic acinar cells were virally transfected with myc-tagged Orai1 overnight, before PFA fixation, permeabilisation and staining with an antibody against the myc epitope. Scale bar represents 10 μm.

5.4 Summary

Orai1 is a PM Ca^{2+} influx channel activated by STIM after the latter has translocated to ER-PM junctions following depletion of the ER Ca^{2+} store. Orai1 has a strong apical presence in pancreatic acinar cells, and co-localises with IP_3Rs at this site (Lur *et al.*, 2011). This is despite the fact that STIM (the main activator of Orai1) does not translocate towards the apical region upon store-depletion, instead travelling to the basolateral membrane where it forms puncta with a separate pool of Orai1 situated basolaterally (Lur *et al.*, 2009). The function of apical Orai1, if not forming a SOCE complex with STIM, is currently unknown.

The previous study that found that Orai1 and IP_3Rs co-localise at the apical region of acinar cells did not determine the cellular structure in which these two proteins are located (Lur *et al.*, 2011). This part of the investigation therefore more precisely determined the localisation of apical Orai1, i.e. determined whether this pool of Orai1 is inserted into the PM in its usual orientation or is instead located in an intracellular organelle. To achieve this I used two main immunocytochemical approaches. The first used a custom antibody that recognises an epitope at the extracellular terminus of Orai1, using immunofluorescence protocols both with and without a permeabilisation step. If Orai1 at the apical region of the acinar cell is at the plasma membrane in its usual configuration, there should be no difference in the ability of the antibody to detect Orai1 regardless of permeabilisation status, as in both conditions the extracellular epitope which the antibody recognises would be accessible for binding. If on the other hand, staining were only visible after permeabilisation this would suggest that the epitope is not extracellular. Data from these experiments suggest that the

endogenous Orai1 in acinar cells is not present in its usual orientation at the apical PM (Figures 5.3 – 5.4), as apical staining of Orai1 was only seen after permeabilisation. These experiments also confirmed the existence of Orai1 in the basolateral membrane, in agreement with previous work by Lur et al (Lur *et al.*, 2011) but in contradiction to other work by Hong et al in parotid and pancreatic acinar cells (Hong *et al.*, 2011).

The second approach was to express a viral Orai1 construct with a myc-tag at its extracellular terminal. This myc epitope is easily identifiable using readily available commercial antibodies that give much more consistent staining than an antibody against the endogenous Orai1 protein. Exogenous expression means that levels of the protein are also higher and hence the localisation is easier to determine. Images of fixed non-permeabilised acinar cells showed that the myc-epitope, which was inserted into the extracellular domain of Orai, is located at the basolateral membrane (Figure 5.5). This suggests that the normal SOCE channel functions of Orai will be manifested at this location. Apical staining of the myc epitope was absent in non-permeabilised cells. Staining with fluorescently-conjugated WGA (which stains the PM) confirms that this region of the cell is accessible to fluorophores (the WGA dye is conjugated to an Alexa Fluor® fluorophore). Experiments on permeabilised cells confirm the presence of an intracellular pool of Orai1 in the apical region that is not inserted in the PM of the cell (Figure 5.6).

My experiments indicate that Orai1 may be localised to an intracellular organelle sitting directly beneath the plasma membrane. Orai1 has previously been shown to be continuously recycled in quiescent cells (El-

Jouni *et al.*, 2007; Yu & Machaca, 2009), and internalised during meiosis (Yu *et al.*, 2010), so its presence outside of the PM (excluding during production) is not without precedent. The nature of the Orai decorated organelle will require further investigation.

Depending on the structure where it is found, different functions are possible. Several factors should be taken into consideration: firstly, both Orai1 and IP_3Rs are Ca^{2+} channels, but the IP_3Rs are capable of carrying a much larger current than Orai channels (picosiemens (Rahman & Taylor, 2009) versus femtosiemens respectively (Cahalan, 2009)). Secondly, IP_3Rs are activated by IP_3 (a second messenger) and Ca^{2+} (though the effect of Ca^{2+} is biphasic)(Berridge *et al.*, 2003), whereas Orai is activated by STIM and inhibited by Ca^{2+}. Thirdly, the association between the two proteins is unaffected by agonist stimulation or store-depletion, and finally apical Orai1 distribution is unchanged in cells with simultaneous knockdown of both IP_3R type 2 and 3 (Lur *et al.*, 2011). Also potentially relevant is that the second member of the STIM family – STIM2 – can exist both as an ER-located form, and as a cytosolic form, the latter of which interacts with Orai1 in a store-independent manner and has been shown to regulate several functions including gene expression (Graham *et al.*, 2011).

With these facts in mind, if the co-localisation of apical Orai1 and IP_3Rs is in a specialised region of the ER, the complex could be functioning as a Ca^{2+} efflux channel, to moderate the Ca^{2+} content of the ER and prevent overloading. As the current carried by Orai channels is much smaller than that of IP_3 channels, it would give the cell greater control over the cellular Ca^{2+} content, both in the ER and in the cytosol. Alternatively, the complex could be located in the zymogen granules or condensing vacuoles, again regulating the Ca^{2+} content to modulate the activity of the digestive enzymes

within. At either of these sites, activation of Orai1 by proteins from the STIM family (either cytosolic or ER based) would allow initiation of Ca^{2+} dynamics, increasing the open probability of the IP_3Rs via CICR. Further Ca^{2+} signals via the IP_3Rs would inhibit Orai1 activity. Conversely, if Orai1 were constitutively active in acinar cells, activation of IP_3Rs by IP_3 would initiate Ca^{2+} signals and inhibit Orai1 channel activity.

The above theories are merely suggestions as to what may be occurring in pancreatic acinar cells and how the complex of IP_3Rs and Orai1 channels may be acting. Further work looking into both structural and functional aspects of this complex will help uncover the role and potential importance of this complex in pancreatic acinar cells.

Chapter 6: General Discussion & Concluding Remarks

Chapter 6: General Discussion & Concluding Remarks

6.1 Overview

This investigation aimed to achieve several things, all centred round the form and function of ER-PM junctions and their components. In migrating pancreatic cancer cells I examined the distribution of ER-PM junctions in relation to the polarity of cells, and the dynamics of the junctions throughout the constant turnover of the PM required for cell migration. I also determined the localisation of ER-PM junctions in relation to proteins and structures integral to the migration of cells. Finally, I increased the understanding of ER-PM junctions and SOCE in pancreatic acinar cells by demonstrating the localisation of plasma membrane Orai1 to the basal and lateral regions of the PM, whilst demonstrating that apical Orai1 exists in as yet undetermined subplasmalemmal structure.

6.2 ER-PM junctions and migration

Migrating cells undergo constant rearrangement of internal structures that drives their forward movement. At the leading edge of migrating cells, there is a constant turnover of focal adhesions, of the actin network and of plasma membrane protrusions. Although there is some dispute as to whether ER-PM junctions are pre-formed or form upon store-depletion, it would seem that in the case of migrating cells at least, formation and disassembly of ER-PM junctions would be a necessity, as the PM undergoes constant rearrangement as the cell migrates. Studies showing the Ca^{2+} dependence of many proteins

crucial to migration and the pervasive involvement of Ca^{2+} signalling in migration suggest that the positioning of ER-PM junctions (whether pre-existing or newly formed) in migrating cells may be critical for the regulation of some of the Ca^{2+}-dependent proteins and processes.

I found that there was an increased density of ER-PM junctions at the leading edge of migrating cells, not due to an increase in ER density but partially because development of a filopodial or lamellapodial protrusion was very often accompanied by the creation of new ER-PM junctions at its base. The appearance of new junctions near cellular protrusions coincided with a close spatial relationship between ER-PM junctions and both polymerised actin (the framework the cell uses to migrate) and focal complexes (the structures by which a cell attaches to the substratum to provide traction). Ca^{2+} directly or indirectly regulates many of the proteins involved in regulating actin dynamics and the turnover of focal complexes / adhesions. Ca^{2+} flickers have also been shown to occur at these sites; this occurs through a pathway not abolished by depletion of the internal Ca^{2+} store (Wei *et al.*, 2009). It would be natural to assume therefore that these ER-PM junctions are the critical sites at which Ca^{2+} influx occurs to regulate migration cascades at the leading edge.

Understanding the mechanism by which ER-PM junctions concentrate at the leading edge was a more complex challenge. Although it has been theorised that the polarisation of STIM1 translocation in cells may be due to its interaction with microtubules (Carrasco & Meyer, 2011), this is unlikely to be the case in migrating PANC-1 cells for two reasons. Firstly, the preferential translocation of STIM to junctions at the leading edge of migrating cells occurs even in cells expressing a mutated form of STIM that lacks the ability to interact with microtubules (Chapter 3). Secondly, experiments with

rapamycin-inducible linkers showed that the distribution of ER-PM junctions alone is also polarised, even without store-depletion and the recruitment of STIM (Chapter 4). Whether the interaction of STIM with microtubules plays a role in the polarisation of STIM distribution in stationary pancreatic acinar cells is the subject of another investigation.

The characteristic distribution of ER-PM junctions in migrating cells is also unlikely to be affected by the specific region of the ER undergoing store-depletion. It is expected that the rear of a polarised cell, which would have a higher Ca^{2+} concentration and fewer Ca^{2+} flicker events (Brundage *et al.*, 1991; Wei *et al.*, 2009) , would have a higher, more stable ER Ca^{2+} concentration than the ER nearer the leading edge. It was possible therefore that ER-PM junctions and SOCE complexes were forming preferentially in regions of the cell with a lower $[Ca^{2+}]_{ER}$; again this does not seem to be the case, as was demonstrated using the constitutively active STIM mutant, which distributed similarly to WT STIM whilst being insensitive to ER Ca^{2+} content.

I also ruled out the possibility that the specific distribution of PIs in migrating cells regulates the positioning of ER-PM junctions. Binding to PIs is one mechanism by which STIM translocation upon store-depletion is driven towards the plasma membrane. The PIs involved ($PI(4,5)P_2$ and $PI(3,4,5)P_3$) are found in characteristic locations in migrating cells, $PI(3,4,5)P_3$ is found concentrated at the leading edge and $PI(4,5)P_2$ at the cell rear. Preventing association of STIM to these PIs did cause a noticeable delay in the formation of puncta upon store-depletion. However I observed a close proximity between the puncta that did eventually form to both the leading edge and regions of polymerised actin, similarly to the distribution of WT STIM; this finding excludes a mechanism whereby PI accumulation is

primarily responsible for the positioning of ER-PM junctions at the leading edge.

6.3 SOCE complexes in pancreatic acinar cells

ER-PM junctions and the related SOCE complexes were also investigated in pancreatic acinar cells. In this highly polarised cell type ER-PM junctions are thought to be relatively stationary and SOCE complexes form in the basolateral region to mediate Ca^{2+} influx. Myc-tagged Orai1 was found in the basal and lateral regions of the PM consistent with the function of Orai1 as a SOCE channel. The same distribution was revealed using a mCherry-tagged Orai1 protein, and with antibodies against the endogenous protein. These experiments suggest that the Orai1 present in the correct orientation to serve as the SOCE channel in pancreatic acinar cells is found at the basal and lateral membranes. Apically, the Ca^{2+} channel component of the SOCE complexes – Orai1 – can be found in an intracellular organelle. The functions of this intracellular Orai1 are as yet undetermined.

6.4 Concluding remarks

This investigation uncovered novel and exciting phenomena in the distribution and dynamics of ER-PM junctions in migrating pancreatic cancer cells. It also clarified aspects regarding Orai1 and SOCE in pancreatic acinar cells. Clearly, further work should be done to understand the distribution mechanism of ER-PM junctions in migrating cells and their possible function at the specific locations identified. Understanding the functions of apical Orai1 in pancreatic acinar cells is another subject for further investigation. Hopefully this investigation will provide an excellent basis for future studies of ER-PM junctions in pancreatic cancer and pancreatic acinar cells and will be relevant for understanding important diseases of the exocrine pancreas such as pancreatic cancer and pancreatitis.

References

Abercrombie M, Heaysman JE & Pegrum SM. (1970). The locomotion of fibroblasts in culture. I. Movements of the leading edge. *Exp Cell Res* **59,** 393-398.

Abercrombie M, Heaysman JE & Pegrum SM. (1971). The locomotion of fibroblasts in culture. IV. Electron microscopy of the leading lamella. *Exp Cell Res* **67,** 359-367.

Alicia S, Angelica Z, Carlos S, Alfonso S & Vaca L. (2008). STIM1 converts TRPC1 from a receptor-operated to a store-operated channel: moving TRPC1 in and out of lipid rafts. *Cell Calcium* **44,** 479-491.

Allen WE, Zicha D, Ridley AJ & Jones GE. (1998). A role for Cdc42 in macrophage chemotaxis. *J Cell Biol* **141,** 1147-1157.

Ambrose EJ. (1956). A surface contact microscope for the study of cell movements. *Nature* **178,** 1194.

Ashby MC, Craske M, Park MK, Gerasimenko OV, Burgoyne RD, Petersen OH & Tepikin AV. (2002). Localized Ca^{2+} uncaging reveals polarized distribution of Ca^{2+}-sensitive Ca^{2+} release sites: mechanism of unidirectional Ca2+ waves. *J Cell Biol* **158,** 283-292.

Baba Y, Hayashi K, Fujii Y, Mizushima A, Watarai H, Wakamori M, Numaga T, Mori Y, Iino M, Hikida M & Kurosaki T. (2006). Coupling of STIM1 to store-operated Ca^{2+} entry through its constitutive and inducible movement in the endoplasmic reticulum. *Proc Natl Acad Sci U S A* **103,** 16704-16709.

Ballestrem C, Hinz B, Imhof BA & Wehrle-Haller B. (2001). Marching at the front and dragging behind: differential alphaVbeta3-integrin turnover regulates focal adhesion behavior. *J Cell Biol* **155,** 1319-1332.

Barrow SL, Voronina SG, da Silva Xavier G, Chvanov MA, Longbottom RE, Gerasimenko OV, Petersen OH, Rutter GA & Tepikin AV. (2008). ATP depletion inhibits Ca^{2+} release, influx and extrusion in pancreatic acinar cells but not pathological Ca^{2+} responses induced by bile. *Pflugers Arch* **455,** 1025-1039.

Beardsley A, Fang K, Mertz H, Castranova V, Friend S & Liu J. (2005). Loss of caveolin-1 polarity impedes endothelial cell polarization and directional movement. *J Biol Chem* **280,** 3541-3547.

Berridge MJ. (1993). Inositol trisphosphate and calcium signalling. *Nature* **361,** 315-325.

Berridge MJ, Bootman MD & Roderick HL. (2003). Calcium signalling: dynamics, homeostasis and remodelling. *Nat Rev Mol Cell Biol* **4,** 517-529.

Berridge MJ, Lipp P & Bootman MD. (2000). The Versatility and Universality of Calcium Signalling. *Nat Rev Mol Cell Biol* **1,** 11-21.

Bers DM. (2002). Cardiac excitation-contraction coupling. *Nature* **415,** 198-205.

Blaustein MP & Lederer WJ. (1999). Sodium/calcium exchange: its physiological implications. *Physiol Rev* **79,** 763-854.

Bogeski I, Kummerow C, Al-Ansary D, Schwarz EC, Koehler R, Kozai D, Takahashi N, Peinelt C, Griesemer D, Bozem M, Mori Y, Hoth M & Niemeyer BA. (2010). Differential redox regulation of ORAI ion channels: a mechanism to tune cellular calcium signaling. *Sci Signal* **3,** ra24.

Bolender RP. (1974). Stereological analysis of the guinea pig pancreas. I. Analytical model and quantitative description of nonstimulated pancreatic exocrine cells. *J Cell Biol* **61,** 269-287.

Borgese N, Francolini M & Snapp E. (2006). Endoplasmic reticulum architecture: structures in flux. *Curr Opin Cell Biol* **18,** 358-364.

Borisy GG & Svitkina TM. (2000). Actin machinery: pushing the envelope. *Curr Opin Cell Biol* **12,** 104-112.

Brandt PW, Reuben JP, Girardier L & Grundfest. (1965). Correlated morphological and physiological studies on isolated single muscle fibers. I. Fine structure of the crayfish muscle fiber. *J Cell Biol* **25,** Suppl:233-260.

Brazer SC, Singh BB, Liu X, Swaim W & Ambudkar IS. (2003). Caveolin-1 contributes to assembly of store-operated Ca^{2+} influx channels by regulating plasma membrane localization of TRPC1. *J Biol Chem* **278,** 27208-27215.

Brundage RA, Fogarty KE, Tuft RA & Fay FS. (1991). Calcium gradients underlying polarization and chemotaxis of eosinophils. *Science* **254,** 703-706.

Burdakov D, Petersen OH & Verkhratsky A. (2005). Intraluminal calcium as a primary regulator of endoplasmic reticulum function. *Cell Calcium* **38,** 303-310.

Burridge K & Feramisco JR. (1981). Non-muscle alpha actinins are calcium-sensitive actin-binding proteins. *Nature* **294,** 565-567.

Cahalan MD. (2009). STIMulating store-operated Ca^{2+} entry. *Nat Cell Biol* **11,** 669-677.

Calloway N, Owens T, Corwith K, Rodgers W, Holowka D & Baird B. (2011). Stimulated association of STIM1 and Orai1 is regulated by the balance of PtdIns(4,5)P_2 between distinct membrane pools. *J Cell Sci* **124,** 2602-2610.

Camello P, Gardner J, Petersen OH & Tepikin AV. (1996). Calcium dependence of calcium extrusion and calcium uptake in mouse pancreatic acinar cells. *J Physiol* **490,** 585-593.

Carrasco S & Meyer T. (2011). STIM Proteins and the Endoplasmic Reticulum-Plasma Membrane Junctions. *Annu Rev Biochem* **80,** 973-1000.

Chen H, Cohen DM, Choudhury DM, Kioka N & Craig SW. (2005). Spatial distribution and functional significance of activated vinculin in living cells. *J Cell Biol* **169,** 459-470.

Chvanov M, Walsh CM, Haynes LP, Voronina SG, Lur G, Gerasimenko OV, Barraclough R, Rudland PS, Petersen OH, Burgoyne RD & Tepikin AV. (2008). ATP depletion induces translocation of STIM1 to puncta and formation of STIM1-ORAI1 clusters: translocation and re-translocation of STIM1 does not require ATP. *Pflugers Arch* **457,** 505-517.

Copeland DE & Dalton AJ. (1959). An association between mitochondria and the endoplasmic reticulum in cells of the pseudobranch gland of a teleost. *J Biophys Biochem Cytol* **5,** 393-396.

Csordas G, Varnai P, Golenar T, Roy S, Purkins G, Schneider TG, Balla T & Hajnoczky G. (2010). Imaging interorganelle contacts and local calcium dynamics at the ER-mitochondrial interface. *Mol Cell* **39,** 121-132.

DeHaven WI, Jones BF, Petranka JG, Smyth JT, Tomita T, Bird GS & Putney JW, Jr. (2009). TRPC channels function independently of STIM1 and Orai1. *J Physiol* **587,** 2275-2298.

Di Leva F, Domi T, Fedrizzi L, Lim D & Carafoli E. (2008). The plasma membrane Ca^{2+} ATPase of animal cells: structure, function and regulation. *Arch Biochem Biophys* **476,** 65-74.

Dietrich A, Kalwa H, Storch U, Mederos y Schnitzler M, Salanova B, Pinkenburg O, Dubrovska G, Essin K, Gollasch M, Birnbaumer L & Gudermann T. (2007). Pressure-induced and store-operated cation influx in vascular smooth muscle cells is independent of TRPC1. *Pflugers Arch* **455,** 465-477.

Eisenberg BR & Eisenberg RS. (1982). The T-SR junction in contracting single skeletal muscle fibers. *J Gen Physiol* **79,** 1-19.

El-Jouni W, Haun S, Hodeify R, Hosein Walker A & Machaca K. (2007). Vesicular traffic at the cell membrane regulates oocyte meiotic arrest. *Development* **134,** 3307-3315.

English AR, Zurek N & Voeltz GK. (2009). Peripheral ER structure and function. *Curr Opin Cell Biol* **21,** 596-602.

Engstrom H. (1958). On the double innervation of the sensory epithelia of the inner ear. *Acta Otolaryngol* **49,** 109-118.

Ercan E, Momburg F, Engel U, Temmerman K, Nickel W & Seedorf M. (2009). A conserved, lipid-mediated sorting mechanism of yeast Ist2 and mammalian STIM proteins to the peripheral ER. *Traffic* **10,** 1802-1818.

Etienne-Manneville S & Hall A. (2002). Rho GTPases in cell biology. *Nature* **420,** 629-635.

Eylenstein A, Gehring EM, Heise N, Shumilina E, Schmidt S, Szteyn K, Munzer P, Nurbaeva MK, Eichenmuller M, Tyan L, Regel I, Foller M, Kuhl D, Soboloff J, Penner R & Lang F. (2011). Stimulation of Ca^{2+}-

channel Orai1/STIM1 by serum- and glucocorticoid-inducible kinase 1 (SGK1). *FASEB J* **25,** 2012-2021.

Ezratty EJ, Partridge MA & Gundersen GG. (2005). Microtubule-induced focal adhesion disassembly is mediated by dynamin and focal adhesion kinase. *Nat Cell Biol* **7,** 581-590.

Fawcett DW & Revel JP. (1961). The sarcoplasmic reticulum of a fast-acting fish muscle. *J Biophys Biochem Cytol* **10,** 89-109.

Feske S, Gwack Y, Prakriya M, Srikanth S, Puppel S, Tanasa B, Hogan P, Lewis RS, Daly M & Rao A. (2006). A mutation in Orai1 causes immune deficiency by abrogating CRAC channel function. *Nature* **441,** 179-185.

Fill M & Copello JA. (2002). Ryanodine receptor calcium release channels. *Physiol Rev* **82,** 893-922.

Franzini-Armstron C. (1974). Freeze fracture of skeletal muscle from the Tarantula spider. Structural differentiations of sarcoplasmic reticulum and transverse tubular system membranes. *J Cell Biol* **61,** 501-513.

Friedman JR, Webster BM, Mastronarde DN, Verhey KJ & Voeltz GK. (2010). ER sliding dynamics and ER-mitochondrial contacts occur on acetylated microtubules. *J Cell Biol* **190,** 363-375.

Fujimoto T, Hagiwara H, Aoki T, Kogo H & Nomura R. (1998). Caveolae: from a morphological point of view. *J Electron Microsc (Tokyo)* **47,** 451-460.

Futatsugi A, Nakamura T, Yamada MK, Ebisui E, Nakamura K, Uchida K, Kitaguchi T, Takahashi-Iwanaga H, Noda T, Aruga J & Mikoshiba K. (2005). IP_3 receptor types 2 and 3 mediate exocrine secretion underlying energy metabolism. *Science* **309,** 2232-2234.

Galione A, White A, Willmott N, Turner M, Potter BV & Watson SP. (1993). cGMP mobilizes intracellular Ca^{2+} in sea urchin eggs by stimulating cyclic ADP-ribose synthesis. *Nature* **365,** 456-459.

Gardiner DM & Grey RD. (1983). Membrane junctions in Xenopus eggs: their distribution suggests a role in calcium regulation. *J Cell Biol* **96,** 1159-1163.

Gerasimenko OV, Gerasimenko JV, Belan PV & Petersen OH. (1996). Inositol trisphosphate and cyclic ADP-ribose-mediated release of Ca^{2+} from single isolated pancreatic zymogen granules. *Cell* **84,** 473-480.

Gerasimenko OV, Gerasimenko JV, Rizzuto RR, Treiman M, Tepikin AV & Petersen OH. (2002). The distribution of the endoplasmic reticulum in living pancreatic acinar cells. *Cell Calcium* **32,** 261-268.

Giancotti FG & Ruoslahti E. (1999). Integrin signaling. *Science* **285,** 1028-1032.

Giorgi C, De Stefani D, Bononi A, Rizzuto R & Pinton P. (2009). Structural and functional link between the mitochondrial network and the endoplasmic reticulum. *Int J Biochem Cell Biol* **41,** 1817-1827.

Graham SJ, Dziadek MA & Johnstone LS. (2011). A cytosolic STIM2 preprotein created by signal peptide inefficiency activates ORAI1 in a store-independent manner. *J Biol Chem* **286,** 16174-16185.

Grande-Garcia A & del Pozo MA. (2008). Caveolin-1 in cell polarization and directional migration. *Eur J Cell Biol* **87,** 641-647.

Grande-Garcia A, Echarri A, de Rooij J, Alderson NB, Waterman-Storer CM, Valdivielso JM & del Pozo MA. (2007). Caveolin-1 regulates cell polarization and directional migration through Src kinase and Rho GTPases. *J Cell Biol* **177,** 683-694.

Grigoriev I, Gouveia SM, van der Vaart B, Demmers J, Smyth JT, Honnappa S, Splinter D, Steinmetz MO, Putney JW, Jr., Hoogenraad CC & Akhmanova A. (2008). STIM1 is a MT-plus-end-tracking protein involved in remodeling of the ER. *Curr Biol* **18,** 177-182.

Groenendyk J & Michalak M. (2005). Endoplasmic reticulum quality control and apoptosis. *Acta Biochim Pol* **52,** 381-395.

Gupta GP & Massague J. (2006). Cancer metastasis: building a framework. *Cell* **127,** 679-695.

Gwack Y, Srikanth S, Feske S, Cruz-Guilloty F, Oh-hora M, Neems D, Hogan P & Rao A. (2007). Biochemical and Functional Characterization of Orai Proteins. *J Biol Chem* **282,** 16232-16243.

Heo WD, Inoue T, Park WS, Kim ML, Park BO, Wandless TJ & Meyer T. (2006). PI(3,4,5)P_3 and PI(4,5)P_2 lipids target proteins with polybasic clusters to the plasma membrane. *Science* **314,** 1458-1461.

Higgs HN & Pollard TD. (2001). Regulation of actin filament network formation through ARP2/3 complex: activation by a diverse array of proteins. *Annu Rev Biochem* **70,** 649-676.

Holthuis JC & Levine TP. (2005). Lipid traffic: floppy drives and a superhighway. *Nat Rev Mol Cell Biol* **6,** 209-220.

Hong JH, Li Q, Kim MS, Shin DM, Feske S, Birnbaumer L, Cheng KT, Ambudkar IS & Muallem S. (2011). Polarized but differential localization and recruitment of STIM1, Orai1 and TRPC channels in secretory cells. *Traffic* **12,** 232-245.

Honnappa S, Gouveia SM, Weisbrich A, Damberger FF, Bhavesh NS, Jawhari H, Grigoriev I, van Rijssel FJ, Buey RM, Lawera A, Jelesarov I, Winkler FK, Wuthrich K, Akhmanova A & Steinmetz MO. (2009). An EB1-

binding motif acts as a microtubule tip localization signal. *Cell* **138,** 366-376.

Hoover PJ & Lewis RS. (2011). Stoichiometric requirements for trapping and gating of Ca^{2+} release-activated Ca^{2+} (CRAC) channels by stromal interaction molecule 1 (STIM1). *Proc Natl Acad Sci U S A* **108,** 13299-13304.

Hoth M, Fanger CM & Lewis RS. (1997). Mitochondrial regulation of store-operated calcium signaling in T lymphocytes. *J Cell Biol* **137,** 633-648.

Huang GN, Zeng W, Kim JY, Yuan JP, Han L, Muallem S & Worley PF. (2006). STIM1 carboxyl-terminus activates native SOC, I_{crac} and TRPC1 channels. *Nat Cell Biol* **8,** 1003-1010.

Ingram VM. (1969). A side view of moving fibroblasts. *Nature* **222,** 641-644.

Itoh RE, Kurokawa K, Ohba Y, Yoshizaki H, Mochizuki N & Matsuda M. (2002). Activation of rac and cdc42 video imaged by fluorescent resonance energy transfer-based single-molecule probes in the membrane of living cells. *Mol Cell Biol* **22,** 6582-6591.

Jamieson JD & Palade GE. (1967). Intracellular transport of secretory proteins in the pancreatic exocrine cell. I. Role of the peripheral elements of the Golgi complex. *J Cell Biol* **34,** 577-596.

Jousset H, Frieden M & Demaurex N. (2007). STIM1 knockdown reveals that store-operated Ca^{2+} channels located close to sarco/endoplasmic Ca^{2+} ATPases (SERCA) pumps silently refill the endoplasmic reticulum. *J Biol Chem* **282,** 11456-11464.

Kar P, Nelson C & Parekh AB. (2011). Selective Activation of the Transcription Factor NFAT1 by Calcium Microdomains near Ca^{2+} Release-activated Ca^{2+} (CRAC) Channels. *J Biol Chem* **286,** 14795-14803.

Kaufman. (2004). A trip to the ER: coping with stress. *Trends Cell Biol* **14,** 20-28.

Kaverina I, Krylyshkina O & Small JV. (1999). Microtubule targeting of substrate contacts promotes their relaxation and dissociation. *J Cell Biol* **146,** 1033-1044.

Kaverina I & Straube A. (2011). Regulation of cell migration by dynamic microtubules. *Semin Cell Dev Biol* **22,** 968-974.

Krapivinsky G, Krapivinsky L, Stotz SC, Manasian Y & Clapham DE. (2011). POST, partner of stromal interaction molecule 1 (STIM1), targets STIM1 to multiple transporters. *Proc Natl Acad Sci U S A* **108,** 19234-19239.

Kraynov VS, Chamberlain C, Bokoch GM, Schwartz MA, Slabaugh S & Hahn KM. (2000). Localized Rac activation dynamics visualized in living cells. *Science* **290,** 333-337.

Laukaitis CM, Webb DJ, Donais K & Horwitz AF. (2001). Differential dynamics of alpha 5 integrin, paxillin, and alpha-actinin during formation and disassembly of adhesions in migrating cells. *J Cell Biol* **153,** 1427-1440.

Lee J, Ishihara A, Oxford G, Johnson B & Jacobson K. (1999). Regulation of cell movement is mediated by stretch-activated calcium channels. *Nature* **400,** 382-386.

Lee KP, Yuan JP, Hong JH, So I, Worley PF & Muallem S. (2010). An endoplasmic reticulum/plasma membrane junction: STIM1/Orai1/TRPCs. *FEBS Lett* **584,** 2022-2027.

Lee MC, Miller EA, Goldberg J, Orci L & Schekman R. (2004). Bi-directional protein transport between the ER and Golgi. *Annu Rev Cell Dev Biol* **20,** 87-123.

Lefkimmiatis K, Srikanthan M, Maiellaro I, Moyer M, Curci S & Hofer AM. (2009). Store-operated cyclic AMP signalling mediated by STIM1. *Nat Cell Biol* **11,** 433-442.

Lengsfeld AM, Low I, Wieland T, Dancker P & Hasselbach W. (1974). Interaction of phalloidin with actin. *Proc Natl Acad Sci U S A* **71,** 2803-2807.

Levine T & Loewen C. (2006). Inter-organelle membrane contact sites: through a glass, darkly. *Curr Opin Cell Biol* **18,** 371-378.

Lewis RS. (2007). The molecular choreography of a store-operated calcium channel. *Nature* **446,** 284-287.

Lieber M, Mazzetta J, Nelson-Rees W, Kaplan M & Todaro G. (1975). Establishment of a continuous tumor-cell line (panc-1) from a human carcinoma of the exocrine pancreas. *Int J Cancer* **15,** 741-747.

Liou J, Fivaz M, Inoue T & Meyer T. (2007). Live-cell imaging reveals sequential oligomerization and local plasma membrane targeting of stromal interaction molecule 1 after Ca^{2+} store depletion. *Proc Natl Acad Sci U S A* **104,** 9301-9306.

Liou J, Kim ML, Heo WD, Jones JT, Myers JW, Ferrell JE & Meyer T. (2005). STIM Is a Ca^{2+} Sensor Essential for Ca^{2+}-Store-Depletion-Triggered Ca^{2+} Influx. *Curr Biol* **15,** 1235-1241.

Lockwich TP, Liu X, Singh BB, Jadlowiec J, Weiland S & Ambudkar IS. (2000). Assembly of Trp1 in a signaling complex associated with caveolin-scaffolding lipid raft domains. *J Biol Chem* **275,** 11934-11942.

Luik RM, Wang B, Prakriya M, Wu MM & Lewis RS. (2008). Oligomerization of STIM1 couples ER calcium depletion to CRAC channel activation. *Nature* **454,** 538-542.

Luik RM, Wu MM, Buchanan J & Lewis RS. (2006). The elementary unit of store-operated Ca^{2+} entry: local activation of CRAC channels by STIM1 at ER-plasma membrane junctions. *J Cell Biol* **174,** 815-825.

Lur G, Haynes LP, Prior IA, Gerasimenko OV, Feske S, Petersen OH, Burgoyne RD & Tepikin AV. (2009). Ribosome-free terminals of rough ER allow formation of STIM1 puncta and segregation of STIM1 from IP_3 receptors. *Curr Biol* **19,** 1648-1653.

Lur G, Sherwood MW, Ebisui E, Haynes L, Feske S, Sutton R, Burgoyne RD, Mikoshiba K, Petersen OH & Tepikin AV. (2011). InsP_3 receptors and Orai channels in pancreatic acinar cells: co-localization and its consequences. *Biochem J* **436,** 231-239.

Malli R, Naghdi S, Romanin C & Graier WF. (2008). Cytosolic Ca^{2+} prevents the subplasmalemmal clustering of STIM1: an intrinsic mechanism to avoid Ca^{2+} overload. *J Cell Sci* **121,** 3133-3139.

Manjarres IM, Rodriguez-Garcia A, Alonso MT & Garcia-Sancho J. (2010). The sarco/endoplasmic reticulum Ca^{2+} ATPase (SERCA) is the third element in capacitative calcium entry. *Cell Calcium* **47,** 412-418.

Mato JM, Losada A, Nanjundiah V & Konijn TM. (1975). Signal input for a chemotactic response in the cellular slime mold Dictyostelium discoideum. *Proc Natl Acad Sci U S A* **72,** 4991-4993.

Mercer JC, Dehaven WI, Smyth JT, Wedel B, Boyles RR, Bird GS & Putney JW, Jr. (2006). Large store-operated calcium selective currents due to co-expression of Orai1 or Orai2 with the intracellular calcium sensor, Stim1. *J Biol Chem* **281,** 24979-24990.

Michalak M, Robert Parker JM & Opas M. (2002). Ca^{2+} signaling and calcium binding chaperones of the endoplasmic reticulum. *Cell Calcium* **32,** 269-278.

Mierke CT. (2009). The role of vinculin in the regulation of the mechanical properties of cells. *Cell Biochem Biophys* **53,** 115-126.

Mogami H, Gardner J, Gerasimenko OV, Camello P, Petersen OH & Tepikin AV. (1999). Calcium binding capacity of the cytosol and endoplasmic reticulum of mouse pancreatic acinar cells. *J Physiol* **518,** 463-467.

Mullins FM, Park CY, Dolmetsch RE & Lewis RS. (2009). STIM1 and calmodulin interact with Orai1 to induce Ca^{2+}-dependent inactivation of CRAC channels. *Proc Natl Acad Sci U S A* **106,** 15495-15500.

Mullins RD, Heuser JA & Pollard TD. (1998). The interaction of Arp2/3 complex with actin: nucleation, high affinity pointed end capping, and formation of branching networks of filaments. *Proc Natl Acad Sci U S A* **95,** 6181-6186.

Neher E & Augustine GJ. (1992). Calcium gradients and buffers in bovine chromaffin cells. *J Physiol* **450,** 273-301.

Nicke B, Tseng MJ, Fenrich M & Logsdon CD. (1999). Adenovirus-mediated gene transfer of RasN17 inhibits specific CCK actions on pancreatic acinar cells. *Am J Physiol* **276,** G499-506.

Nobes CD & Hall A. (1995). Rho, rac, and cdc42 GTPases regulate the assembly of multimolecular focal complexes associated with actin stress fibers, lamellipodia, and filopodia. *Cell* **81,** 53-62.

Noegel A, Witke W & Schleicher M. (1987). Calcium-sensitive non-muscle alpha-actinin contains EF-hand structures and highly conserved regions. *FEBS Lett* **221,** 391-396.

Northrop J, Weber A, Mooseker MS, Franzini-Armstrong C, Bishop MF, Dubyak GR, Tucker M & Walsh TP. (1986). Different calcium

dependence of the capping and cutting activities of villin. *J Biol Chem* **261,** 9274-9281.

Orci L, Ravazzola M, Le Coadic M, Shen WW, Demaurex N & Cosson P. (2009). From the Cover: STIM1-induced precortical and cortical subdomains of the endoplasmic reticulum. *Proc Natl Acad Sci U S A* **106,** 19358-19362.

Orrenius S, Zhivotovsky B & Nicotera P. (2003). Regulation of cell death: the calcium-apoptosis link. *Nat Rev Mol Cell Biol* **4,** 552-565.

Padfield PJ, Elliott AC & Baldassare JJ. (1998). Adenovirus-mediated gene expression in isolated rat pancreatic acini and individual pancreatic acinar cells. *Pflugers Arch* **436,** 782-787.

Pani B, Ong HL, Brazer S-CW, Liu X, Rauser K, Singh BB & Ambudkar IS. (2009). Activation of TRPC1 by STIM1 in ER-PM microdomains involves release of the channel from its scaffold caveolin-1. *Proc Natl Acad Sci USA* **106,** 20087-20092.

Pani B, Ong HL, Liu X, Rauser K, Ambudkar IS & Singh BB. (2008). Lipid rafts determine clustering of STIM1 in endoplasmic reticulum-plasma membrane junctions and regulation of store-operated Ca^{2+} entry (SOCE). *J Biol Chem* **283,** 17333-17340.

Pani B & Singh BB. (2009). Lipid rafts/caveolae as microdomains of calcium signaling. *Cell Calcium* **45,** 625-633.

Parekh AB. (2003). Mitochondrial regulation of intracellular Ca^{2+} signaling: more than just simple Ca^{2+} buffers. *News Physiol Sci* **18,** 252-256.

Parekh AB. (2008). Mitochondrial regulation of store-operated CRAC channels. *Cell Calcium* **44,** 6-13.

Parekh AB. (2011). Decoding cytosolic Ca^{2+} oscillations. *Trends Biochem Sci* **36,** 78-87.

Parekh AB & Muallem S. (2011). Ca^{2+} signalling and gene regulation. *Cell Calcium*.

Park C, Hoover P, Mullins F, Bachhawat P, Covington E, Raunser S, Walz T, Garcia K, Dolmetsch R & Lewis RS. (2009). STIM1 Clusters and Activates CRAC Channels via Direct Binding of a Cytosolic Domain to Orai1. *Cell* **136,** 876-890.

Petersen OH. (2003). Localization and regulation of Ca^{2+} entry and exit pathways in exocrine gland cells. *Cell Calcium* **33,** 337-344.

Petersen OH & Tepikin AV. (2008). Polarized calcium signaling in exocrine gland cells. *Annu Rev Physiol* **70,** 273-299.

Petrie RJ, Doyle AD & Yamada KM. (2009). Random versus directionally persistent cell migration. *Nat Rev Mol Cell Biol* **10,** 538-549.

Porter KR & Palade GE. (1957). Studies on the endoplasmic reticulum. III. Its form and distribution in striated muscle cells. *J Biophys Biochem Cytol* **3,** 269-300.

Putney JW. (1986). A model for receptor-regulated calcium entry. *Cell Calcium* **7,** 1-12.

Putney JW. (2007). Recent breakthroughs in the molecular mechanism of capacitative calcium entry (with thoughts on how we got here). *Cell Calcium* **42,** 103-110.

Putney JW & Bird GS. (2008). Cytoplasmic calcium oscillations and store-operated calcium influx. *J Physiol* **586,** 3055-3059.

Rahman T & Taylor CW. (2009). Dynamic regulation of IP_3 receptor clustering and activity by IP_3. *Channels (Austin)* **3,** 226-232.

Reger JF. (1961). The fine structure of neuromuscular junctions and the sarcoplasmic reticulum of extrinsic eye muscles of Fundulus heteroclitus. *J Biophys Biochem Cytol* **10,** 111-121.

Ridley AJ, Paterson HF, Johnston CL, Diekmann D & Hall A. (1992). The small GTP-binding protein rac regulates growth factor-induced membrane ruffling. *Cell* **70,** 401-410.

Ridley AJ, Schwartz MA, Burridge K, Firtel RA, Ginsberg MH, Borisy G, Parsons JT & Horwitz AR. (2003). Cell migration: integrating signals from front to back. *Science* **302,** 1704-1709.

Rizzuto R & Pozzan T. (2006). Microdomains of intracellular Ca^{2+}: molecular determinants and functional consequences. *Physiol Rev* **86,** 369-408.

Rizzuto RR, Pinton P, Carrington W, Fay FS, Fogarty KE, Lifshitz LM, Tuft RA & Pozzan T. (1998). Close contacts with the endoplasmic reticulum as determinants of mitochondrial Ca^{2+} responses. *Science* **280,** 1763-1766.

Roos J, DiGregorio P, Yeromin A, Ohlsen K, Lioudyno M, Zhang S, Safrina O, Kozak J, Wagner S, Cahalan M, Velicelebi G & Stauderman K. (2005). STIM1, an essential and conserved component of store-operated Ca^{2+} channel function. *J Cell Biol* **169,** 435-445.

Rosenbluth J. (1962). Subsurface cisterns and their relationship to the neuronal plasma membrane. *J Cell Biol* **13,** 405-421.

Rossi AE & Dirksen RT. (2006). Sarcoplasmic reticulum: the dynamic calcium governor of muscle. *Muscle Nerve* **33,** 715-731.

Saarikangas J, Zhao H & Lappalainen P. (2010). Regulation of the Actin Cytoskeleton-Plasma Membrane Interplay by Phosphoinositides. *Physiol Rev* **90,** 259-289.

Schafer C, Rymarczyk G, Ding L, Kirber M & Bolotina VM. (2012). Role of molecular determinants of store-operated Ca^{2+} entry (Orai1, phospholipase A2 group 6 and STIM1) in focal adhesion formation and cell migration. *J Biol Chem* **287,** 40745-40757.

Schwaller B. (2010). Cytosolic Ca^{2+} buffers. *Cold Spring Harb Perspect Biol* **2,** a004051.

Shen WW, Frieden M & Demaurex N. (2011). Remodelling of the endoplasmic reticulum during store-operated calcium entry. *Biol Cell* **103,** 365-380.

Shimizu Y & Hendershot LM. (2007). Organization of the functions and components of the endoplasmic reticulum. *Adv Exp Med Biol* **594,** 37-46.

Singaravelu K, Nelson C, Bakowski D, de Brito OM, Ng SW, Di Capite J, Powell T, Scorrano L & Parekh AB. (2011). Mitofusin 2 Regulates STIM1 Migration from the Ca^{2+} Store to the Plasma Membrane in Cells with Depolarized Mitochondria. *J Biol Chem* **286,** 12189-12201.

Smyth J, DeHaven W, Bird G & Putney J. (2008). Ca^{2+}-store-dependent and independent reversal of Stim1 localization and function. *J Cell Sci* **121,** 762-772.

Smyth JT, DeHaven WI, Bird GS & Putney JW, Jr. (2007). Role of the microtubule cytoskeleton in the function of the store-operated Ca^{2+} channel activator STIM1. *J Cell Sci* **120,** 3762-3771.

Srikanth S & Gwack Y. (2012). Orai1, STIM1, and their associating partners. *J Physiol* **590,** 4169-4177.

Srikanth S, Jew M, Kim KD, Yee MK, Abramson J & Gwack Y. (2012). Junctate is a Ca^{2+}-sensing structural component of Orai1 and stromal interaction molecule 1 (STIM1). *Proc Natl Acad Sci U S A* **109,** 8682-8687.

Srikanth S, Jung HJ, Kim KD, Souda P, Whitelegge J & Gwack Y. (2010). A novel EF-hand protein, CRACR2A, is a cytosolic Ca^{2+} sensor that stabilizes CRAC channels in T cells. *Nat Cell Biol* **12,** 436-446.

Srinivasan S, Wang F, Glavas S, Ott A, Hofmann F, Aktories K, Kalman D & Bourne HR. (2003). Rac and Cdc42 play distinct roles in regulating PI(3,4,5)P_3 and polarity during neutrophil chemotaxis. *J Cell Biol* **160,** 375-385.

Sun HQ, Yamamoto M, Mejillano M & Yin HL. (1999). Gelsolin, a multifunctional actin regulatory protein. *J Biol Chem* **274,** 33179-33182.

Tabas I & Ron D. (2011). Integrating the mechanisms of apoptosis induced by endoplasmic reticulum stress. *Nat Cell Biol* **13,** 184-190.

Tashiro M, Samuelson L, Liddle R & JA W. (2004). Calcineurin mediates pancreatic growth in protease inhibitor-treated mice. *Am J Physiol Gastrointest Liver Physiol* **286,** G784-790.

Terasaki M, Chen LB & Fujiwara K. (1986). Microtubules and the endoplasmic reticulum are highly interdependent structures. *J Cell Biol* **103,** 1557-1568.

Tinel H, Cancela JM, Mogami H, Gerasimenko JV, Gerasimenko OV, Tepikin AV & Petersen OH. (1999). Active mitochondria surrounding the pancreatic acinar granule region prevent spreading of inositol trisphosphate-evoked local cytosolic Ca^{2+} signals. *EMBO J* **18,** 4999-5008.

Treves S, Franzini-Armstrong C, Moccagatta L, Arnoult C, Grasso C, Schrum A, Ducreux S, Zhu M, Mikoshiba K, Girard T, Smida-Rezgui S, Ronjat M & Zorzato F. (2004). Junctate Is a Key Element in Calcium Entry Induced by Activation of $InsP_3$ Receptors and/or Calcium Store Depletion. *J Cell Biol* **166,** 537-548.

Tsai FC & Meyer T. (2012). Ca^{2+} Pulses Control Local Cycles of Lamellipodia Retraction and Adhesion along the Front of Migrating Cells. *Curr Biol* **22,** 837-842.

Tu JC, Xiao B, Yuan JP, Lanahan AA, Leoffert K, Li M, Linden DJ & Worley PF. (1998). Homer binds a novel proline-rich motif and links group 1 metabotropic glutamate receptors with IP3 receptors. *Neuron* **21,** 717-726.

Varnai P, Thyagarajan B, Rohacs T & Balla T. (2006). Rapidly inducible changes in phosphatidylinositol 4,5-bisphosphate levels influence multiple regulatory functions of the lipid in intact living cells. *J Cell Biol* **175,** 377-382.

Várnai P, Tóth B, Tóth DJ, Hunyady L & Balla T. (2007). Visualization and manipulation of plasma membrane-endoplasmic reticulum contact sites indicates the presence of additional molecular components within the STIM1-Orai1 Complex. *J Biol Chem* **282,** 29678-29690.

Vasiliev JM, Gelfand IM, Domnina LV, Ivanova OY, Komm SG & Olshevskaja LV. (1970). Effect of colcemid on the locomotory behaviour of fibroblasts. *J Embryol Exp Morphol* **24,** 625-640.

Voeltz GK, Rolls MM & Rapoport TA. (2002). Structural organization of the endoplasmic reticulum. *EMBO Rep* **3,** 944-950.

Walsh C, Barrow S, Voronina S, Chvanov M, Petersen OH & Tepikin A. (2009). Modulation of calcium signalling by mitochondria. *Biochim Biophys Acta* **1787,** 1374-1382.

Walsh CM, Chvanov M, Haynes LP, Petersen OH, Tepikin AV & Burgoyne RD. (2010a). Role of phosphoinositides in STIM1 dynamics and store-operated calcium entry. *Biochem J* **425,** 159-168.

Walsh CM, Doherty MK, Tepikin AV & Burgoyne RD. (2010b). Evidence for an interaction between Golli and STIM1 in store-operated calcium entry. *Biochem J* **430,** 453-460.

Wary KK, Mariotti A, Zurzolo C & Giancotti FG. (1998). A requirement for caveolin-1 and associated kinase Fyn in integrin signaling and anchorage-dependent cell growth. *Cell* **94,** 625-634.

Waterman-Storer CM, Gregory J, Parsons SF & Salmon ED. (1995). Membrane/microtubule tip attachment complexes (TACs) allow the assembly dynamics of plus ends to push and pull membranes into tubulovesicular networks in interphase Xenopus egg extracts. *J Cell Biol* **130,** 1161-1169.

Webb DJ, Parsons JT & Horwitz AF. (2002). Adhesion assembly, disassembly and turnover in migrating cells -- over and over and over again. *Nat Cell Biol* **4,** E97-100.

Wei C, Wang X, Chen M, Ouyang K, Song LS & Cheng H. (2009). Calcium flickers steer cell migration. *Nature* **457,** 901-905.

Wei C, Wang X, Zheng M & Cheng H. (2012). Calcium gradients underlying cell migration. *Curr Opin Cell Biol* **24,** 254-261.

Willoughby D, Wachten S, Masada N & Cooper DM. (2010). Direct demonstration of discrete Ca^{2+} microdomains associated with different isoforms of adenylyl cyclase. *J Cell Sci* **123,** 107-117.

Wu MM, Buchanan J, Luik RM & Lewis RS. (2006). Ca^{2+} store depletion causes STIM1 to accumulate in ER regions closely associated with the plasma membrane. *J Cell Biol* **174,** 803-813.

Wuytack F, Raeymaekers L & Missiaen L. (2002). Molecular physiology of the SERCA and SPCA pumps. *Cell Calcium* **32,** 279-305.

Xiao B, Coste B, Mathur J & Patapoutian A. (2011). Temperature-dependent STIM1 activation induces Ca^{2+} influx and modulates gene expression. *Nat Chem Biol* **7,** 351-358.

Xu P, Lu J, Li Z, Yu X, Chen L & Xu T. (2006). Aggregation of STIM1 underneath the plasma membrane induces clustering of Orai1. *Biochem Biophys Res Commun* **350,** 969-976.

Yamazaki D, Kurisu S & Takenawa T. (2005). Regulation of cancer cell motility through actin reorganization. *Cancer Sci* **96,** 379-386.

Yang S, Zhang JJ & Huang X-Y. (2009). Orai1 and STIM1 are critical for breast tumor cell migration and metastasis. *Cancer Cell* **15,** 124-134.

Yin HL & Stossel TP. (1979). Control of cytoplasmic actin gel-sol transformation by gelsolin, a calcium-dependent regulatory protein. *Nature* **281,** 583-586.

Yu F & Machaca K. (2009). Orai1 internalization and STIM1 clustering inhibition modulate SOCE inactivation during meiosis. *Proc Natl Acad Sci U S A* **106,** 17401-17406.

Yu F, Sun L & Machaca K. (2010). Constitutive recycling of the store-operated Ca^{2+} channel Orai1 and its internalization during meiosis. *J Cell Biol* **191,** 523-535.

Yule DI. (2010). Pancreatic acinar cells: molecular insight from studies of signal-transduction using transgenic animals. *Int J Biochem Cell Biol* **42,** 1757-1761.

Zamir E & Geiger B. (2001). Molecular complexity and dynamics of cell-matrix adhesions. *J Cell Sci* **114,** 3583-3590.

Zeng W, Yuan JP, Kim MS, Choi YJ, Huang GN, Worley PF & Muallem S. (2008). STIM1 gates TRPC channels, but not Orai1, by electrostatic interaction. *Mol Cell* **32,** 439-448.

Zhang SL, Yu Y, Roos J, Kozak JA, Deerinck TJ, Ellisman MH, Stauderman KA & Cahalan MD. (2005). STIM1 is a Ca^{2+} sensor that activates CRAC channels and migrates from the Ca^{2+} store to the plasma membrane. *Nature* **437,** 902-905.

Appendix 1: Video Legends

Video 1.1 Two potential mechanisms for ER-PM junction formation and dynamics during cell migration: sliding junctions and saltatory junction formation. In the first part of the video, a depiction of sliding junctions is shown, in which preformed junctions slide into new locations as a cell migrates. In the latter part of the video, a depiction of saltatory junction formation is shown, in which there is continual turnover of ER-PM junctions during cell migration.

Video 3.1 There is a concentration of junctions at the cell periphery that follows the leading edge during cell migration. PANC-1 cells expressing TK-YFP-STIM1 were treated with 15 μM CPA to deplete the intracellular Ca^{2+} store, kept in media with reduced Ca^{2+} (1 mM) and imaged on a confocal microscope overnight, at 37 °C, 5% CO_2. Scale bar represents 10 μm.

Video 3.2 STIM1(NN) puncta can concentrate at the periphery of migrating PANC-1 cells, following the leading edge as the cell migrates. PANC-1 cells expressing CMV-STIM1(NN)-YFP were treated with 10 μM CPA in media with reduced Ca^{2+} (1 mM) and imaged live on a confocal microscope (at 37 °C, 5% CO_2). Time indicates relative time (from start of video); scale bar represents 10 μm.

Video 3.3 Junction formation at the leading edge of migrating cells is saltatory. PANC-1 cells expressing TK-YFP-STIM1 were treated with 15 μM CPA in media with reduced Ca^{2+} (1 mM) and imaged live on a confocal microscope (at 37 °C, 5% CO_2). Scale bar represents 10 μm.

Video 3.4 STIM1 puncta at the leading edge form in a saltatory fashion in heat-treated cells. TK-YFP-STIM1 transfected PANC-1 cells were imaged live on a confocal microscope at 40 °C (and 5% CO_2) in full media. Scale bar represents 10 μm.

Video 3.5 Puncta found in the tail of migrating cells can travel long distances during tail retraction. PANC-1 cells expressing TK-YFP-STIM1 were treated with 15 μM CPA in media with reduced Ca^{2+} (1 mM) and imaged on a confocal microscope (at 37 °C, 5% CO_2). Scale bar represents 10 μm.